NUCLEATION DURING BOILING

WITH SPECIAL REFERENCE TO ITS CESSATION AT LOW PRESSURE

by

H.H.JAWUREK

being a thesis submitted for the degree of Master of Science in Chemical Engineering at the University of Cape Town.

October, 1962.

ABSTRACT

A critical review of the mechanisms, models and heat-transfer correlations for nucleate boiling is presented. The importance of nucleation is stressed. It is pointed out that the bulk of correlations are based on the erroneous notion that the energy transferred away from the heating surface by bubbles as such, in the form of latent heat, contributes insignificantly to the total flux. - A critical review of the correlations for the upper limit of the nucleate boiling regime - the peak flux is also presented.

The theory of nucleation during boiling is reviewed and extended in an attempt to explain the complete absence of the nucleate regime, noted in preliminary tests conducted at low pressures. The following equation characterizing nucleation is derived

$$r_c = \frac{\sigma(T_w + T_s)\, v_V}{\lambda_V (T_w - T_s)\, J}$$

where r_c is the mouth radius of the smallest cavity for which nucleation can proceed under the conditions reflected in the right-hand terms of the equation; T_w is the (absolute) wall temperature; T_s is the (absolute) saturation temperature corresponding to the system pressure; σ is the surface tension; λ_V is the latent heat of vaporization; v_V is the specific volume of the vapour; (all physical properties evaluated at $(T_w + T_s)/2$); and J is the mechanical equivalent of heat.

The nucleation mechanism embodied in this equation is the one according to which the nucleation superheat for a particular surface cavity is determined by the equilibrium (expressed by the Gibbs equation) of a vapour cap formed over a cavity mouth, with the bubble radius of curvature equal to the cavity mouth radius.

Experimental data are reported for benzene and ethanol boiling from the same surface at various pressures. At atmospheric and moderate subatmospheric pressures the usual stable boiling curves are obtained. In an intermediate region a hitherto unreported, permanently unstable, nucleate boiling regime exists, which is characterized by erratic bubble behaviour and by boiling curves of unusual shape. At even lower pressures the nucleate regime is altogether absent, the heat-transfer changing from natural convection straight to film boiling as the wall superheat is raised.

Application of the nucleation equation to the stable runs and to the point of disappearance of the last bubble on a stable boiling curve (flux decreasing) allows the prediction of the size range of surface cavities available for nucleation. A method is given to determine the point where this size range becomes zero, and where the above mechanism ceases to operate. Comparison with the experimental

data shows remarkably quantitatively that when this mechanism ceases to operate - a situation that can occur in the middle of a boiling curve - nucleate boiling changes from stable to unstable and the bubble behaviour becomes erratic. Thus a method of predicting the threshold of unstable nucleation which becomes operative before complete cessation of nucleation occurs, is presented.

Photomicrographs of the heating surface employed are shown, which illustrate the existence of cavities of such sizes as are required by the theory.

CONTENTS

SECTION I INTRODUCTION

1.0 GENERAL

Boiling, a heat transfer mode capable of accommodating fluxes in the order of several millions of Btu/hr.ft^2, has, with the recent advent of such high heat flux equipment as nuclear reactors, jet engines and rocket engines assumed a major position in heat transfer research.

Despite man's long acquaintance with the phenomenom of boiling and the intensive research to which it has been subjected in the last three or so decades, our present knowledge of the physical processes underlying it is insufficient even for the semi-empirical derivation of correlations capable of predicting boiling heat transfer rates under all conditions.

In this study consideration is limited to one of the 19 possible modes of boiling which have been recognized[1], namely, to the important case of saturated nucleate pool boiling, i.e. the case of boiling with vapour emination from discrete sites on the heating surface, the bulk of the liquid being at its boiling point and circulation of the liquid occurring by natural convection in a large vessel.

1.1 THE IMPORTANCE OF NUCLEATION.

The remark on the absence of satisfactory correlations for the prediction of heat transfer rates applies particularly to nucleate boiling. The reason for this lies in the highly surface-dependent nature of the process.

Nucleate boiling involves the processes of nucleation (the formation of microscopic bubbles capable of growth) and the subsequent growth of these bubbles. Now nucleation, as has been shown analytically and experimentally (2, 3, 4, 5) takes place mainly from a pre-existing vapour phase entrapped in microscopic surface cavities. Clearly, different surfaces, even of the same material, will have

different micro-structures and hence different nucleation characteristics. Even one particular surface, subjected to no such thermal or mechanical treatment as might change its microstructure, will, with different previous histories and hence different entrapped gases and vapours, behave differently (3, 6, 7, 8, 9, 10). It is therefore not surprising that the many attempts at general correlations of nucleate boiling heat transfer, along the traditional lines of dimensional analysis, neglecting surface variables important in nucleation, have failed.

The processes basic to nucleate boiling are, to repeat, nucleation followed by growth. There is, as pointed out by Westwater (11) "no reason to believe that the important variables for these two processes are the same, or that either one of the two processes will be rate controlling under all conditions." Thus a satisfactory correlation will have to take into consideration both nucleation and growth.

The problem of the growth of nuclei into full-size bubbles has received attention recently (12, 13, 14, 15, 16). Expressions which fit well with experimental data for the growth of steam bubbles in superheated water (17) were obtained and employed alone in the derivation of heat transfer correlations (18, 19). A recent Russian correlation (20) was derived along similar lines. As is to be expected, these expressions, based only on the growth aspect, are of limited validity.

Our present knowledge of heterogeneous nucleation and the means available for surface characterization are, however, insufficient to afford the derivation of a heat transfer equation inclusive of the effects of both processes basic to nucleate boiling.

This insufficiency of knowledge concerning nucleation is one reason for the initiation of the work here reported.

1.2 THE CESSATION OF NUCLEATION AT LOW PRESSURES

In the course of a number of saturated boiling runs conducted at subatmospheric pressure, the present author observed the absence

of the nucleate regime below roughly 120 mm Hg for several organic liquids. Instead of the usual transitions from heat transfer by natural convection to nucleate boiling, through the peak flux and then (for the case of boiling from electrically heated wires) to film boiling, the wire remained in natural convection without any bubble formation and at some high surface-to-bulk temperature difference burst into film boiling.

This phenomenon had once been previously and accidentally observed by van Straten (21) during the low pressure boiling of water. The observations in this Department were made independently and without knowledge of van Straten's work.

The absence of the nucleate regime at low pressure presents a remarkable problem in nucleation. It was felt that an attempt at the explanation of the phenomenon on the basis of the theories of Bankoff (2) and Griffith and Wallis (5) would serve as a useful indication of the status of heterogeneous nucleation theory.

1.3 OBJECTS OF PRESENT WORK

The objects of the present work, then, are the following:

(1) To present a critical review, in the light of remarks made under section 1.1, of the mechanisms and correlations proposed for nucleate boiling, together with a similar review for the upper limit thereof, i.e. the peak flux or burnout point.

(2) To discuss heterogeneous nucleation theory as applicable to boiling, and to attempt an explanation of the cessation of nucleation at low pressure along the lines suggested by the theories of Bankoff (2) and Griffith and Wallis (5).

(3) To present further experimental data on low pressure boiling and accurate evidence of the cessation of nucleation phenomenon.

(4) To conduct such experimental work as is dictated by the considerations under (2) above.

SECTION II A CRITICAL REVIEW OF THE MECHANISMS, MODELS, AND CORRELATIONS FOR POOL BOILING AND THE PEAK FLUX

2.00 MECHANISMS, MODELS, AND APPROACHES TO THE CORRELATION OF NUCLEATE POOL BOILING

Apart from early, empirical relationships, defensible on no grounds other than simple dimensional analysis (22, 23, 24, 25, 26), and a recent statistical analysis of no theoretical significance (27), all pool boiling correlations published to date have been derived on the basis of one of the approaches or mechanisms listed below. Such proposed mechanisms or models as have not lead to correlations are included.

(a) The high heat transfer rates observed in nucleate boiling are attributed to vigorous convection currents set up in the super-heated layer near the heating surface by growing and departing bubbles, direct latent heat transport being negligable. See section 2.000

(b) The heat transferred away from the surface by bubbles as such, due to their latent heat of formation, is the major contributor to the total boiling flux. See section 2.001.

(c) The formation of a liquid microlayer under a growing bubble and its rapid vaporization into the bubble are considered of importance. See section 2.002.

(d) A vapour-liquid exchange mechanism is postulated, whereby growing bubbles push hot liquid away from the surface, and upon departure allow cooler liquid to rush to the surface. See section 2.003.

(e) Wave motion in the superheated layer is considered of prime importance in determining boiling fluxes. See section 2.004.

(f) Departing bubbles are postulated to induce flow patterns identical to those encountered in laminar stagnation-flow but in the opposite direction. See section 2.005

Of the many proposed correlations only the ones in more common use will be discussed.

2.000 BUBBLE-INDUCED FORCED CONVECTION NEAR THE HEATING SURFACE.

It is the generally held view that in nucleate boiling the energy transferred away from the heating surface by bubbles as such, in the form of latent heat, contributes insignificantly to the total flux. The postulated thermal path is: from the hot solid into the superheated liquid layer and from there into the rising bubbles, only an insignificant part flowing into attached bubbles. This view appears to be based on photographic data of Jakob (28) on the low flux boiling of water, and on that of Gunther and Kreith (29) and Rohsenow and Clark (30) on subcooled nucleate boiling. Only subsequent to the derivation of the correlations here presented was this central assumption checked by Rallis and his co-workers (10, 31). It was shown that in saturated pool boiling the assumption does not even hold at low fluxes and is entirely in error at high fluxes (see section 2.001).

Meanwhile the heat transfer rates were attributed to bubble-induced agitation near the heating surface. The problem was thus formulated as one of turbulent forced convection with correlations of the general form

$$Nu = \text{const.}\ Re^{m}.\ Pr^{n} \quad \ldots \quad \ldots \quad (2.1)$$

where the constant and the exponents are determined from experiment.

Inasmuch as the heat transfer rates in nucleate boiling appear to be independent of system geometry, bubble dimensions, rather than apparatus dimensions, were used as characteristic lengths. The difference of proposed correlations arises out of the use of different bubble dimensions and different definitions of the dimensionless groups.

2.0000 ROHSENOW'S CORRELATION

In Rohsenhow's analysis (32, 33) the bubble dynamics at departure were considered of prime importance. Hence the bubble diameter at departure, correlated by Fritz (34) as

$$D_d = C_1 \beta \left[\frac{2 g_c \sigma}{g(\rho_L - \rho_V)} \right]^{\frac{1}{2}} \quad \ldots \quad \ldots \quad (2.2)$$

was chosen as characteristic length. If bubbles are approximated by spheres, and the bubble population is (N/A) sites per unit area then the bubble mass flow rate becomes

$$G_b = \frac{\pi}{6} D_d^3 \rho_V f(N/A) \ldots \quad \ldots \quad (2.3)$$

and

$$G_b = \frac{(q/A)_b}{\lambda_V} \quad \ldots \quad \ldots \quad (2.4)$$

In addition it had been observed by Jakob (28) during the low flux boiling of water, that

$$(q/A) = C_2 (q/A)_b \quad \ldots \quad \ldots \quad (2.5)$$

This relation was assumed to hold generally. Combining equations (2.2), (2.4) and (2.5) permits the formulation of a bubble Reynold number as

$$Re = \frac{G_b D_d}{\mu_L} = \frac{C_3 \beta (q/A)}{\mu_L \lambda_V} \left[\frac{g_c \sigma}{g(\rho_L - \rho_V)} \right]^{\frac{1}{2}} \quad \ldots \quad (2.6)$$

The Nusselt number was formulated, using equation (2.2), as

$$Nu = \frac{h D_d}{k_L} = \frac{h \beta}{k_L} \left[\frac{g_c \sigma}{g(\rho_L - \rho_V)} \right]^{\frac{1}{2}} \quad \ldots \quad \ldots \quad (2.7)$$

The Prandtl number was based on liquid properties.

The assumption that the contact angle, β, is independent of flux for a particular solid-fluid combination, together with the above, produces the final correlation

$$\frac{h}{k_L} \left[\frac{g_c \sigma}{g(\rho_L - \rho_V)} \right]^{\frac{1}{2}} = \frac{1}{C_{sf}} \left[\left(\frac{(q/A)}{\mu_L \lambda_V} \right) \left(\frac{g_c \sigma}{g(\rho_L - \rho_V)} \right)^{\frac{1}{2}} \right]^{\frac{3}{7}} \left[\frac{C_L \mu_L}{k_L} \right]^{-0.7} \quad \ldots (2.8)$$

The exponents of the dimensionless groups were determined from experimental data on water (23, 35) and on three organic liquids (36) boiling on different surfaces and under different pressures. The constant C_{sf} was found to be different for each solid-fluid combination and varied from 0.0027 to 0.015, that is by a factor of five. Since these constants were chosen to fit particular data the correlation predicts nothing but the slope of the nucleate boiling curve. For any particular pressure the expression reduces to approximately

$$(q/A) = \text{const.} \ (T_w - T_s)^3 \quad \ldots \quad \ldots \quad (2.9)$$

i.e. the slope of the boiling curve is always 3 which is, of course, not the case, Courty and Fouse (3) and Kurihara and Myers (37), among others, having shown that variations in the exponent, ranging from 3 to 25 may be effected by polishing a surface with different grades of emery paper. Such mechanical treatment changes the nucleation characteristics of a surface (but not by changing the primary roughness which is not generally of a size and shape conducive to the nuclei formation, but by changing the smaller, second-order roughness formed statistically by the fracture of the solid). The nucleation characteristics, more specifically the number and size distribution of cavities, influence the entire shape of the boiling curve, including therefore the value of the exponent. This will be more fully discussed later.

It must, however, be pointed out that these findings were published after Rohsenow's equation. Inasmuch as it is one of the first theoretical attempts to correlate nucleate boiling it is highly laudible.

2.0001 THE FORSTER-ZUBER EQUATION

Forster and Zuber (18) considered growth velocities of attached bubbles, rather than velocities of departing bubbles as the major contributors to sublayer turbulence. Since the velocities involved in bubble growth are roughly one order of magnitude larger

than those associated with macroscopic bubble movement (38) their view is justified.

For the formulation of the dimensionless moduli in equation (2.1), on the above basis, it was necessary to obtain expressions for the bubble radius, R, and for the rate of radial bubble growth, $\dot{R}$.

Plesset and Zwick (15) and Forster and Zuber (15) considered the rate of bubble growth in a uniformly superheated liquid. From their growth equations they obtained the relation

$$R = \frac{(T_w - T_s)\, c_L\, \rho_L}{\rho_V\, \lambda_V} \sqrt{\pi a_L t} \quad \ldots \quad (2.10)$$

Substitution of a relevant time constant for the time, t, would result in a characteristic length. By a complex analysis considering the isothermal advance of a vapour front (18) the relation

$$t = R_o \sqrt{\frac{\rho_L}{\Delta P}} \quad \ldots \quad \ldots \quad (2.11)$$

was obtained, where ΔP is the vapour pressure difference corresponding to the superheat, and R_o is the initial bubble radius given by

$$R_o = \frac{2\sigma}{\Delta P} \quad \ldots \quad \ldots \quad (2.12)^*$$

Combining equations (2.10), (2.11) and (2.12) results in the formulation of the characteristic length

$$R = \left[\frac{(T_w - T_s)\, c_L \rho_L \sqrt{\pi a_L}}{\rho_V\, \lambda_V}\right]\left[\frac{2\sigma}{\Delta P}\right]^{\frac{1}{2}}\left[\frac{\rho_L}{\Delta P}\right]^{\frac{1}{4}} \quad \ldots \quad (2.13)$$

It follows from equation (2.10) that the product of bubble radius, R and radial bubble growth rate, $\dot{R}$, as required for the formulation of the bubble Reynolds number, is independent of time and given by

$$2R\dot{R} = \left[\frac{(T_w - T_s)\, c_L\, \rho_L \sqrt{\pi a_L}}{\rho_V\, \lambda_V}\right]^2 \quad \ldots \quad (2.14)$$

---

* This equation will be discussed more fully later

Thus the bubble Reynolds number was given by

$$Re = \frac{2R\dot{R}\rho_L}{\mu_L} \quad \ldots \quad \ldots \quad (2.15)$$

with the product $R\dot{R}$ substituted from equation (2.14) and the bubble Nusselt number by

$$Nu = \frac{R(q/A)}{k_L (T_w - T_s)} \quad \ldots \quad \ldots \quad (2.16)$$

with R substituted from equation (2.13). The Prandtl number was based on liquid properties. The final correlation was

$$Nu = 0.0015\ Re^{0.62}\ Pr^{\frac{1}{3}} \quad \ldots \quad (2.17)$$

i.e.

$$\left[\frac{c_L \rho_L \sqrt{\pi \alpha_L}\ (q/A)}{k_L \rho_V \lambda_V}\right]\left[\frac{2\sigma}{\Delta P}\right]^{\frac{1}{2}}\left[\frac{\rho_L}{\Delta P}\right]^{\frac{1}{4}}$$

$$= 0.0015 \left[\frac{\rho_L}{\mu_L}\left(\frac{c_L \rho_L (T_w - T_s)\sqrt{\pi \alpha_L}}{\rho_V \lambda_V}\right)^2\right]^{0.62}\left[\frac{c_L \mu_L}{k_L}\right]^{\frac{1}{3}}$$

where the values of the constant and the exponents of the dimensionless moduli were determined from experimental data on three organic liquids (36) boiling at nor near the critical flux. The applicability of the correlation to data on water was tested with the peak flux data of Addoms (35) and Kazakova (39) and was found satisfactory. Unlike in Rohsenow's relation, all data fell on the same line.

Since the constants in equation (2.17) were obtained from peak flux data, the correlation should be more applicable to high flux conditions than others.

Like the bulk of correlations, the Forster-Zuber equation does not take the nucleation characteristics of the surface into account. Its success must stem from the relative similarity (with respect to nucleation) of the "smooth" chrome, nickel and platinum surfaces generally used in boiling runs.

In a subsequent publication (40) Zuber has attempted to show that the inclusion of the critical bubble radius, R_o, in the formulation of the bubble radius takes nucleation into account. The remarks apply only to homogeneous nucleation (i.e. nucleation within the liquid bulk); in fact, the correlation is derived on the basis of boiling in the bulk and predicts identical fluxes for homogeneous and heterogeneous ebbulation.

It has, incidentally, been shown by Zuber and Fried (41) that the equation of Engelberg-Forster and Greif (42) i.e. equation (29) in ref.(42), derived by dimensional analysis, is, in fact identical with equation (2.18), the difference stemming from a substitution for ΔP in terms of the Clausius-Clapeyron equation.

2.0002 LABUNTZOV'S CORRELATION

It is reported (41) that Labuntzov has obtained a correlation based on a model similar to that of Forster and Zuber.

A new concept, apparently derived from experiments (unspecified, no reference given) is that the liquid is superheated to a distance R_o from the surface, where R_o is the critical bubble radius given by equation (2.12). The enthalpy of the liquid film (above the saturation temperature) is then $AR_o\, c_L\, \rho_L (T_w - T_s)$. If all the stored energy is used for vaporization, then the maximum distance, ℓ^*, which a vapour front can advance is given by

$$A\,\ell^*\,\rho_V\,\lambda_V = A\,R_o\,\rho_L\,c_L(T_w - T_s) \quad \ldots \quad (2.19)$$

This relation, together with equation (2.12) with the ΔP term expressed in terms of superheat temperature difference as

$$R_o = \frac{2\sigma T_s}{(T_w - T_s)} \frac{(\rho_L - \rho_V)}{\rho_L \rho_V \lambda_V} \quad \ldots \quad \ldots \quad (2.20)$$

permits the formulation of a characteristic length as

$$\ell^* = \frac{c_L \rho_L}{\rho_V \lambda_V} \cdot \frac{2\sigma T_s}{\rho_V \lambda_V} \left(\frac{\rho_L - \rho_V}{\rho_L} \right) \quad \ldots \quad \ldots \quad (2.21)$$

which, by neglecting the term in brackets and dropping the 2 may be expressed as

$$\ell^* = \frac{c_L \rho_L \sigma T_s}{(\rho_V \lambda_V)^2} \quad \ldots \quad \ldots \quad (2.22)$$

From the concept of a superheat layer thickness of R_o, and the Fourier equation it further follows that

$$\frac{q}{A} = \frac{k_L (T_w - T_s)}{R_o} \quad \ldots \quad \ldots \quad (2.23)$$

Substitution of equation (2.23) into the Forster-Zuber Reynolds modulus with the constant dropped, and further substitution from or of equations (2.20) and (2.22) yields

$$Re = \frac{\rho_L (q/A)}{\mu_L \rho_V \lambda_V} \ell^* = \frac{\rho_L (q/A) c_L \rho_L \sigma T_s}{\mu_L (\rho_V \lambda_V)^2} \quad \ldots \quad (2.24)$$

Using equation (2.22) the Nusselt number was formulated as

$$Nu = \frac{h \ell^*}{k_L} = \frac{h c_L \rho_L \sigma T_s}{k_L (\rho_V \lambda_V)^2} \quad \ldots \quad \ldots \quad (2.25)$$

The Prandtl number was based on liquid properties. The final correlation was

$$Nu = 0.125\, Re^{0.65}\, Pr^{\frac{1}{3}} \quad \text{for} \quad Re > 10^{-2} \quad \ldots \quad (2.26a)$$

and

$$Nu = 0.0625\, Re^{0.5}\, Pr^{\frac{1}{3}} \quad \text{for} \quad Re < 10^{-2} \quad \ldots \quad (2.26b)$$

It is reported (41) that these equations correlate boiling fluxes for a large variety of liquids including liquid metals.

The limitations of equations based purely on bubble growth and neglecting nucleation has already been discussed.

2.0003 KUTATELADZE'S AND MICHENKO'S CORRELATIONS

It is reported (41) that Kutateladze has obtained a correlation based on a model similar to that first proposed by Rohsenow.

As characteristic length he chose (as did Rohsenow) the bubble diameter at departure, as correlated by Fritz's relation, equation (2.2).

The conversion factor g_c was dropped, the MLθT system of units being employed.

Following Jakob (43), the assumption is made that the superficial liquid velocity towards the surface equals the superficial vapour velocity away from the surface; then the superficial liquid velocity may be used as characteristic velocity. This is given by

$$U_L = \frac{(q/A)}{\rho_V \lambda_V} \quad \ldots \quad \ldots \quad (2.27)$$

The Reynolds modulus thus becomes

$$Re = \beta \frac{\rho_L}{\mu_L} \frac{(q/A)}{\rho_V \lambda_V} \left[\frac{\sigma}{g(\rho_L - \rho_V)} \right]^{\frac{1}{2}} \quad \ldots \quad (2.28)$$

The Nusselt modulus is the same as Rohsenow's, see equation (2.7), except that g_c is excluded.

The Prandtl number was based on liquid properties.

The contact angle, β , was apparently assumed constant and dropped from the formulation of Re and Nu .

These three dimensionless groups were insufficient to correlate data. Kutateladze found it necessary to make use of a pressure group defined by

$$Ku = \left[\frac{P}{\sigma g(\rho_L - \rho_V)} \right]^{\frac{1}{2}} \quad \ldots \quad \ldots \quad (2.29)$$

which is dimensionless in the MLθT system of units. It has been shown (41) that this group expresses the effect of system pressure upon the ratio D_d/R_o.

The final correlation was

$$\frac{h}{k_L} \left[\frac{\sigma}{g(\rho_L - \rho_V)} \right]^{\frac{1}{2}} = 7.0 \times 10^{-4} \left[\frac{\rho_L (q/A)}{\mu_L \rho_V \lambda_V} \left(\frac{\sigma}{g(\rho_L - \rho_V)} \right) \right]^{0.7} . Pr_L^{0.35} . Ku^{0.7}$$

$$\ldots \quad (2.30)$$

which is reported to correlate data for a large variety of solid-liquid combinations and pressures.

More recently, Michenko, as reported (41), using the same dimensionless groups obtained an equally satisfactory correlation given by

$$Nu = 8.7 \times 10^{-4} \left[\frac{1}{a} \frac{(q/A)}{\rho_V \lambda_V} \frac{\sigma}{g(\rho_L - \rho_V)} \right]^{0.7} Ku^{0.7} \quad \ldots (2.31)$$

where the term in square brackets may be interpreted as a Peclet number (= Re.Pr) for boiling.

Inasmuch as these correlations may, at a particular pressure, be reduced to

$$(q/A) = \text{const.}(T_w - T_s)^m \quad \ldots \quad \ldots \quad (2.32)$$

with m a constant, their limited applicability is clear.

2.0004 OTHER CORRELATIONS

Two further well known correlations based on bubble induced turbulence in the sublayer, but being of somewhat lower status than those discussed above, are mentioned for the sake of completeness.

Gilmour (44) using the same dimensionless groups as Kutateladze and Michenko and a further dimensionless ratio, D_d/D, was able to correlate reasonably (within 45%) data on boiling from tubes with the tube diameter as D in the length ratio. In correlating data for the boiling from disks he found it "necessary to select a diameter which is not the diameter of the disk". It was not specified how this diameter was selected.

Levy (19), employing the bubble growth equations of Forster and Zuber (13) was able to derive a correlation without specifying the bubble Reynolds and Nusselt numbers. His equation contains a dimensional factor which on the basis of theory ought to be a constant, but was, in fact, found to be pressure dependent. This factor is given in graphical form as a function of the enthalpy content, $\rho_V \rho_V$.

2.0005 ADVANCES

For the nucleate boiling of a particular substance at a particular pressure, the heat flux is not a single valued function of the superheat, but depends upon the superheat temperature difference and the bubble population. The bubble population, in turn, depends on the nucleating characteristics of the surface, that is, on the number and size distribution of nucleation cavities.

While there are at present no means available for the required micro-characterization of surfaces, the interrelation between heat flux, bubble population and superheat temperature difference has received attention.

It is reported (37, 45, 46) that the flux is not directly proportional to the site concentration, (N/A), as originally proposed by Jakob (47), but proportional to a fractional power thereof. In the region where boiling is the principal mechanism of heat transfer this exponent varies from 0.33 to 0.46 for various investigations. This interrelation has been shown to be unaffected by surface contamination, surface-active agents, dissolved salts or the degree of macroroughness.

Further, Kurihara and Myers (37), by forming dimensionless groups similar to those of Rohsenow (32), obtained an equation which correlated fluxes of water and several organic in terms of physical properties and bubble population. The liquids were boiled on widely differing surfaces with a large range of slopes of the boiling curve. Their relation is

$$\frac{h}{k_L} = 820\left[\frac{\rho_V}{\mu_L}\right]^{\frac{1}{3}}\left[\frac{N}{A}\right]^{\frac{1}{3}} Pr_L^{-0.89} \quad \ldots \quad (2.33)$$

the bubble population appearing to the $\frac{1}{3}$ power. In similarity to Rohsenow's equation (2.8) the Prandtl number enters with a negative exponent which seems incompatible with the bubble-induced turbulence model.

It appears (41) that Zuber, in a report submitted for publication, has on the basis of a new model derived a Reynolds number including a bubble population term. The group is given by

$$Re = \text{const.}\ \beta \frac{\rho_L}{\mu_L} \left[\frac{(T_w - T_s)\ c_L\ \rho_L}{\rho_V \lambda_V} \right]^2 \pi a \left[\frac{N}{A} \right]^{\frac{1}{2}} \left[\frac{\sigma}{g(\rho_L - \rho_L)} \right]^{\frac{1}{2}} \quad \ldots \quad \ldots \quad (2.34)$$

These formulations, while not providing the solution to the problems of correlating boiling fluxes, are believed by the present author to be steps in the right direction.

2.001 LATENT HEAT TRANSPORT

As was pointed out at the beginning of section 2.000, the assumption that direct latent heat transport by departing bubbles contributes but insignificantly to the total boiling flux, is central to the derivation of every boiling correlation published to date. The notion is based on Jakob's data (28) on the low flux boiling of water, and on boiling tests with the bulk subcooled (29, 30). Only in 1960 was this basic assumption tested by Rallis and his co-workers (10, 31) in the range to which it was principally applied, namely in fully developed saturated pool boiling. It was shown that latent heat transport is at no time insignificant.

It is instructive to illustrate this with Rallis' actual results. Taking one of his figures for the boiling of water (fig. 6 in reference 10), on which both the total flux and the photographically determined flux due to latent heat transport by bubbles is plotted, we note:

(a) At the very low flux of 10,000 Btu/hr.ft^2 (the boiling curve having separated from the natural convection curve at approximately 7,500 Btu/hr.ft^2) direct latent heat transport accounts for 3,000 Btu/hr.ft^2, i.e. for 30% of the total flux.

(b) At the low flux of 30,000 Btu/hr.ft^2 the latent heat contribution is roughly 16,000 Btu/hr.ft^2, i.e. 53%

(c) At the intermediate flux of 100,000 Btu/hr.ft^2 it is 80,000 Btu/hr.ft^2, i.e. 80%

(d) At the high flux of 200,000 Btu/hr.ft^2 (typical peak fluxes are 300,000-400,000) the latent heat contribution is approximately 190,000 Btu/hr.ft^2, i.e. 95%.

Except at low fluxes, latent heat transport is seen to account for the major portion of the total flux.

Similar results were subsequently obtained for water, using a more accurate photographic technique (31). Ethyl alcohol exhibits similar behaviour (10). These results may be considered conclusive.

With regard to the correlations of section 2.000, one is faced with a staggering instance of the use of unjustified assumptions.

Rallis has attempted a correlation. By summing the direct latent heat transport and the natural convection flux based on an undisturbed surface, and noting that this sum exceeds the experimentally observed flux, he has shown that latent heat transport by departing bubbles together with natural convection can account adequately for the fluxes observed in saturated nucleate boiling.

This leaves the conclusive evidence of insignificant latent heat transport in subcooled boiling (29, 30) to be dealt with.

If the high fluxes observed in this form of boiling are, as is generally assumed, attributable to the bubble-induced turbulence in the boundary layer, then it should be immaterial whether the bubbles are filled with vapour or inert gas. While it has been shown (48) that non-boiling fluxes may be increased considerably by the electrolytic generation of inert gas bubbles from the heating surface, the observed fluxes, even at the highest gas generation rate, were nowhere near those observed in high flux nucleate boiling.

The explanation seems to lie rather in mass transfer through the attached bubbles. This view originates from remarks made by Zmola during the discussion of Rohsenow and Clark's report (30) and has received considerable theoretical and experimental support (49,50). In subcooled boiling the mechanism that accounts for the major portion of the total flux is almost certainly that of evaporation near the superheated base of the attached bubble and condensation on the cooler parts towards the top of the bubble. The mechanism cannot to any significant degree apply to saturated boiling (see results of Rallis.)

2.002 MICROLAYER VAPORIZATION

It does, however, imply a process applicable to saturated boiling. It implies, as pointed out by Bankoff (50) among others (51), the existence of a thin liquid film at the base of the bubble from which vaporization would proceed. The temperature of this film would be expected to drop significantly after mass transfer had begun.

Now rapid surface temperature fluctuations during nucleate boiling have been investigated (51, 52). Moore and Mesler (51), by employing a thermocouple having an extremely short response time and capable of measuring the temperature of a very small area, this couple being linked to an oscilloscope, were able to record surface temperature drops of 20°F to 30°F occurring in about 2 msec during the nucleate boiling of water. These temperature dips were followed by slower recoveries to the original temperature.

These results were analysed theoretically and interpreted with care. The only mechanism consistent with the observed fluctuations was found to be one which involves vaporization at the base of the bubble, with the following detailed events: (quoting from the original) "As a bubble grows on the surface it exposes the heating surface wet with a microlayer of liquid to the interior of the bubble. This microlayer rapidly vaporizes removing heat rapidly from the surface until it is completely vaporized." The temperature dip corresponds to the microlayer vaporization the recovery and the interval till the next

dip corresponds to the time between completion of vaporization and recommencement of vapourization of the microlayer under the next bubble.

The hypothesis of bubble-induced boundary layer agitation and the consequent correlations cannot predict the observed temperature drops.

These findings ought to be of importance in correlating bubble growth and frequency, which in conjunction with effective surface characterization and hence prediction of bubble population, and Rallis' latent heat transport mechanism might provide the ideal correlation.

2.003 VAPOUR-LIQUID EXCHANGE ACTION

The mechanism of Engelberg-Forster and Greif (42), proposed prior to the above findings, would appear at first sight to predict the observed temperature drops.

The action basic to the suggested mechanism is one in which the space in the superheated layer vacated by a departing bubble (or in the case of subcooled boiling, a collapsing bubble) is occupied by cold liquid rushing in. Thus bubbles mechanically pump cooler liquid to the hot surface. This action predicts temperature fluctuations at a particular spot on the heating surface. However, a careful analysis by Moore and Mesler (51) shows that for the observed temperature dips to occur the inrushing water would have to be 147°F below the metal temperature, while the actual bulk saturation temperature was only 10°F to 30°F below the surface temperature. Further, the mechanism does not predict the sudden arrest of cooling which was observed.

It is hardly probable that vapour-liquid exchange action is a controlling factor in nucleate boiling. The approach has not led to a correlation.

2.004 CHANG'S WAVE THEORY

This approach will not be discussed in detail, but is mentioned for the sake of completeness.

Chang (53, 54) has proposed a generalized wave theory for

both natural convection and boiling which has led to a correlation.

Above the heating surface a boundary layer is postulated whose thickness depends upon the heat flux. This layer is in wave motion, stable at low fluxes, but unstable at higher fluxes. Bubble-eminating sites appear at the nodes of these waves. The theory predicts that the wave length and hence the spacing of nucleating sites should be an increasing function of surface temperature. This has been confirmed by experiment.

Inasmuch as the bubble population depends not only upon the surface temperature, but also on the number and size distribution of nucleation cavities, and further, since not ordered geometrical pattern of active sites, as predicted, has been observed, the approach seems limited.

The assumption that latent heat transport is insignificant, except near the peak flux, is basic to the approach.

2.005 INVERTED STAGNATION-FLOW MODEL

Tien (55) has very recently suggested a new hydrodynamic model for boiling. Since the publication was read at the very time of writing and has not been studied exhaustively only a few comments are offered.

In the region of low bubble population rising bubbles are postulated to set up flow patterns identical to those of laminar stagnation flow normal to a horizontal plate, but opposite in sign. At high bubble populations with mutual interaction flow patterns become more complicated. As a first approximation the model for the "isolated bubbles region" is used for the entire range of fluxes. The published relations governing heat transfer in laminar stagnation-flow against a wall are employed. Clearly the number of such flow sources is important, hence the bubble population enters into the correlation. The final equation is

$$\frac{q}{A} = 61.3\ Pr_L^{0.33}\ k_L \left(\frac{N}{A}\right)^{0.5} (T_w - T_s) \quad \ldots \quad (2.35)$$

The relation correlates (with quite a large deviation) the data for boiling of various substances from widely differing surfaces (37, 45, 46).

In the light of the work of Rallis (10, 31), it seems, as the author suggests, highly probable that "considerable error is introduced ... through the neglect of the vapour phase."

2.01 CONCLUSIONS

All saturated boiling correlations published to date are based on the erroneous notion of insignificant latent heat transport.

Correlations based entirely on physical properties of liquid and vapour cannot possibly predict heat fluxes under all conditions. The means available for surface characterization are insufficient to predict the nucleation properties of a surface. Correlations including bubble population terms are steps in the right direction.

Microlayer vaporization into attached bubbles should be of importance in the derivation of bubble growth and frequency predictions. These, in conjunction with nucleation predictions, a relation for bubble diameter at departure and the latent heat transport mechanism, could result in the ideal correlation.

2.10 THE CRITICAL FLUX

As the heat flux is raised during nucleate boiling both surface temperature and bubble population increase. At the critical flux the bubble population has increased to the point of coalescence, the surface, as observed photographically (56) being covered with an irregular, highly unstable vapour film. This hydrodynamic crisis marking the end of the nucleate regime and the beginning of transition boiling represents an operational limit of power level controlled boiling systems.

The limit arises from the following: Inasmuch as the mechanism which yielded high heat transfer rates in the nucleate regime is non-operational in transition boiling, the surface temperature rises if the power level is maintained; the film becomes increasingly more stable and the system proceeds towards film boiling. Stable operation in this region is possible only if (a) a heat transfer rate by combined conduction and radiation through the film, equal to the power input is attained prior to failure of the heating surface by melting, and (b) if the surface temperature corresponding to the temperature difference associated with stable film boiling at the power input level is below the melting point of the surface. In many instances the requirements are not satisfied. The material melts locally. This occurrence is commonly referred to as burnout.

The reason for the intensive attempts at the correlation of the critical flux is highly apparent.

2.11 APPROACHES TO THE CORRELATION OF THE CRITICAL FLUX.

Apart from early, highly empirical or otherwise unsatisfactory correlations (26, 36) all expressions for the critical flux proposed to date have been derived by employing one of the approaches listed below.

(a) A situation of close packed bubbles with adjacent bubbles touching each other on the heating surface is postulated as a burnout criterian. See 2.110.

(b) Dimensional analysis, in conjunction with various equations of motion, energy, heat transfer and boundary conditions, is employed. See 2.111 .

(c) The critical flux is considered to occur when a condition of coalescence of successive bubbles eminating from the same site occurs. See 2.112.

(d) The problem is formulated as one of hydrodynamic instability of a two-phase mixture. See 2.113.

2.110 ROHSENOW AND GRIFFITH'S SQUARE-CLOSE-PACKED BUBBLES MODEL

Rohsenow and Griffith (57) advance a model of square-close-packed bubbles touching each other on the heating surface. Burnout is considered to take place probably before this idealized condition arises, in fact at a bubble population differing from such close packing by a constant factor. The product of this factor and another unknown constant arising from the inclusion of their earlier finding (32) that the heat transferred to the bubbles is proportional to the total flux, was determined from experiment. Their derivation further assumes the product of bubble frequency and diameter at departure as constant for all liquids. This constancy had been observed by Jakob (58) for carbon tetrachloride and water boiling at low fluxes. The final correlation takes the form

$$\frac{(q/A)_c}{\lambda_V \rho_V} = C_1 \left[\frac{\rho_L - \rho_V}{\rho_V} \right]^n \quad \ldots \quad \ldots \quad (2.36)$$

where C_1 and n are experimentally determined constants having values of 143 ft/hr. and 0.6, respectively. The group on the left is a superficial vapour velocity obtained from the considerations of close packing; the group on the right may be considered a buoyancy force per unit mass of vapour. Their relation by a power function was assumed.

Equation (2.36) correlates satisfactorily Braunlich's and Addom's data on water (59, 55) and Cichelli and Bouilla's data for four organic liquids (36).

A theoretical objection to the correlation arises from subsequent investigations (60, 61) indicating that Jokob's relation

$$f.D_d = \text{const.} \quad \ldots \quad \ldots \quad (2.37)$$

does not hold generally, and certainly is in error in the region of the critical flux. The most recent work (62) produces strong theoretical and experimental support for the relation

$$f.D_d^{\frac{1}{2}} = \text{const.} \quad \ldots \quad \ldots \quad (2.38)$$

apparently first suggested by Deissler, as reported (61).

2.111 DIMENSIONAL ANALYSIS - RUSSIAN CORRELATIONS

Inasmuch as the publications advancing the correlations here discussed were not read in the originals, the equations will be presented with little comment. Reviews (61, 63) were consulted.

Apparently it was Kutateladze (64) who first remarked on burnout in terms of instability of two-phase flow. However, he did not apply stability analysis. "Starting from the non-linear Euler equation of motion for the two phases and the heat transfer equation"* he derived the following relation by dimensional analysis

$$\frac{(q/A)_c}{\lambda_V \rho_V^{\frac{1}{2}} [\sigma g(\rho_L - \rho_V)]^{\frac{1}{4}}} = K = \text{const.} \quad \ldots (2.39)$$

The value of K was determined from experiments as 0.16 .

Sherman (65) "utilizing the equation for convective heat transfer with a heat source, an equation describing the transfer of heat due to boiling from the laminar-transition layers to the turbulent core and the dimensionless groups resulting from the equation of motion, obtains, also by means of dimensional analysis, an expression identical to equation (2.39)" **

Borishanskii (66), extending Kutateladze's analysis to include the effects of viscosity, employed dimensional analysis to derive the relation

$$\frac{(q/A)_c}{\lambda_V \rho_V^{\frac{1}{2}} [\sigma g(\rho_L - \rho_V)]^{\frac{1}{4}}} = 0.13 + 4N^{-0.4} \quad \ldots (2.40)$$

where

$$N = \frac{\rho_L \sigma^{3/2}}{\mu_L^2 [\sigma g(\rho_L - \rho_V)]^{\frac{1}{2}}} \quad \ldots (2.41)$$

---

* quoted from (63)

** quoted from (61)

The viscosity thus appears only in the correlation factor N. Its effect is apparently (63) quite small.

The agreement of the above three relationships with experimental data is good, as may be observed from a figure reproduced (67) from Borishanskii's paper.

2.112 COALESCENCE OF SUCCESSIVE BUBBLES

Two correlations have been advanced, postulating the critical flux to occur when the rate at which bubbles rise from a flat horizontal heating surface is just insufficient to keep them clear of their successors.

Deissler, as reported (61) considered the effects of both drag and buoyancy on the rising bubbles; Bragg and Smith (68) considered buoyancy only.

2.1120 DEISSLER'S DRAG-BUOYANCY MODEL

Deissler, equating buoyancy force and drag force on a freely rising vapour bubble, obtained an expression for bubble velocity, u_b, which, in combination with his coalescence criterion

$$f.D_d = u_b \quad \ldots \quad \ldots \quad (2.42)$$

gives an expression for bubble frequency at burn out in terms of bubble diameter, drag coefficient and physical properties. This frequency and the relation of Fritz (34) between bubble diameter and contact angle at break-off were apparently substituted into an equation identical to that used by Rohsenow and Griffith (57) relating the critical flux with the product $f.D_d$. The correlation, as reported, was

$$\frac{(q/A)_c}{\lambda_V \rho_V^{\frac{1}{2}} [\sigma g(\rho_L - \rho_V)]^{\frac{1}{4}}} = C_2 \frac{\beta^{\frac{1}{2}}}{C_D^{\frac{1}{2}}} \quad \ldots \quad (2.43)$$

where C_2 is a constant.

The contact angle was assumed constant for all liquid-solid combinations. The drag coefficient was assumed to be a function of a bubble Reynolds number. Substitution of the above expressions for bubble velocity and diameter into the Reynolds number yielded the relationship

$$X = f\left[\frac{\rho_V^{\frac{1}{2}}\,\sigma^{\frac{3}{4}}}{\mu_V\left[g(\rho_L - \rho_V)\right]^{\frac{1}{4}}}\right] \quad \ldots \quad \ldots \quad (2.44)$$

where X is the left hand side of equation (2.42) and f indicates some function. No significant trend of X with the group in brackets was found. Thus the drag coefficient was considered constant. The final correlation was thus

$$\frac{(q/A)_c}{\lambda_V \rho_V^{\frac{1}{2}}\left[\sigma g(\rho_L - \rho_V)\right]^{\frac{1}{4}}} = K = \text{const.}$$

which is identical with equation (2.39).

The constancy of the drag coefficient with respect to the bubble Reynolds number and the relation

$$f.D_d^{\frac{1}{2}} = \text{const.} \quad \ldots \quad \ldots \quad (2.38)$$

implied in Deissler's analysis, have been verified by Cole (61) by direct measurement; he also showed (61) that Fritz's relation (34) does not apply at the critical flux. The dependence of contact angle upon surface conditions is, of course, well known.

2.1121 BRAGG AND SMITH'S BUOYANCY MODEL

Recently there appeared a rather naive attempt by Bragg and Smith (68) to rederive equation (2.39) and to determine the value of the constant purely analytically, on the basis of a highly simplified model.

In the face of previous experimental evidence to the contrary (61) the drag force on the rising bubble was assumed negligable because of "the small dispatch velocities involved" * . Buoyancy was thus considered to be the sole force acting on a rising bubble, which for some reason was assumed hemispherical. The acceleration, a,

*quoted from the original paper (68)

corresponding to this force was determined. An expression for the bubble diameter at departure, D_d, identical to that of Fritz (34) except for the absence of a contact angle term, was derived, assuming $\beta = 90^{\circ}$. Inasmuch as Fritz's expression, as previously shown (61) is inapplicable at the critical flux, and the contact angle is known to depend upon surface conditions, this step introduces two further errors. At the point of coalescence, the centre of gravity of the preceding hemispherical bubble was considered to have moved upwards a distance $D_d/2$ in the time, t, taken for a new bubble to form. Thus their critical flux criterion takes the form

$$\frac{D_d}{2} = \tfrac{1}{2} a t^2 \quad \ldots \quad \ldots \quad (2.45)$$

Assuming a burnout condition of total vapour coverage of the surface, and the entire flux to be by latent heat transport to attached hemispherical bubbles - an impossible situation - a simple expression for t was obtained. Substitution of the expressions for bubble diameter, acceleration and time of formation of a bubble into equation (2.45) yields, remarkably, the final correlation

$$\frac{(q/A)_c}{\lambda_V \rho_V^{\frac{1}{2}} [\sigma . g . g_c (\rho_L - \rho_V)]^{\frac{1}{4}}} = 0.62 \quad \ldots \quad (2.46)$$

which is of the required form of equation (2.39).

Needless to say, the value of the constant is about four times as large as that observed experimentally.

2.113 HYDRODYNAMIC INSTABILITY - ZUBER'S CORRELATIONS

Following Kutateladze's suggestion (64), Zuber and his co-workers approached the problem of the critical flux from the point of view of hydrodynamic instability of two-phase flow.

2.1130 THE TAYLOR INSTABILITY MODEL

Examining the photographs of Westwater and Santangelo (56), Zuber (63) concluded that no solid-liquid contact exists in transition boiling, the liquid being supported by an irregular vapour blanket.

It seemed promising to approach the critical flux from this region and to characterize it by the breaking down of the vapour blanket.

Experimental evidence pointing to the existence of capillary waves on the interface of a thin film in two-phase flow was noted; in especial the occurrence of ripples in film boiling (56, 69) and the wave shadows noticed by Chang (53) on photographs of nucleate boiling (56). It seemed natural to invesitage transition boiling and its breakdown to the critical flux by considering wave stability.

The effect of viscosity on the waves was neglected. The vapour film thickness was considered small compared with the radius of the cross section of the heating element, thus allowing the use of the plane approximation. The problem was thus formulated as one of instability of a plane vortex sheet separating two inviscid fluids in relative motion, the denser fluid being supported by the less dense fluid, i.e. as a problem in Taylor instability. The classical equations of Helmholtz, Kelvin and Rayleigh (70) were applied, governing the propogation of small disturbances, and the stability of such a vortex sheet oscillating under the influence of surface tension. These, together with an energy balance assuming the interface to break at the nodes and that vapour slugs are approximated by spheres, result in the final correlation

$$\frac{(q/A)_c}{\lambda_V \rho_V^{\frac{1}{2}} [\sigma g(\rho_L - \rho_V)]^{\frac{1}{4}}} = \frac{\pi}{24}\left[\frac{\rho_L + \rho_V}{\rho_L}\right]^{\frac{1}{2}} \quad \ldots \quad (2.47)$$

Except at very high pressures the density ratio term on the right hand side approximates to unity and equation (2.47) reduces to equation (2.39). The agreement between Borishanskii's experimental constant of 0.13 in equation (2.40) and $\frac{\pi}{24}$ (= 0.131) is remarkable.

The relation correlates satisfactorily the data of several investigations (56, 36, 35, 71).

It was subsequently shown by Zuber and Tribus (72) that the constant $\frac{\pi}{24}$ in equation (2.47) is actually an average value having theoretical limits, arising from the wave length spectrum of unstable disturbances, of 0.157 and 0.12 .

Fundamental to the Zuber treatment is the notion of absence of any solid-liquid contact during transition boiling. Hence the nucleation characteristics of the solid heating surface are immaterial, the heat flux being determined entirely by hydrodynamic effects in a region removed from the surface. However, in the light of more recent experimental studies (73, 74), showing strong surface dependence of transition fluxes, it appears highly probable that momentary contacts between liquid and solid do occur. Bankoff and Mehra (75) have, in fact, advanced a "quenching theory" for transition boiling which accommodates these contacts.

Thus the Taylor instability model is probably incompatible with the physical process it is supposed to simulate.

2.1131 THE COMBINED TAYLOR AND HELMHOLTZ INSTABILITY MODEL

More recently Zuber, Tribus and Westwater (67) approached the critical flux from the point of view of combined Taylor and Helmholtz instability of two-phase flow.

The similarity between nucleate boiling and the process of gas bubbling from a porous surface is noted by observing the similarity between the plots of Kurihara and Myers (37) relating the heat flux with temperature difference for various surface roughnesses, with those of Siemes and Borchers (76) relating the superficial gas velocity and the pressure drop across porous plates of various pore sizes. Early remarks pointing out the similarity between burn out in boiling and flooding in bubbling mass transfer systems (26, 77) are noted. These considerations and the similarity between Rohsenow and Griffith's peak flux correlation (57)

$$\frac{(q/A)_c}{\lambda_V \rho_V} = \begin{matrix}\text{superficial}\\ \text{vapour velocity}\\ \text{at burnout}\end{matrix} = C_1\left[\frac{\rho_L - \rho_V}{\rho_V}\right]^{0.6} \quad \ldots \quad (2.36)$$

and Souders and Brown's flodding correlation for bubble-cap columns (78)

$$U_c = \begin{matrix}\text{superficial}\\ \text{vapour velocity}\\ \text{at flooding}\end{matrix} = C\left[\frac{\rho_L - \rho_V}{\rho_V}\right]^{\frac{1}{2}} \quad \ldots \quad (2.48)$$

suggest a flooding model for the critical flux.

As the flux in nucleate boiling is raised, bubble population and bubble frequency increase. At the critical flux the frequency of emission is considered to have increased to the point of coalescence of rising bubbles with their predecessors resulting in the formation of continuous vapour columns. Quoting from the original (67): "The number of vapour columns increases as the flux approaches the critical value. However, the number cannot increase indefinitely. Each new vapour column occupies space formerly occupied by liquid. Like in the flooding phenomenom the discontinuous (vapour) phase and the continuous (liquid) phase compete for the free volume. As the cross section of space available to the liquid becomes smaller and smaller the liquid which must move towards the heating surface moves faster. Thus, we visualize jets of vapour rising from the solid, while between these jets are liquid jets moving in the opposite direction. Because of Helmholtz instability (70, 79) this countercurrent flow of liquid and vapour may become hydrodynamically unstable. The maximum heat flux occurs when the hydrodynamuc crisis arises. At the crisis the relative velocity of the liquid and vapour is as great as it can be; an increase is impossible; it would either cause the vapour to drag the liquid back away from the heating surface or liquid jets to drag vapour back to the heating source".

The problem was thus formulated, again using the plane approximation, as that of finding the value of the critical velocity corresponding to (Helmholtz) instability of a circular vapour jet.

The diameter of this jet was determined from considerations of Taylor instability: An instant was imagined at which the liquid is supported by a blanket of vapour. The two streams will not be permitted to move in opposite directions as described unless the liquid-vapour interface is broken. It was postulated that the interface will tend to break up in a definite pattern corresponding

to a critical wave-length spectrum (70, 79) associated with Taylor instability of the vorter sheet. The diameter of the critical vapour columns was taken to be half this critical wave-length, or range of wave-lengths, corresponding to the points of inflection of the critical two-dimensional disturbance.

Using this diameter, the critical velocity for Helmholtz instability of the circular vapour jet was obtained using classical equations (70, 79). This, together with an energy balance produced the final correlation

$$0.15 \geq \frac{(q/A)_c}{\lambda_V \rho_V^{\frac{1}{2}} [\sigma g(\rho_L - \rho_V)]^{\frac{1}{4}}} \geq 0.12 \quad \ldots \quad (2.49)$$

which is seen to be identical with their earlier relation.

Inasmuch as these equations were derived entirely analytically and correlate data on such diverse media as various organic liquids (56, 36), water (35, 71) and liquid hydrogen (80, 81) see also (41), they are highly impressive. The assumption of absence of liquid-solid contact at the critical flux, basic to their derivation, is, however, open to serious doubt (see 2.1130). As equations (2.39) etc., they are not dimensionally homogeneous in the MLθTFH system of units; g_c, the conversion factor from force to mass units, having been omitted in the group in square brackets.

3.0 INTRODUCTION

This section deals in some detail with the questions of what a nucleation site is, how a surface may be characterized with respect to nucleation and how system variables, in particular pressure, affect the number of nucleation sites on a surface. An explanation of the cessation of nucleation at low pressure (see section 1.2 and Fig. 3.6) is attempted on the basis of published theory or on extension of such theory.

Before dealing with these problems it is appropriate to define some of the terms used in nucleation theory.

3.00 BASIC CONSIDERATIONS AND DEFINITIONS

On the basis of the kinetic theory the superheated liquid from which bubble formation is to take place may be considered to contain some molecules having energies considerably greater than the energy of average molecules. A cluster of molecules having sufficiently high energy may be considered a vapour cluster, this cluster having arisen from collisions of activated molecules with average molecules or other activated molecules. When the number of molecules in the vapour cluster is sufficiently large, the cluster is a vapour bubble. These bubbles are cooler than the liquid bulk, thus the process of bubble formation is, strictly speaking, irreversible.

The superheat constitutes a driving force between liquid and vapour; surface tension tends to crush the tiny bubble and tends to cause its collapse. A nucleus is a tiny vapour bubble that will not collapse but grow spontaneously.

It is possible to formulate the work required to form a vapour embryo of any shape. On the basis of the generally accepted simplifying approximation of reversibility of bubble growth, this work, W, equals the increase in (Gibbs) free energy, ΔF, of the total system. ΔF or W is obtained by considering the chemical potential of vapour and liquid, or PV work, and from the work required to create the liquid-vapour interface. A maximum on the ΔF or W vs. vapour volume curve will represent a situation of metastability and growth beyond this point will be spontaneous. This maximum marks a critical condition.

Consider the simplest possible case, that of nucleation within the liquid bulk (homogeneous nucleation). Westwater (82), among others, has derived the relation between ΔF and the bubble volume, V. On the assumption that vapour embryos are spherical, vapour volume was represented by bubble radius, R. A plot of the function is given in Fig. 3.1 (see overleaf).

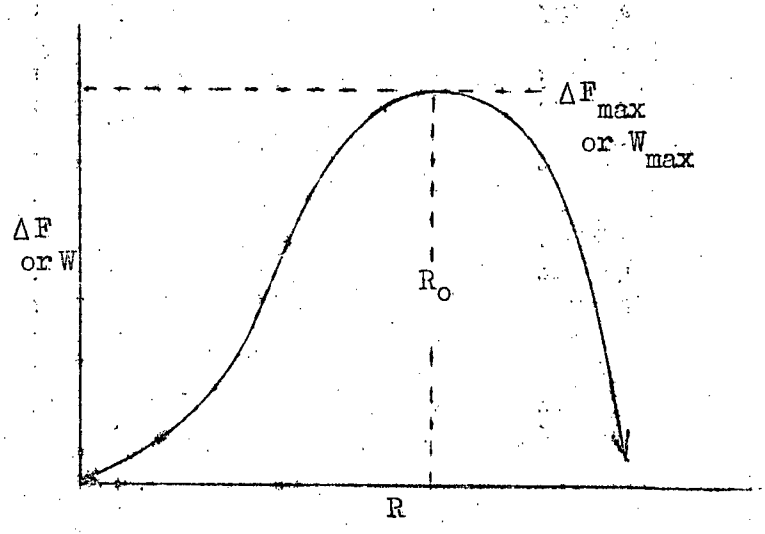

Fig. 3.1 Plot of Work of Formation vs. Radius - Homogeneous Case

The function passes through a maximum. Only bubbles of radius R_o are stable, and only as long as they do not change in radius. The slightest change in size, arising, say, from the loss or gain of one molecule would cause spontaneous collapse or spontaneous growth of the bubble, accompanied by a decrease in free energy and an increase in entropy. A bubble of size R_o is called a nucleus and the radius of the nucleus is called the critical radius. For bubbles to grow to macroscopic size it is thus necessary to exceed the free energy barrier ΔF max i.e. the work barrier W max.

Consider now vapour nucleation from a solid-liquid interface. If the embryo grows from some surface irregularity, say a cavity, it is possible that the W vs V curve has more than one maximum. In this case the highest maximum marks the critical condition and must be exceeded for growth to macroscopic size to occur. The bubble radius of curvature associated with this maximum is now the critical radius.

3.1 THE NATURE OF NUCLEATION SITES

In this subsection the various previously proposed conditions considered conducive to nucleation, and the generally received view that nucleation occurs from a pre-existing vapour phase in steep-walled unwetted cavities are discussed in detail. A controlling nucleation mechanism is proposed. Experimental evidence supporting the adopted model and mechanism will be quoted.

3.10 PREVIOUSLY POSTULATED LIKELY SITES

The physical nature of nucleation sites in boiling has received a thorough examination in the important paper of Bankoff's of 1957 (2). The various possible and previously postulated requirements for vapour nucleation were analysed theoretically and then compared with experimental results.

Homogeneous nucelation and nucelation at a plane surface were considered first. The analysis is here presented to illustrate the method of attack.

Volmer's original expression (83) for the reversible work of formation of a vapour nucleus having the shape of a spherical sector on a plane solid surface (Fig. 3.2) was rederived and corrected. The maximum of this expression,

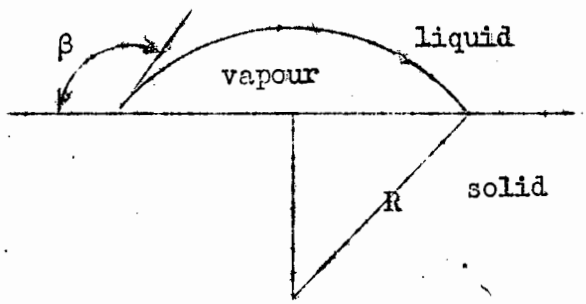

Fig. 3.2 Nucleation on Plane Surface

corresponding to a vapour nucleus of critical size is given in its corrected form, by

$$W_{max} = \frac{16\pi\sigma^3}{3(P_B - P_L)^2} f(\beta) \quad \ldots \quad \ldots \quad (3.1)$$

where $$f(\beta) = \frac{2 + 3\cos\beta - \cos^3\beta}{4} \quad \ldots \quad (3.2)$$

The size of the critical bubble is unknown; hence P_B, the pressure inside this bubble is unknown and equation (3.1) is not directly useful. Resort was made to the work of Fisher (84) who treated nucleation during cavitation. Fisher's analysis is directly applicable to superheated liquids, yielding the expression for the rate of formation of vapour nuclei in a mole of superheated liquid

$$\frac{dN}{dt} = \frac{NkT}{h} \exp\left[- \frac{(\Delta f_o^* + W_{max})}{kT} \right] \quad \ldots \quad (3.3)$$

where N is the Avogadro number, and Δf_o^* is the activation energy for the motion of a liquid molecule past its neighbours into or away from the bubble surface. Fisher has shown its effect to be generally negligable. Equation (3.3) was applied to homogeneous nucleation. For the homogeneous case $f(\beta)$ in equations (3.1) and (3.2) is equal to unity. Further, the term $(P_B - P_L)$ in equation (3.1) was related to the superheat-vapour-pressure difference, ΔP, by means of the Thomson correction

$$(P_B - P_L) = \Delta P \frac{\rho_L - \rho_V}{\rho_L} \quad \ldots \quad (3.4)$$

Hence

$$\frac{dN}{dt} = \frac{NkT}{h} \exp - \left[\frac{16\pi\sigma^3}{3(\Delta P)^2} \left(\frac{\rho_L}{\rho_L - \rho_V} \right)^2 \frac{1}{kT} \right] \quad \ldots \quad (3.5)$$

Fisher (84) has further shown that the fracture pressure for cavitation is very insensitive to the waiting time for the first bubble. On the basis of this property Bankoff selected a value of unity for dN/dt in equation (3.5) and solved for the superheat-vapour-pressure difference

$$\Delta P = \frac{\rho_L}{\rho_L - \rho_V} \left[\frac{16\pi\sigma^3}{3kT \ln(NkT/h)} \right]^{\frac{1}{2}} \quad \ldots \quad (3.6)$$

ΔP in equation (3.6) should approximate the theoretical fracture pressure for the cavitation of liquids, which is "in the neighbourhood of hundreds to thousands of atmospheres".** The highest experimentally observed superheats correspond to ΔP's of only a few atmospheres. Nucleation from the homogeneous liquid does therefore not take place.

Similarly for nucleation at a plane solid surface, the superheat-vapour-pressure difference is given by

$$\Delta P = \frac{\rho_L}{\rho_L - \rho_V} \left[\frac{16\pi\sigma^3 f(\beta)}{3kT \ln(NkT/h)} \right]^{\frac{1}{2}} \quad \ldots \quad (3.7)$$

where $f(\beta)$ is given by equation (3.2). Within the range of observed contact angle, β, the ΔP obtained from equation (3.7) is in excess of experimentally observed ΔP's by some orders of magnitude. Hence nucleation in ebullition does not take place from plane surfaces.

** quoted from (2)

Nucleation from surface projections was considered next. The solid projections were considered to be spherical sectors of radius r_s. An expression for W_{max} identical to equation (3.1) except for a different geometry function was obtained. This geometry function was shown to be of the same order of magnitude as $f(\beta)$ in equations (3.1) and (3.2) for the case of r_s = critical radius of vapour embryo; in fact, for $\beta = 90^{\circ}$ the work to form a nucleus is greater than that required to form a nucleus in the homogeneous liquid. For the cases of r_s tending towards infinity and r_s tending towards zero the work of nucleation tends towards that determined for the previously treated plane surface case. Thus the possibility of nucleation from surface projections may be dismissed.

Nucleation from conical cavities was considered next. For well-wetted (low β) surface-fluid combinations the work required for nucleation was shown to be of the same order of magnitude, irrespective of the depth of the cavity, as the work required to form a nucleus within the liquid bulk.

Before dealing with the all-important case of unwetted cavities, Bankoff's reasoning for the rejection of surface crevices as possible nucleation sites will be given. The cavities are considered to be grooves with a wedge-shaped profile. If the walls are wetted, approximately the same considerations will apply as for wetted cavities. Thus wetted crevices may be dismissed from consideration. If the crevice walls are unwetted, the work required to tear the liquid away from a small area at the apex will be less than for the wetted case; but the resulting vapour phase will have to grow along the entire length of the crevice apex before growing out of the crevice. Hence nucleation will rather take place from unwetted cavities than from unwetted crevices. However, should a well wetted crevice contain a short unwetted section, then the vapour embryo need not extend past the unwetted portion, and the crevice will act as an unwetted cavity. Such a contamination effect is not unlikely.

Up to this point the discussion has been a summary of Bankoff's important paper of 1957 (2).

3.11 STEEP-WALLED UNWETTED CAVITIES

The remarks made so far apply to static determinations of superheat in the absence of any pre-existing gaseous phase. Such considerations are insufficient for the treatment of boiling nucleation from steep-walled, unwetted conical cavities. While Bankoff (2) has indicated, though not strictly quantitatively, that conditions for nucleation in the absence of a pre-existing gaseous phase are more favourable in unwetted cavities than in any other possible site, it appears that during the dynamic process of ebullition such cavities will always contain a vapour phase from which bubbles grow. The postulate that nucleation occurs from a

pre-existing gaseous phase in cavities actually goes back to Fisher (84) and Courty and Foust (3). The first postulation of surface cavities as boiling nucleation sites is, incidentally, due to Andreev who studied cylindrical pores, and dates back to 1945, as reported (85).

Now by considering the unidirectional advance of a liquid front over an irregular surface, Bankoff (86, 87) has derived a quantitative procedure for determining whether a surface cavity of a particular shape and size will entrap gas and vapour or not. For entrapment to occur it is assumed that the liquid front in advancing down one wall of a depression makes contact with the opposite wall before displacing all the gas. The study indicates that unwetted, steep-walled cavities, as are here considered, are highly efficient vapour traps.

Let us initially consider nucleation in the absence of a pre-existing gaseous phase from a steep-walled, unwetted, conical cavity, (Fig. 3.3), of such a size as to let the maximum on the work vs. volume curve, analogous to the homogeneous critical condition, occur while the vapour phase is near the apex of the cavity, i.e. when $R'_o \leq R_c$.

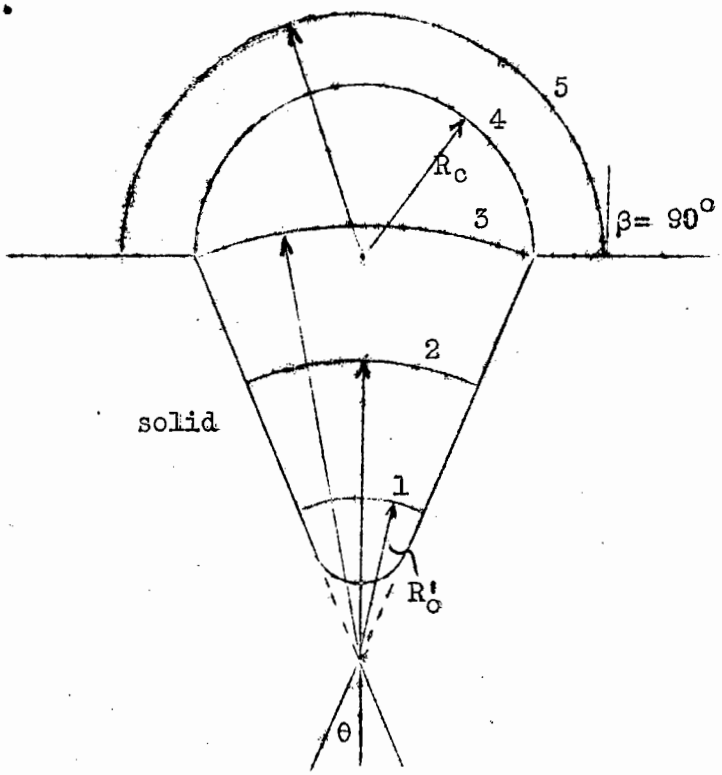

Fig. 3.3 Successive Bubble Profiles - Unwetted Cavity

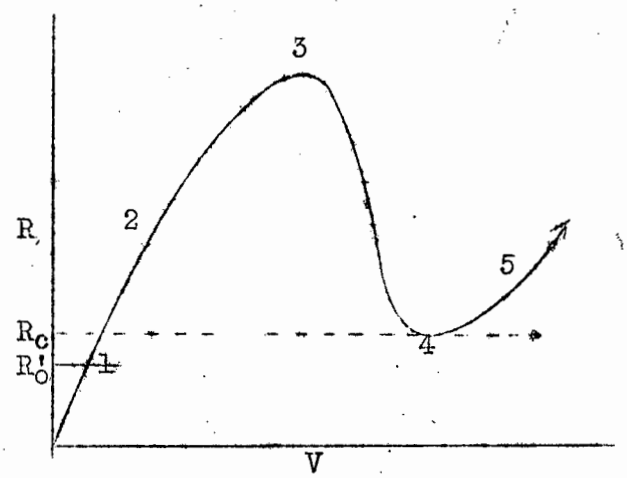

Fig. 3.4 Radius of Curvature vs. Volume - Growth in above Cavity

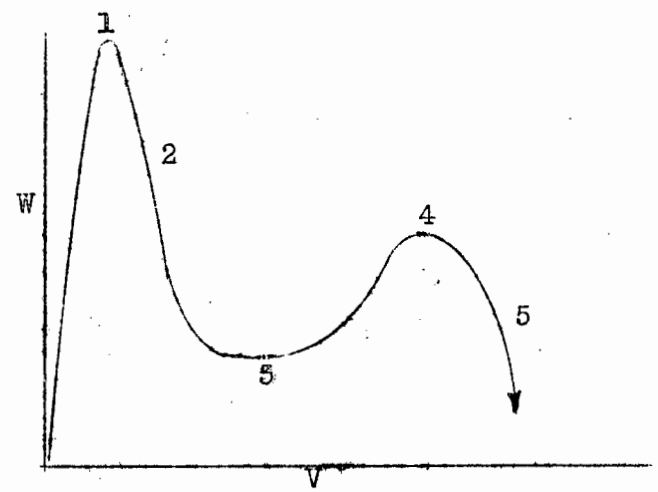

Fig. 3.5 Work vs. Volume - Growth in above Cavity

Let us consider the case of $\beta = 90^{\circ}$; let the cavity mouth radius = r_c. In Fig. 3.5 successive bubble profiles are drawn. An appropriate plot of the variation of radius of curvature with bubble volume is given in Fig. 3.4. It is proposed that the work vs. volume curve is of the shape given in Fig. 3.5.

R'_o (situation 1 in Fig. 3.3) is the radius of curvature, analogous to the homogeneous critical radius R_o, associated with the first maximum on the W vs. V curve. Growth from this point

onwards will be spontaneous until situation 3 is reached. From the arrows in Fig. 3.3 marking radii of curvature of the interface and from Fig. 3.4, it is seen that a sudden reduction in radius of curvature is necessary before a hemispherical vapour cap of radius $R_c = r_c$ can be formed over the cavity mouth, i.e. before situation 4 is realised. Further growth is accompanied by a regular increase in radius of curvature. At this point we recall the Gibbs equation, applicable to a situation of static mechanical equilibrium

$$(P_B - P_L) = \frac{2\sigma}{R} \qquad \ldots \quad \ldots \quad (3.8)$$

where P_B is the pressure inside the bubble, P_L is the bulk liquid pressure, and R is the radius of curvature of an interface which is a segment of a sphere. If we approximate each stage of growth beyond and including R'_o, by an equilibrium situation, it is seen that R'_o, and the minimum on the R vs. V curve (Fig. 3.4), R_c, correspond to situations of maximum $(P_B - P_L)$. An exact equation relating $(P_B - P_L)$ with superheat will be given later. For the present we follow the bulk of investigators by using the approximation

$$(P_B - P_L) \cong \Delta P . \qquad \ldots \quad (3.9)$$

where ΔP is the superheat-vapour-pressure difference. Thus R'_o and R_c correspond to conditions of maximum superheat-vapour-pressure difference and hence superheat. For the case of $R'_o < R_c$, here considered, R'_o requires the higher superheat. This argument qualifies the postulate (Fig. 3.5) that R'_o is associated with the highest maximum on the W vs. V curve. Thus R'_o is the critical radius and controls the superheat necessary for nucleation, if the cavity is originally liquid filled.

From Fig. 3.3 drawn for the case of R'_o being just fractionally smaller than R_c, we note that for steep-walled unwetted cavities of such a size as to let $R'_o < R_c$, R'_o occurs towards the very apex of the cavity. Considerations of vapour entrapment (86. 87) indicate that a vapour volume corresponding to $R \geqslant R'_o$ will be very likely to pre-exist in cavities of this type. In this case the "cap-over-mouth" situation becomes controlling and $R_c = r_c$ is the critical radius and determines the superheat.

For cavities of the same type but of smaller size, such that $R'_o > R_c$ but still occurs inside the cavity, consideration of the Gibbs equation indicates that a higher superheat will be required to form R_c than R'_o. Thus for this case also $R_c = r_c$ is the critical radius and determines the superheat; in this case irrespective of vapour entrapment.

If the cavity is so small as to let R'_o be reached only after the vapour phase has grown out of the cavity, the system approaches the plane surface case, previously dismissed.

It is perhaps here appropriate to point out that whereas the homogeneous critical radius, R_o, is unique for a particular liquid at a particular temperature and pressure, R'_o is not, being in addition dependent upon the surface configuration from which the vapour phase grows and upon the contact angle.

We have till now limited consideration to the case of $\beta = 90^\circ$ and have postulated that for this case the cavity mouth radius, r_c, controls the superheat. It may be shown (5) that this model actually covers a large range of conditions, in that as long as the limitation

$$\theta < \beta < 90^\circ \qquad \ldots \quad \ldots \quad (3.10)$$

applies, the minimum on the R vs. V curve (Fig. 3.4) is constant, and the critical radius equals the cavity mouth radius. Thus for surface-liquid combinations for which equation (3.10) applies, the superheat necessary for the initiation of boiling from a cavity will be determined by the mouth radius of the cavity. If $\beta < \theta$ no minimum will exist in Fig. 3.4; but is $\beta > 90^\circ$ the required superheat will be reduced.

It is proposed in the present study, as in that of Griffith and Wallis (5), to characterize all nucleation during boiling by the formation of a vapour cap of radius R_c over a conical cavity of mouth radius r_c under the conditions given by equation (3.10), i.e. with $R_c = r_c$. It is further proposed that r_c is controlling in the static sense of the Gibbs equation.

The question now arises as to which extent equation (3.10) is representative of actual boiling conditions. As far as θ is concerned we may safely assume that all surfaces will have cavities of various shapes present on them. These will not generally be represented by the macroroughness which is predominantly in the form of grooves arising from the cutting action used in the production of most surface finishes; rather, such cavities will be represented by second-order roughness, formed statistically by the fracture of the solid during cutting. In the case of surfaces formed by sand-casting, anodizing or etching etc., cavities will presumably be present as primary roughness. - Thus one would expect nucleation to occur at lower driving forces on being essentially of the cavity type. This is strikingly confirmed by the experiments of Kerneen, McGraw and Parkin (88) on cavitation from an anodized aluminium surface, and by the boiling runs of Jakob and Fritz (89) who employed a heating surface fitted with square cavities of length, depth and spacing of about 0.25 mm, which required a temperature difference of only about 1°C for the initiation of ebullition of water.

With regard to contact angle, β, it appears (5) - at least for the case of water - that inasmuch as contact angles differ from zero, they are due to contamination. Any surface held in air for any length of time will have $\beta > 0$; no solvent will remove the last traces of contaminant. Water on "clean" and oily stainless steel exhibits contact angles between 30° and 90° at temperatures above 40°C (5). Recent measurements in the M.I.T. Heat Transfer Laboratory (90), and those of Courty and Foust (3) indicate that contact angles for boiling organics from various surfaces generally lie between 40° and 60°.

Thus it appears that the limitations imposed by equation (3.10) may reasonably be obeyed.

While it is generally considered established that boiling nucleation occurs from cavities with a pre-existing gaseous phase, the view supporting the "cap-over-mouth" mechanism as controlling in the static sense of the Gibbs equation, has been questioned. Bankoff in particular (91, 92) has advocated a mechanism based on considerations of the stability of cavities as nucleation sites. His mechanism involves a complex analysis of the relative rates of heating in a cavity and vapour collapse into a cavity. Which of the proposed mechanisms is actually controlling can be determined by the quality of the correlation obtained when experimental results are handled in the manner dictated by the particular mechanism. A comparison (90) of the quality of an equation of Bankoff's based on his mechanism with that of the equation of Griffith and Wallis based on "cap-over-mouth" mechanism as controlling in the sense of the Gibbs equation, establishes the superiority of the latter approach, which is also adopted in the present study.

Some experimental evidence supporting the views advanced in this subsection will now be mentioned.

3.110 EXPERIMENTAL EVIDENCE.

While wellnigh every phenomenon observed in nucleate boiling has been subjected to interpretations based on the model and mechanism proposed in section 3.11, only particularly striking evidence, or such studies which were directed at a particular aspect of the proposals will here be mentioned.

3.1100 CAVITY SITES.

In the important work of Clark, Strenge and Westwater (4) photography during and after nucleate boiling was used to identify active bubble-producing sites. Ether and pentane were tested on vertical surfaces of pure zinc and on an aluminium alloy at atmospheric pressure. Numerous still photographs at magnifications ranging from 160 to 864 and a few electron micrographs at a magnification of 25,000 were taken. These, in addition to motion

pictures having a magnification of 13 on the negative showed that cavities with diameters between 3×10^{-5} and 3×10^{-4} ft. were active nucleation sites. The observations are adequate proof that nucleation does proceed mainly from surface pits or cavities. A few scratches and crevices, as predicted by Bankoff, as well as a mobile speck of unidentified material were also active sites. In no case did bubbles form at grain boundaries. No difference in activity could be observed for the various crystal faces of zinc having different atomic densities.

Trefethen (93) examined nucleation from an extreme case of a smooth surface - from a liquid-liquid interface which has no roughness in the usual sense. A drop of a third liquid, immiscible with the other two, more volatile that the other two, and of intermediate density, was introduced onto the interface. The whole system was heated, or the pressure was reduced. Superheats, considerably higher than those observed in nucleate boiling could be sustained. The process was usually limited not by the nucleation of the superheated drop, but by the saturation temperature of the more volatile of the enclosing liquids. This may be considered as further evidence of the necessity of surface irregularities for boiling nucleation.

The study is in apparent contradiction to that of Gordon, Singh and Weissman (94) who obtained nucleate boiling in the ordinary sense and at typical temperature differences for water, ethanol, and methanol heated on a liquid mercury surface. However, it appears that nucleation proceeded not from the mercury surface, but from extraneous solid sites: "Despite great care a clean liquid-liquid interface could never be achieved during a run. Under a strong light a superficially clean surface would show many very small particles like white dust, most probably glass from the tube" (i.e. from the boiling vessel.) "Presumably these served as nucleation sites". * A micro-photographic study of this system, along the lines of Clark, Strenge and Westwater (4) would be of interest.

3.1101 VAPOUR ENTRAPMENT

As evidence of the occurrence of vapour entrapment the study of Dutkiewicz (6) is here reported. Two liquids exhibiting marked different boiling curves - ethanol and water - were studied on one surface. When the heating surface, after prolonged boiling of ethanol and the determination of its boiling curve, was transferred into water and retested, the boiling curve initially approximated or coincided with the ethanol boiling curve. A similar effect was noted when the ethanol boiling curve was determined after surface pre-treatment with water. In all cases the pre-treatment effects decreased with time and vanished after about six hours of boiling. This implies that the bulk of active cavities contained ethanol vapour at the completion of the first test. While the procedure between tests is not accurately reported and it is unknown whether the heating element was actually wet with ethanol or not at the time of immersion in water, such considerations are immaterial. Obviously the element

* quoted from the original

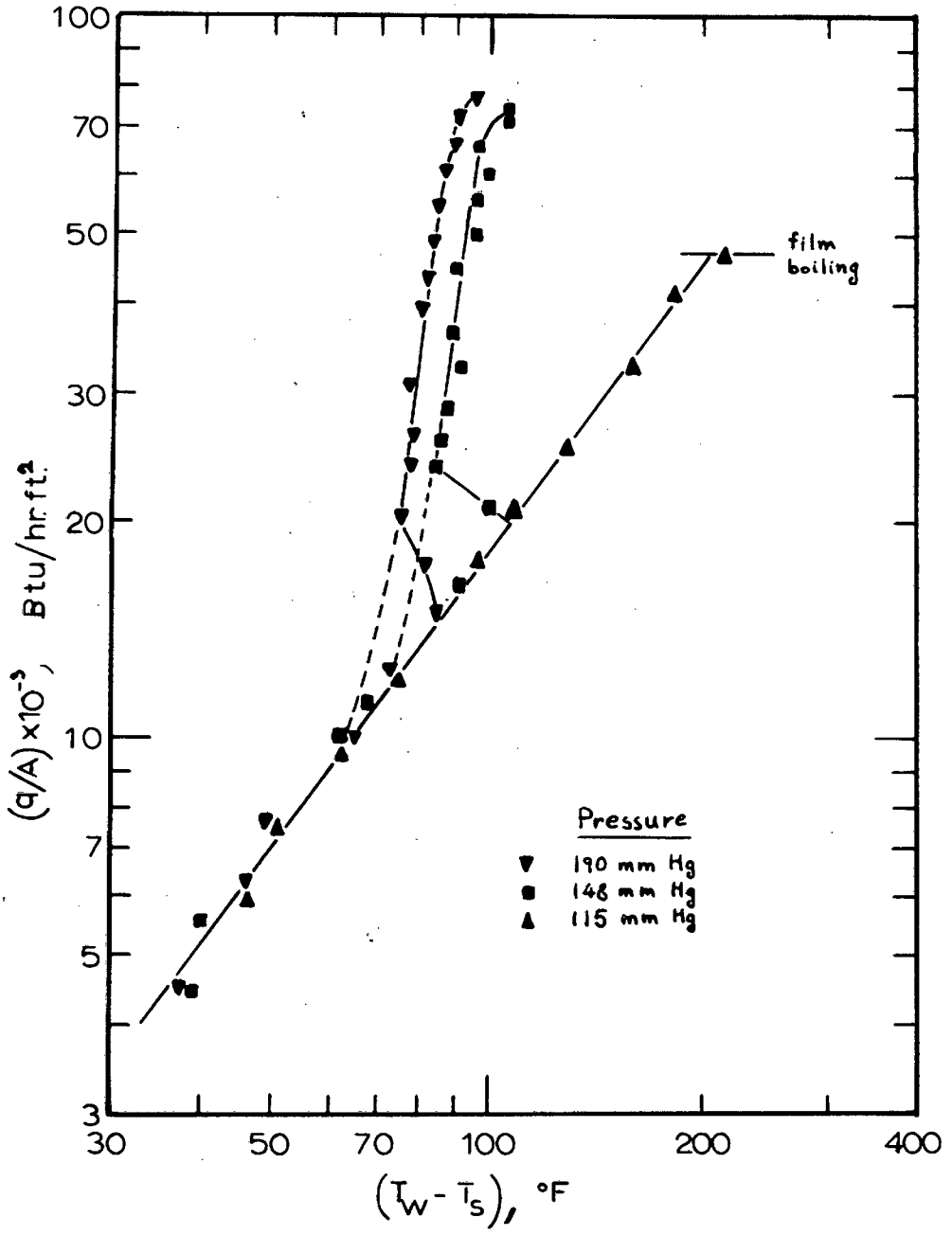

Fig. 3·6 BROMOBENZENE BOILING AT VARIOUS PRESSURES

was not heated to high temperatures between runs. Assuming that the surface was wet with ethanol, it is fairly apparent that at the moment of immersion in water the ethanol present on the "flat" surface was dissolved and affected the bulk liquid properties insubstantially. Such ethanol as was present in cavities, either wholly or partially condensed, would, in the absence of boiling, require considerable time, probably days, to diffuse into the water. Thus as the commencement of ebbulition active cavities predominantly contained ethanol. After bubble formation vapour transport gradually diluted the ethanol vapour with water vapour until finally all ethanol was swept out.

When a fresh heating surface is first immersed in liquid, the cavities can be expected to contain air. Nucleation will initially proceed from these air embryos. After prolonged boiling the air will have been replaced by vapour. If now the liquid is allowed to cool, condensation of the vapour should cause all surface depressions, except those which contain very sharp apeces, to be filled with liquid. The same situation could be realized by prolonged immersion of the fresh heating surface in a cold liquid exhibiting solubility for air. If a boiling test is now commenced with the flux increasing, the surface should remain in natural convection till well past the knee of the boiling curve obtained in stable tests. This temperature overshoot before the surface breaks into nucleate boiling has been observed previously (3, 7) and in the present study. In Fig. 3.6 two preliminary runs exhibiting this effect during the boiling of bromo-benzene from a platinum wire are reported. (The complete cessation of nucleation may be observed in the test conducted at 115 mm Hg; this phenomenon is due to other causes and will be fully discussed later). More extreme cases of the overshoot were observed during the boiling of ethanol and benzene: at low pressures, when the peak flux is low, the nucleate regime could only be obtained by decreasing the flux after the surface had first broken into film boiling. The temperature overshoot before boiling commences may, as indicated above, be attributed to the fact that many potential vapour traps are initially liquid-filled. Once boiling begins these cavities or crevices fill with vapour, most probably by evaporation of their liquid content into a bubble spreading from an adjacent site.

3.1102 THE CONTROLLING MECHANISM.

Griffith and Wallis (5) are the chief proponents of the nucleation mechanism in which a vapour cap of radius r_c, formed over a cavity of mouth radius r_c, dictates the nucleation superheat in the equilibrium sense of the Gibbs equation. Before reporting their experimental work in support of this mechanism, their controlling equation will be given.

For static mechanical equilibrium of the vapour cap of radius r_c the Gibbs equation holds

$$(P_B - P_L) = \frac{2\sigma}{r_c} \quad \ldots \quad \ldots \quad (3.11)$$

The approximation

$$(P_B - P_L) \cong \Delta P \quad \ldots \quad \ldots \quad (3.9)$$

is tacitly applied. Hence

$$\Delta P = \frac{2\sigma}{r_c} \quad \ldots \quad \ldots \quad (3.12)$$

The liquid superheat can be related to ΔP through the Clausius-Clapeyron equation, which in difference form is

$$\frac{\Delta P}{(T_w - T_s)} = \frac{\lambda_V}{T(v_V - v_L)} \quad \ldots \quad (3.13)$$

where v is the specific volume. If ΔP is eliminated between equations (3.12) and (3.13) and if T in equation (3.13) is taken as T_w, then the relation between cavity mouth radius and superheat is obtained:

$$r_c = \frac{2\sigma T_w (v_V - v_L)}{\lambda_V (T_w - T_s) J} \quad \ldots \quad \ldots \quad (3.14)$$

J is the mechanical equivalent of heat and ought to be included if the MLθTΘH engineering system of units is employed.

Equation (3.14) gives the minimum temperature difference necessary for the initiation of ebbilition from a cavity of a given mouth radius; or gives the mouth radius of the smallest cavity which will be active at a given superheat.

This equation was tested by measuring the flux and the wall superheat during the boiling of water from a polished copper surface fitted with about 50 identical steep-walled cavities per sq.inch. The mouth radius was 2.7×10^{-3} in. Cavities were produced by a special punch made of a sharpened gramophone needle placed in a holder having a stop that permitted penetration only to the desired depth. - With this surface one would expect the boiling curve to be vertical. Further, a superheat of $3^{\circ}F$ as obtained from equation (3.14) is expected to produce nucleation. - The boiling curve for a similarly polished surface free from punched cavities was also determined. The curve for the surface with punched cavities showed lower superheats than the curve for the smooth surface. The slope was large, 7 or so, but the line was definitely not vertical. Further, the wall superheat for the surface with artificial cavities was of the order of $20^{\circ}F$ as opposed to the predicted $3^{\circ}F$. The superheat for the smooth surface was about $25^{\circ}F$. - Two possible explanations for these results were suggested: either the mean surface temperature is not the one sensed by the nucleua , or some other mechanism controls nucleation,

and the superheat is determined by properties other than those appearing in equation (3.14).

These possibilities were investigated by two further sets of experiments. In the first, nucleation was studied from a single cavity of known dimensions and at a uniform known temperature. An apparatus was employed which consisted of a glass vessel immersed in an oil bath and connected to a pressure control system. In this vessel a liquid could be maintained at any moderate temperature and at any pressure equal to or less than atmospheric. A surface containing one punched cavity of known geometry was immersed in this liquid. Liquid temperature and pressure were adjusted until boiling from the cavity nearly ceased, and were recorded. The corresponding superheat was calculated from equation (3.14). With experiments performed in this way essentially equilibrium conditions existed in the test vessel. The solid surface which now did not act as a heating element was at the known and uniform bulk liquid temperature. Since the system pressure was varied, variations in all terms of equation (3.14) were obtained, though not independently. Such runs at varying pressure were performed for three cavities of different geometries. In each case recorded superheats were in close agreement with those predicted by equation (3.14). These tests indicate that the theory of bubble nucleation embodied in equation (3.14) is essentially correct and that the specification of a single dimension of length is sufficient to characterize a nucleation site.

In the opinion of Griffith and Wallis (5) these tests further indicate that the discrepancy between observed and predicted superheats in the previous experiments is due to the fact that during the dynamic process of ebullition the surface in the vicinity of a cavity is considerably cooler at the instant of nucleation than the average wall temperature. Now the local rapid surface temperature drops during nucleate boiling, observed by Moore and Mesler (51) - see section 2.002 -, were interpreted to occur during the vaporization of the postulated microlayer after the vapour phase has grown out of and beyond a cavity. The analysis leading to this view appears to be sound and it seems that nucleation occurs when the local surface temperature differs insubstantially from the average surface temperature. However, it must be pointed out that the annular area sensed by the thermocouple of Moore and Mesler was about 30 times as large as the mouth area of the cavities of Griffith and Wallis. This leaves the discrepancy between observed and predicted superheats in the first experiments of Griffith and Wallis without a satisfactory explanation. However, the set of experiments at uniform temperature indicates that the nucleation mechanism embodied in equation (3.14) is essentially correct.

It remained to apply these findings to a real boiling surface containing a range of cavity sizes. Equation (3.14), when applied to a point on a boiling curve, should predict the mouth radius of the smallest cavity active under the conditions of this point. Thus

for a given surface material and method of surface treatment there should be a single value of the number of active cavities, if r_c as obtained from equation (3.14) is the same; that is, if the present mechanism is applicable to real boiling surfaces, then a plot of the active site concentration (N/A) against r_c should be invariant for different fluids boiling at different pressures from essentially identical surfaces. To test this the apparatus used in the first set of experiments was employed again, but in addition the active site concentration was determined photographically. Subcooled boiling runs with water, methanol and ethanol boiling from identically treated copper surfaces were performed. The three liquids yielded quite different (N/A) vs. $(T_w - T_s)$ curves. When (N/A) was plotted against r_c as obtained from equation (3.14) all points fell on the same line approximately. The data of Kurihara and Myers (37) for acetone, hexane, carbon tetrachloride and carbon disulphide boiling from similarly treated surfaces also yielded one line when handled in this manner. Since the fluid properties not appearing in equation (3.14) are different for these liquids it was claimed that they have no influence on nucleation. It was argued that if a mechanism other than the one embodied in equation (3.14) were controlling a correlation of the different liquids would not be possible.

These findings indicate that the "cap-over-mouth" situation is controlling. The superheat necessary for nucleation in a liquid at uniform temperature may be predicted accurately from a relation based upon the Gibbs equation. For the case of a real boiling surface the relation ceases to be quantitative. The nucleation mechanism appears to be the same in both cases.

3.2 AN EQUATION CHARACTERIZING NUCLEATION

An equation relating wall superheat and cavity mouth radius is here presented. It is based upon the nucleation mechanism proposed in Section 3.11. Although very similar to the relation of Griffith and Wallis (5), this equation is both more refined and simpler.

The condition of equilibrium between a bubble and the surrounding liquid at the same temperature is stated by Gibbs (95) as

$$(P_B - P_L) = \sigma\left(\frac{1}{R_1} + \frac{1}{R_2}\right) \qquad \ldots \quad \ldots \quad (3.15)$$

where R_1 and R_2 are the principal radii of curvature of the interface.

This equation is applied to the hemispherical vapour cap

of radius R_c formed over the mouth of a cavity of radius r_c. Thus

$$R_1 = R_2 = R_c = r_c \quad \ldots \quad \ldots \quad (3.16)$$

Equation (3.15) thus reduces to the well-known Gibbs equation given previously

$$(P_B - P_L) = \frac{2\sigma}{r_c} \quad \ldots \quad (3.11)$$

Now $(P_B - P_L)$ differs from ΔP, the superheat-vapour-pressure difference. Their interrelation is given by the Thomson correction (96, 97)

$$(P_B - P_L) = \Delta P \frac{\rho_L - \rho_V}{\rho_L} \quad \ldots \quad (3.4)$$

where the densities are those of liquid and vapour of infinite extent at the prevailing temperature.

The superheat-vapour-pressure difference, ΔP, is related to the superheat, $(T_w - T_s)$, by the Clausius-Clapeyron equation, which in difference form is

$$\frac{\Delta P}{(T_w - T_s)} = \frac{\lambda_V}{T(v_V - v_L)} \quad \ldots \quad (3.13)$$

where T is the absolute temperature.

Combining equations (3.11), (3.4) and (3.13) yields

$$r_c = \frac{2\sigma T \rho_L (v_V - v_L)}{\lambda_V (\rho_L - \rho_V)(T_w - T_s)} \quad \ldots \quad (3.17)$$

It is felt that T ought not, as in the equation of Griffith and Wallis, to be evaluated as the wall temperature. Preliminary calculations on the experimental results of Clark, Strenge and Westwater (4) indicate that the superheat-layer thickness, δ, as obtained very roughly from the relation

$$h\delta = k_L \quad \ldots \quad \ldots \quad (3.18)$$

is of the same order of magnitude as the mouth radius of the cavities which were observed to be active. Thus it seems more appropriate to evaluate T as $(T_w + T_s)/2$. Hence and by simplification

$$r_c = \frac{\sigma(T_w + T_s)v_V}{\lambda_V(T_w - T_s)J} \quad \ldots \quad \ldots \quad (3.19)$$

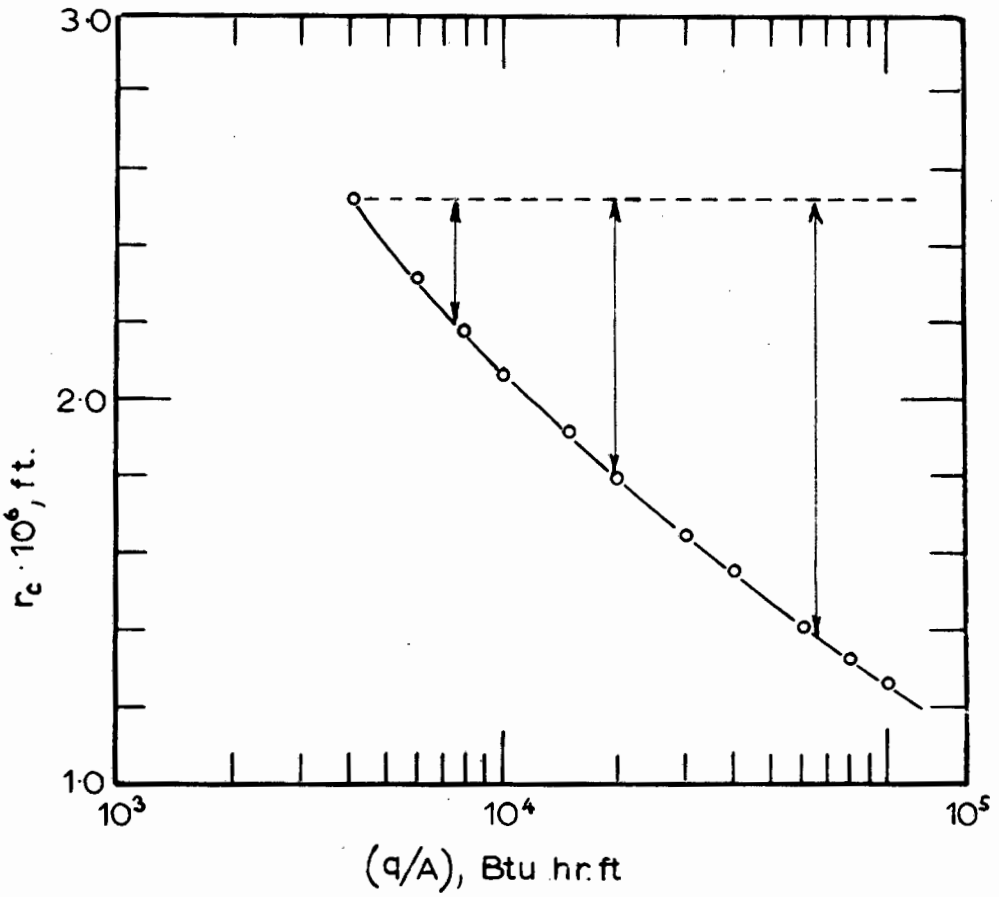

Fig. 3·7 VARIATION OF r_c WITH (q/A)
from data of Dutkiewicz (6),
ethanol boiling from
platinum

of acting as nucleation sites. $r_c = 2.52 \times 10^{-6}$ ft. corresponds to the largest cavity on the surface; this cavity will continue to act as an active site at fluxes above 4200 Btu/hr.ft^2. Thus the size range of active cavities (see arrows Figure 3.7) increases with increasing flux, and the number of bubble-producing sites increases as the integral of the cavity size distribution evaluated between the limits of the range.

3.4 EFFECT OF PRESSURE ON THE NUMBER OF ACTIVE SITES.

The variation of r_c with P_L, the bulk liquid pressure, is now investigated at constant flux. Equation (3.19) is applied to sets of boiling curves of three common liquids boiling under varying pressure. r_c is evaluated at an arbitrarily chosen flux of 60,000 Btu/hr.ft^2. Physical properties (98, 99, 100, 101) are evaluated as saturation values at $(T_w + T_s)/2$. The data which are analysed are those of Cichelli and Bonilla (24), Bonilla and Perry (23) and Mesler and Banchero (102) on ethanol; those of Cichelli and Bonilla, and Mesler and Banchero on benzene; and those of Addoms (29), Braunlich (28), Akin and McAdams (103) (runs W IV - VI), and Micheef (extrapolated from 104)) on water.

On the assumption that during each set of investigations the boiling-surface remained the same (e.g. the wires used by Addoms had similar surface characteristics or the tube of Mesler and Banchero was polished in a similar manner after each run, one would expect a smooth curve to result for the plot of r_c vs P_L for each substance and surface. Such plots are given in Figures 3.8, 3.9 and 3.10. Sets of data fall on separate lines, except for the ethanol data in Figure 3.8 where the best lines through the points of Mesler and Banchero and those of Bonilla and Perry coincide within the range of the scatter. The two surfaces must have had very similar size distributions of cavities.

The important point to note is that in all cases r_c increases as P_L decreases; i.e. as the pressure is lowered at constant flux, the smallest cavity capable of supporting nucelation becomes larger.

If the present theory of nucleation holds, then the largest surface cavity (of mouth radius r_{max}) will be active during nucleation at all pressures. Thus in Figure 3.10 r_{max} = const. for a particular surface may be drawn as a vertical line. The size range of cavities, limited by r_c and r_{max}, is seen to decrease as the pressure decreases at constant flux.

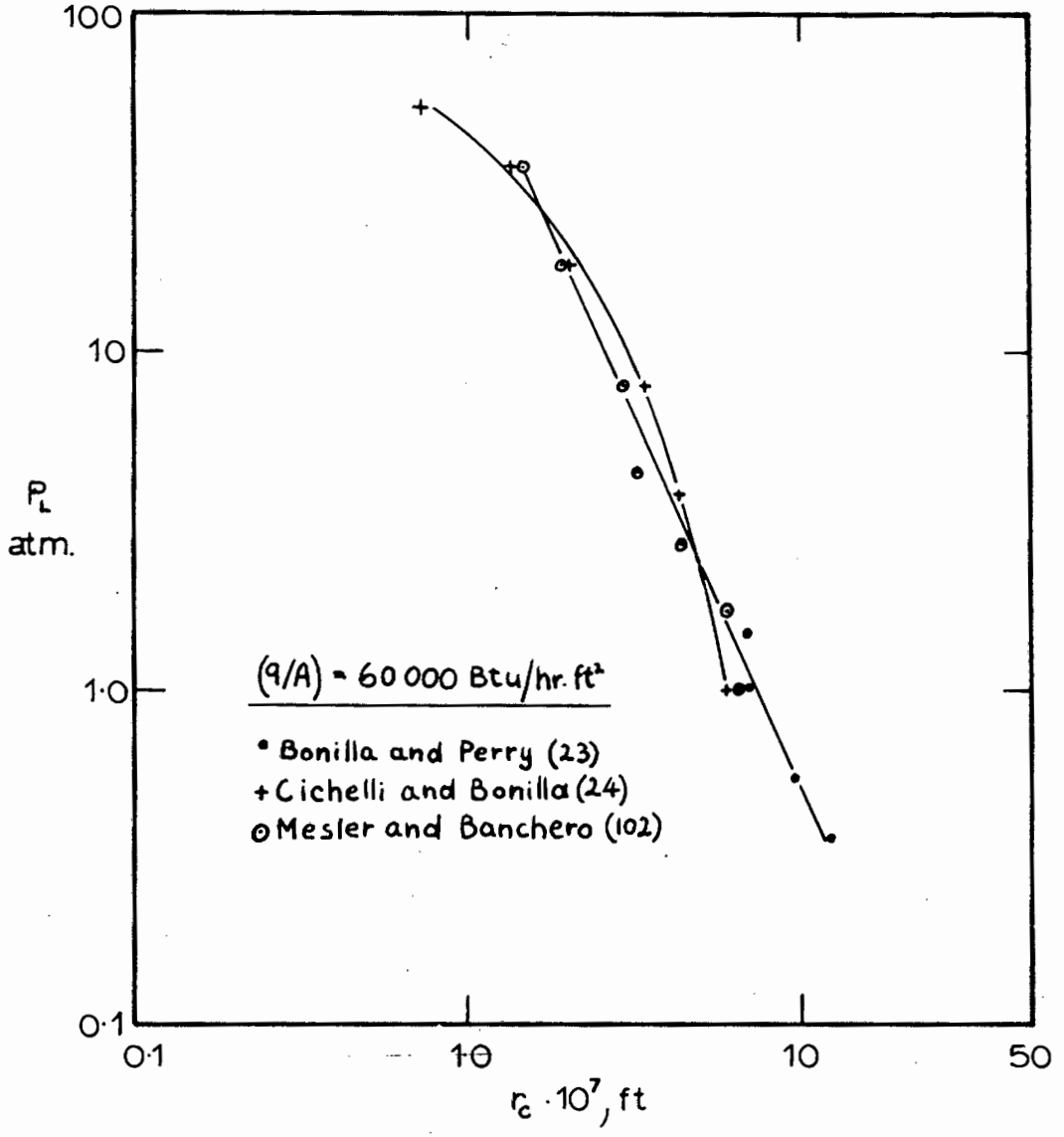

Fig. 3·8 ETHANOL: VARIATION OF r_c WITH P_L AT CONSTANT (q/A)

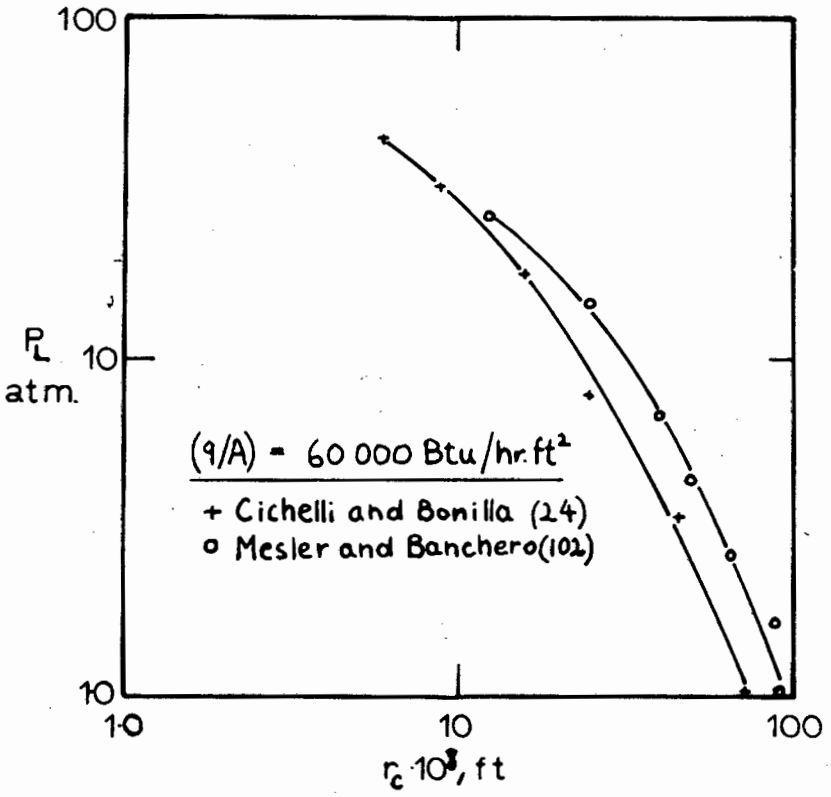

Fig. 39 BENZENE :

VARIATION OF r_c WITH P_L AT CONST. (q/A)

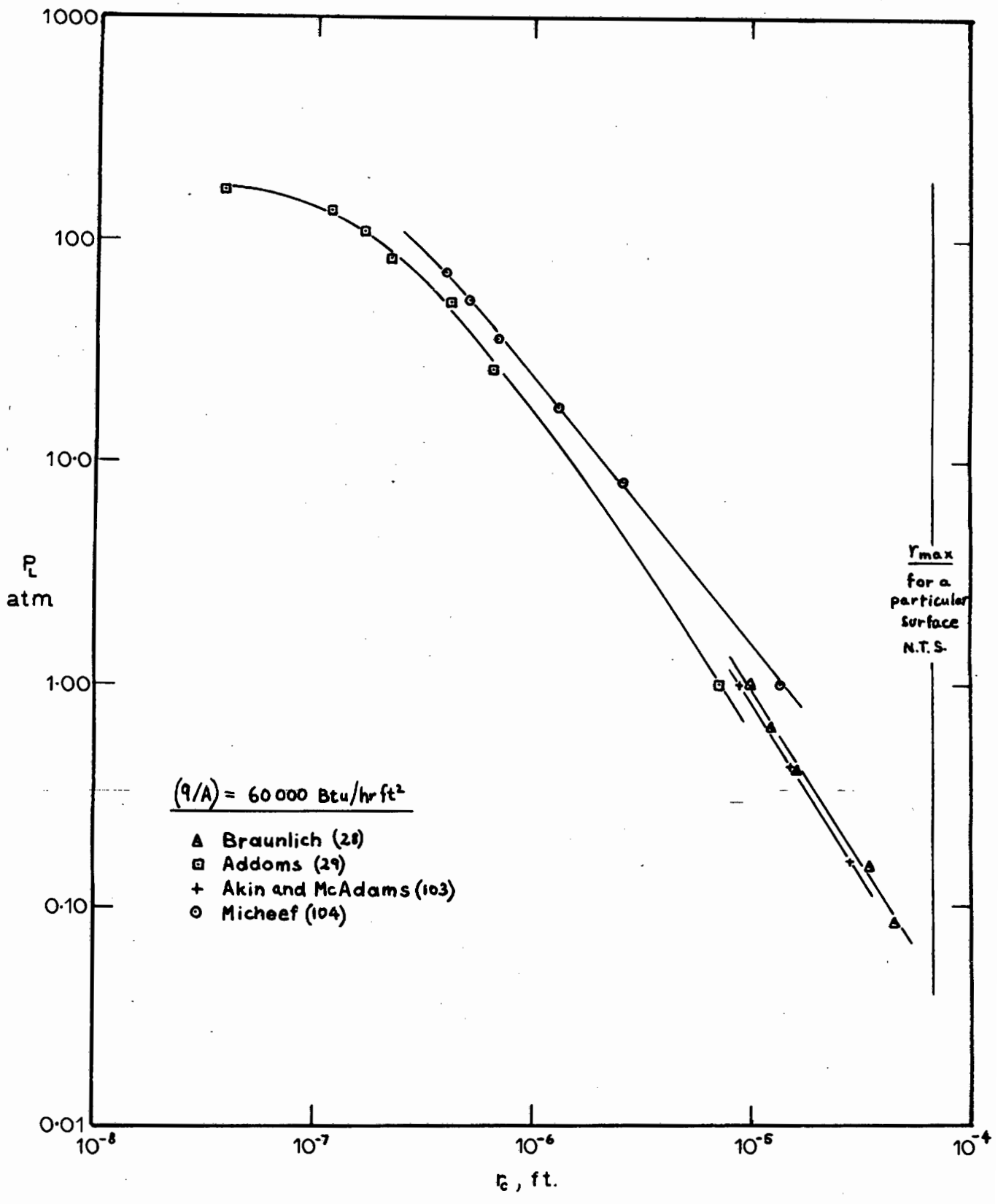

Fig. 3·10 WATER : VARIATION OF r_c WITH P_L AT CONST. (q/A)

3.5 THE CESSATION OF NUCLEATION AT LOW PRESSURE.

When the size range of cavities available for nucleation becomes zero, nucleation ceases. Thus, referring to Fig. 3.9, nucleation will cease at the pressure corresponding to the point of intersection of the r_c curve and the r_{max} line, at the flux for which the r_c curve is drawn. If similar r_c vs. P_L curves are obtained at different fluxes, the resulting family of curves will be of the form of Fig. 3.10.

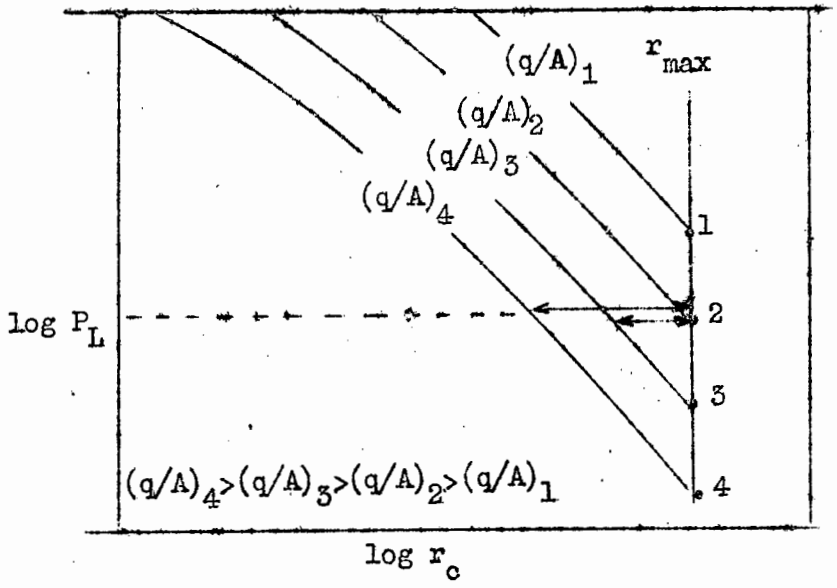

Fig. 3.11 r_c vs P_L curves with Flux as Parameter

Points 1, 2, 3, 4 mark the theoretical cessation of nucleation. It is thus possible to plot (q/A) vs P_L at cessation of nucleation. The resulting plot may be related to the (q/A) vs $(T_w - T_s)$ boiling curves as follows: A particular flux is chosen; the $(T_w - T_s)$ value, satisfying equation (3.19) with $r_c = r_{max}$ and with T_s corresponding to the P_L value read off, is determined by trial and error. If a number of such points are determined, then the theoretical cessation of nucleation curve may be plotted on the same diagram as the boiling curves. Below this curve nucleation by the present mechanism ceases. At low pressures, this curve is expected to lie above the natural convection curves; if it does not, then the analysis is trivial and no cessation of nucleation, other than the normally occurring one when the boiling curve smoothly meets the natural convection curve, is predicted. When the cessation of nucleation curve does lie above the natural convection curves, it should theoretically be possible, during the determination of a boiling curve at some low pressure, to obtain nucleation at high flux and no nucleation at some lower flux,

this lower flux being greater than the natural convection flux corresponding to the existing $(T_w - T_s)$ and P_L; i.e. nucleation should cease "in the middle of a boiling curve". The effect may also be noted in Fig. 3.11: During operation at a particular pressure, a large size range of cavities (top arrow) is available at a flux of $(q/A)_4$; the range is lower at $(q/A)_3$, and zero at $(q/A)_2$.

3.50 THE NEED FOR EXPERIMENTAL WORK

No suitable published data exist which allow this analysis to be carried out. While several sets of boiling curves for a particular liquid boiling from the same surface under subatmospheric pressures have been published (23, 28, 103), the curves were not continued down into the natural convection regime. r_{max} can only be determined by application of equation (3.19) to the points where the last bubble disappears, flux decreasing.

In the following section a number of low-pressure boiling runs are reported, which were determined with particular attention to the point of disappearance of the last bubble, and with a view to obtaining evidence of the cessation of nucleation in the middle of a boiling curve.

SECTION 4 EXPERIMENTAL WORK.

4.0 BOILING RUNS

Two highly pure (A.R.grade) organic liquids of different type, ethanol and benzene, were studied. Each liquid was tested at five pressures ranging from 1.0 to approximately 0.1 atm., the liquid bulk being maintained at the saturation temperature corresponding to the pressure, and under essentially stagnant pool conditions. An electrically heated platinum wire served as heating surface. Details of the apparatus are given in Appendix I. The same wire was used in all ten tests. The relation between flux, (q/A), and wall superheat, $(T_w - T_s)$, was established, great care being taken to avoid the well-known "hysteresis effects" (5, 10). Prior to measurements, both the heating surface and the test liquid were thoroughly degassed. Wire pretreatment and test procedure were standardized so as to yield reproducible results; details are given in Appendix II. Whenever possible the number of active bubble-producing sites were counted visually.

The method of computation of the flux and the temperature difference from electrical measurements is given in Appendix III. An estimate of the experimental error is reported in Appendix IV

4.00 RESULTS

Results are tabulated in Appendix V and are plotted below.

In Fig. 4.1 flux is plotted against wall superheat for runs with ethanol at various pressures. Runs E.1 to E.5 were performed at successively lower system pressure.

During run E.1 at 1.0 atm, run E.2 at 0.677 atm and at higher fluxes during run E.3 at 0.396 atm the well-known boiling curves are traced.

At lower fluxes run E.3 exhibits a highly unusual change in direction. It was immediately suspected that this behaviour is associated with the cessation of the postulated nucleation mechanism. Inspection of Fig. 4.2, in which the number of active sites on the test section, N, is plotted against flux, shows that no dramatic change in the active site concentration occurred at this point. However, nucleation seemed to become unstable: bubbles no longer eminated from the same source in column formation, but appeared to be formed at points shifting on the surface. This effect was particularly noticeable in run E.4 at 0.294 atm where the bubble-producing sites jumped around on the surface in a rapid and apparently random manner. A curve of the shape of run E.3 has been obtained by van Straten (105) for the boiling of a solution of whey in water at 0.132 atm pressure. Boiling as in run E.4 has not hitherto been reported.

The phenomena of runs E.3 and E.4 cannot be attributed to "hysteresis effects" (3,10) or to the temperature overshoot discussed in Section 3.1101, since (a) runs were performed with decreasing flux, (b) the procedure in obtaining runs E.3 and E.4 was identical to that adopted for the stable runs E.1 and E.2, and (c) the behaviour did not die away with time; in fact, on one occasion during operation in the unstable region the flux was maintained at the same setting for over an hour, but the bubble pattern remained irregular; previously, at higher flux, no irregularity was observed.

Run E.5 at 0.136 atm illustrates the complete cessation of nucleation, reported earlier. At a flux slightly higher than that of the last point recorded the surface burst into film boiling. The nucleate regime was entirely absent.

Run E.6 at 1.0 atm is a check on reproducibility. The points are observed to lie nearly perfectly on the previously determined E.1 curve.

The natural convection curve appears to be insensitive to changes in bulk temperature and system pressure within the range of operation.

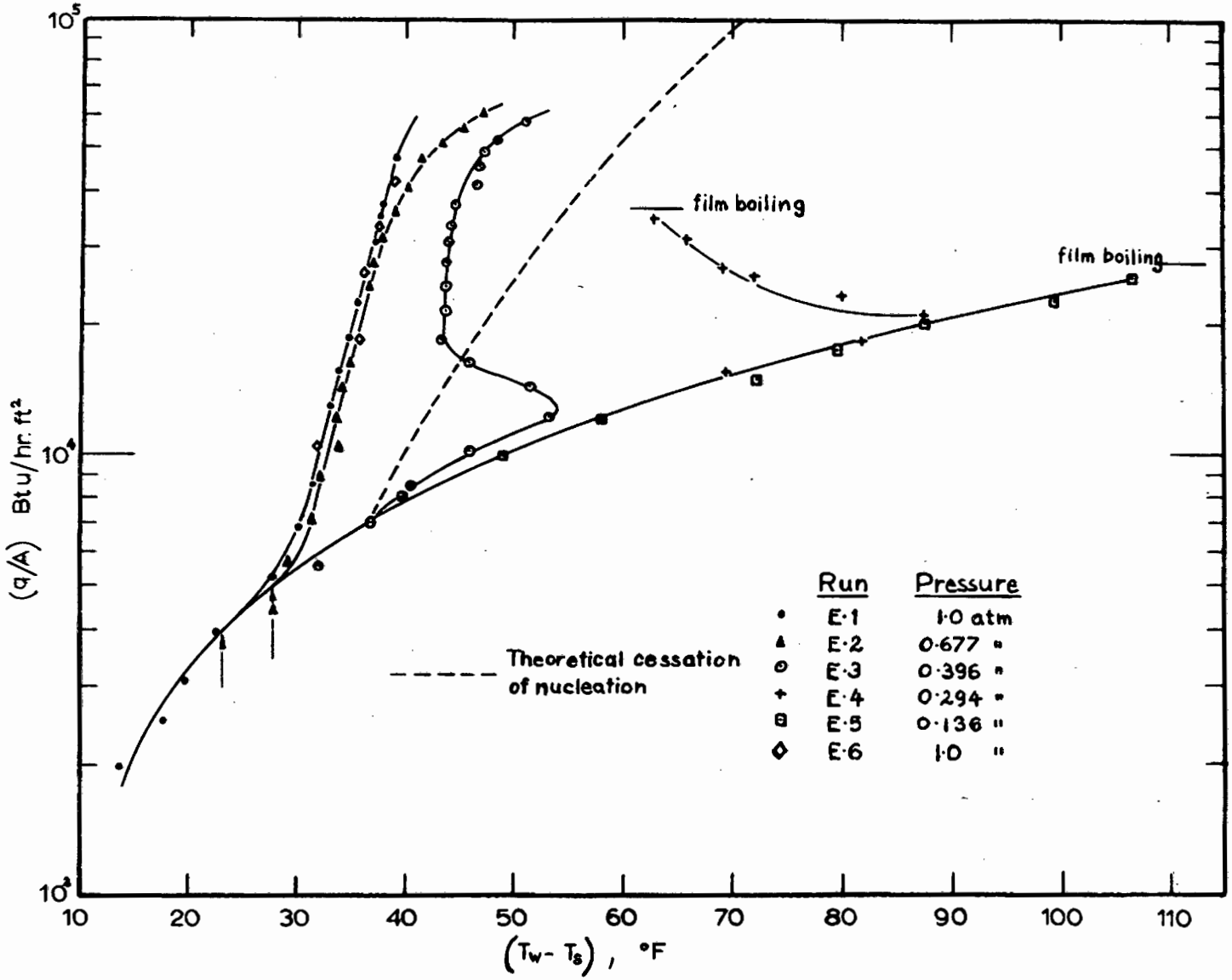

Fig. 4·1 BOILING CURVES FOR ETHANOL AT LOW PRESSURES

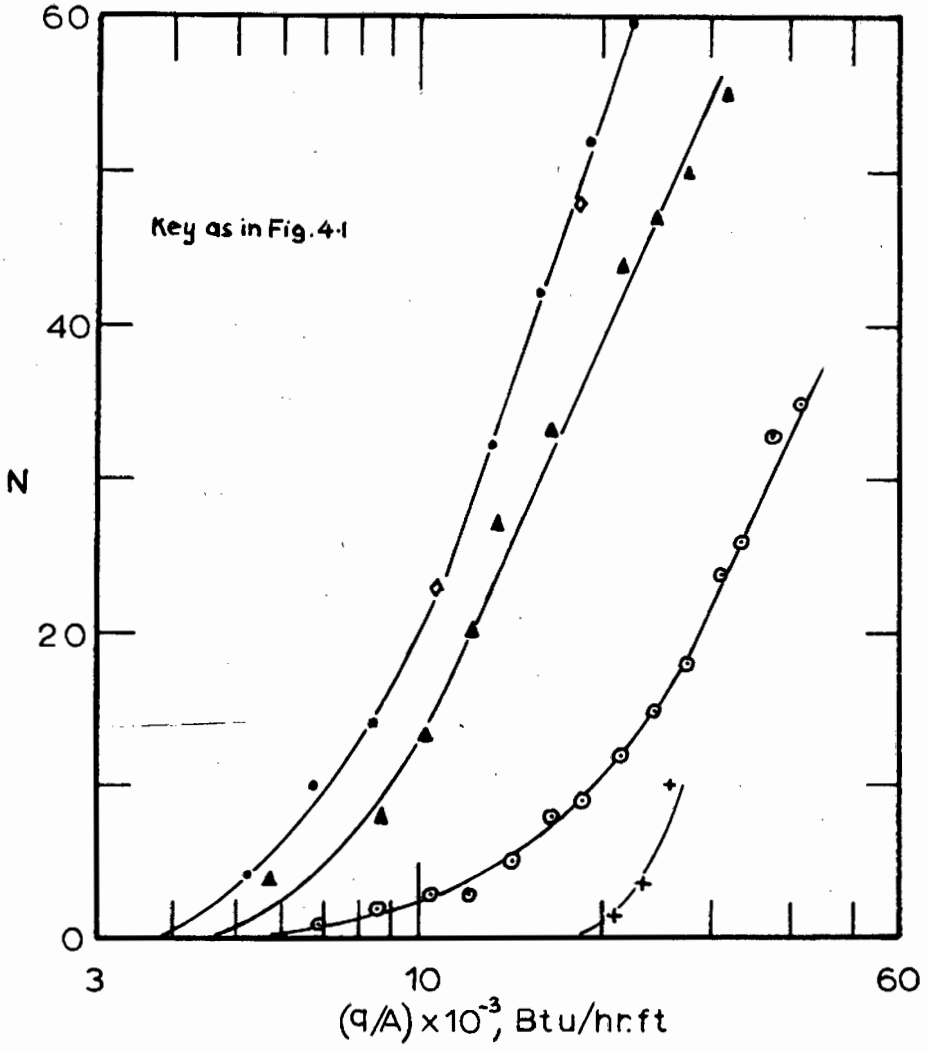

Fig. 4·2 ETHANOL: NUMBER OF ACTIVE SITES ON TEST SECTION

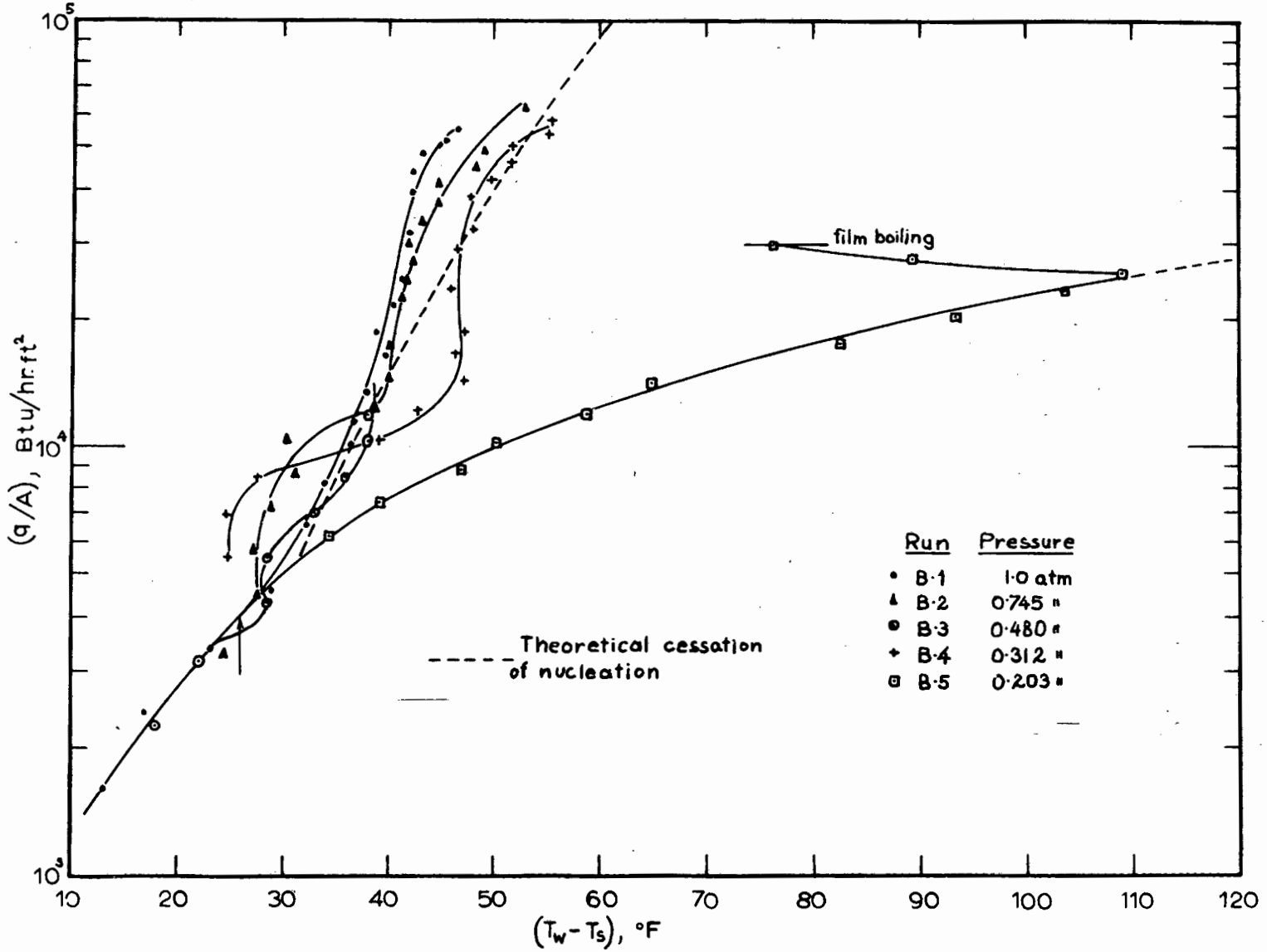

Fig. 43 BOILING CURVES FOR BENZENE AT LOW PRESSURES

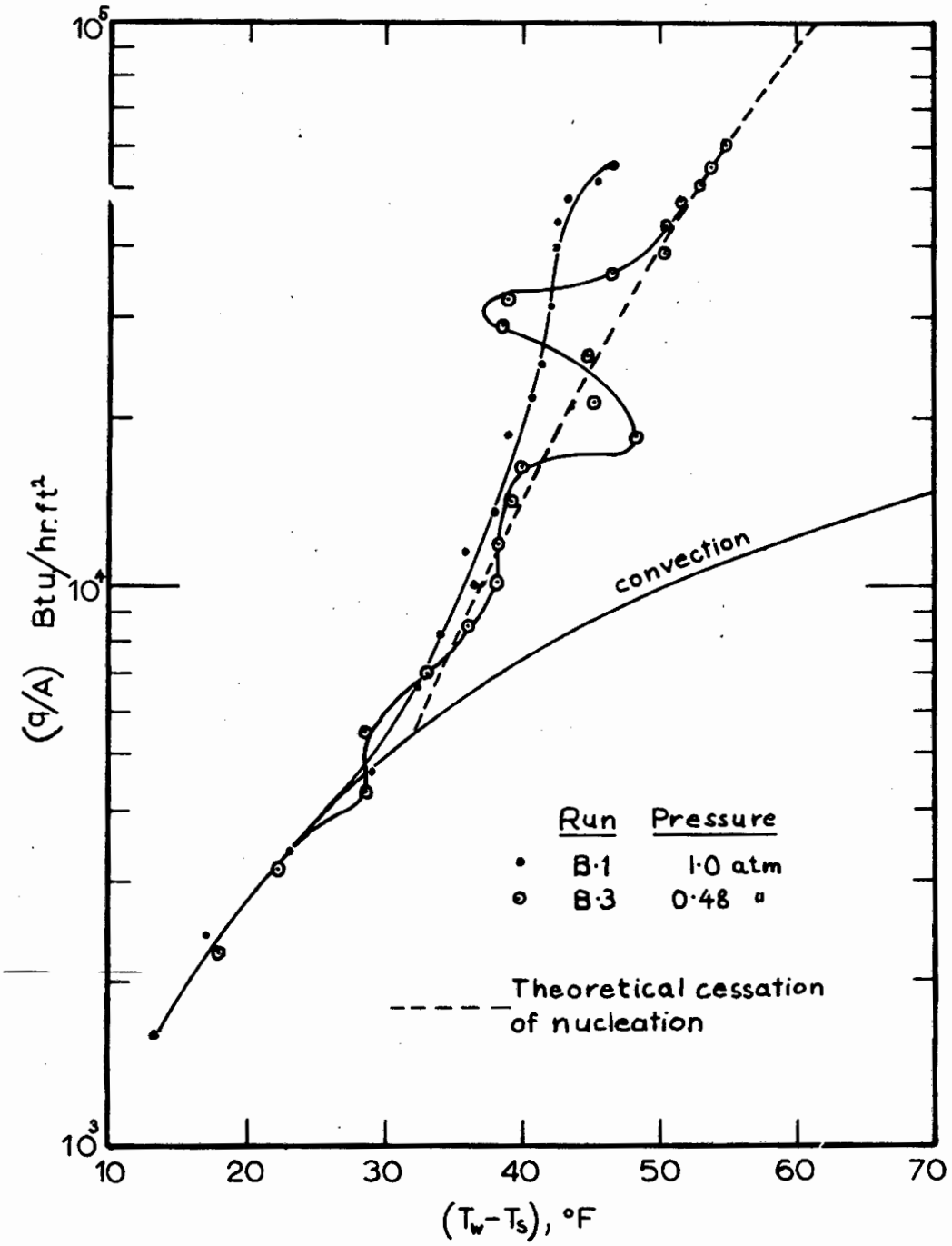

Fig. 4·4 BOILING CURVES FOR BENZENE

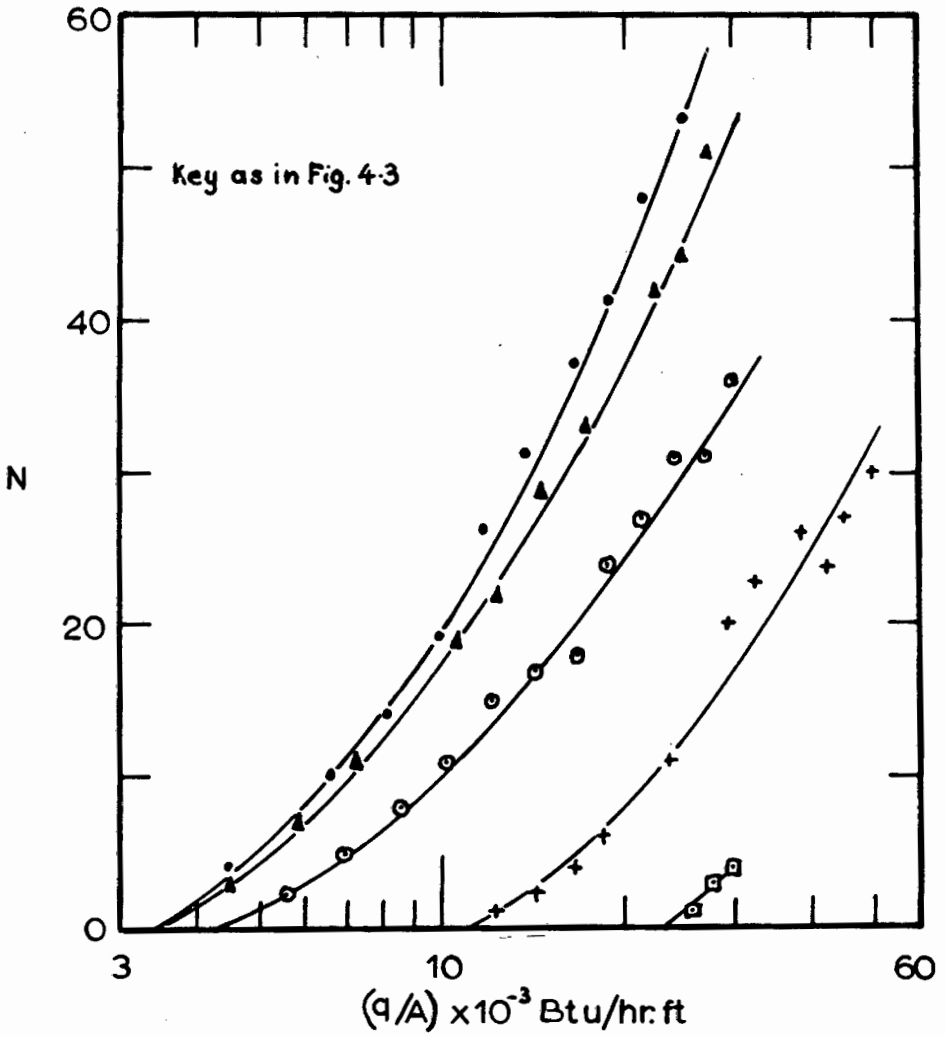

Fig. 4·5 BENZENE : NUMBER OF ACTIVE SITES ON TEST SECTION

Similar tests were performed for benzene. Boiling curves are plotted in Figs. 4.3 and 4.4. Only during run B.1 at atmospheric pressure, and possible in the high flux region of run B.2 at 0.745 atm was stable operation obtained. At intermediate pressures (run B.3 at 0.480 atm and run B.4 at 0.312 atm) and in the low flux region of run B.2, boiling curves exhibit wavy patterns hitherto unreported. The curve of run E.5 at 0.203 atm is of the same shape as run E.4 for ethanol. To avoid confusion of the diagram the entire boiling curve for run B.3 is not plotted on Fig. 4.3. Fig. 4.4 shows the whole curve together with the stable atmospheric curve.

Due to the rapid shifting of active sites the N vs. (q/A) curves shown in Fig. 4.5 are, with the exception of the data at 1.0 atm, highly unreliable.

The earlier remarks as to the inexplicability of these phenomena in terms of hysteresis effects and temperature overshoots are equally applicable to the benzene data.

An analysis of these results along the lines suggested in Section 3.5 is presented in Section 5.

4.1 PHOTOMICROGRAPHIC EXAMINATION OF HEATING SURFACE.

It was considered of interest to examine the surface of the wire employed in the tests under high magnification.

After careful cleaning and drying the test wire was photographed through a microscope employing oblique phase-contrast lighting. Details of the apparatus and the technique are listed in Appendix VI.

Figures 4.6 and 4.7 show two portions of the test surface under a magnification of approximately 400 X. Due to the curvature of the surface only the central portion of the wire is in focus.

It may be observed that the primary roughness is in the form of longtitundinal grooves; these arise from the drawing process employed in the production of the wire.

The second-order roughness is predominantly in the shape of pits, cavities and depressions ranging in diameter from roughly 10^{-5} to 10^{-7} ft. These irregularities are considered to have arisen from the fracture of the metal during drawing.

Fig. 4.6 SURFACE OF HEATING WIRE, MAGNIFIED APPROX. 400 X

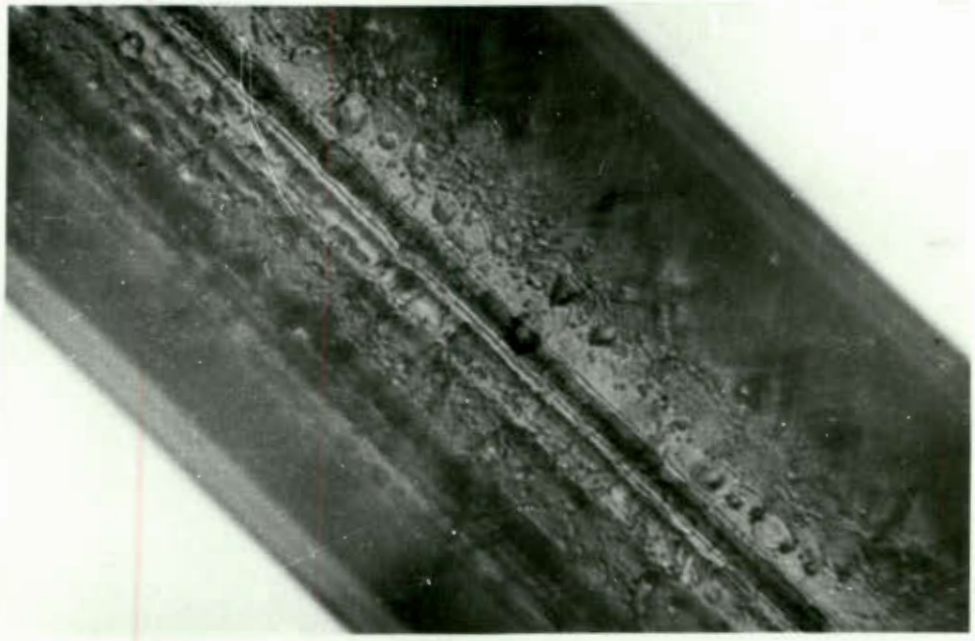

Fig. 4.7 SURFACE OF HEATING WIRE, MAGNIFIED APPROX. 400 X

SECTION 5 ANALYSIS OF RESULTS AND DISCUSSION

The experimental results are now analysed in the manner outlined in Section 3.5 .

5.0 THE MAXIMUM CAVITY SIZE

It is recalled that application of equation (3.19) to the point on a boiling curve where the last bubble just disappears, should give r_{max} i.e. the mouth radius of the largest cavity present on the surface. For a particular surface r_{max}, thus determined, should be independent of pressure and type of liquid. To check this equation (3.19) is applied to the points of disappearance of the last bubble (points marked by vertical arrows in Figs. 4.1 and 4.3) in the three stable runs E.1, E.2 and B.1. Results are listed in Table 5.1

Table 5.1. Calculated r_{max} for surface employed in Present Study

Run	Liquid	P_L atm.	r_{max} ft.
E.1	ethanol	1.0	2.66×10^{-6}
E.2	ethanol	0.677	2.12×10^{-6}
B.1	benzene	1.0	2.53×10^{-6}

For the stable runs the calculated r_{max} is seen to be reasonably constant, as predicted. Unstable runs, with the exception of run E.3 of $r_{max} = 2.46 \times 10^{-6}$ ft., give widely varying and different values of r_{max} . This suggests that the nucleation mechanism embodied in equation (3.19) is correct and applicable during normal boiling. At lower pressures during the unstable boiling runs the mechanism appears to be inoperative. This will be further investigated in Section 5.1.

The few determinations of r_{max} in Table 5.1 are due to the limited subatmospheric pressure range in which stable boiling was obtainable. To offer further evidence of the constancy of r_{max}, as calculated from equation (3.19), the analysis is applied to the data of van Stralen (21) on the low-pressure boiling of water. Unfortunately these runs were not all conducted from one and the same wire; however the wires were of the same type. Results are listed in Table 5.2.

Table 5.2 Calculated r_{max} for data of van Stralen (21)

Run	Liquid	Wire No.	P_L atm.	r_{max} ft.
1	water	1	1.0	(1.17×10^{-5})
2	"	3	1.0	6.84×10^{-6}
3	"	2	0.553	5.76×10^{-6}
4	"	2	0.263	6.41×10^{-6}

It is again seen that, with the exception of Run 1, r_{max} is reasonably constant. Runs 1 and 2 were intended as checks on r_{max} reproducibility; since the points for the two tests do not coincide it is concluded that surface conditions were dissimilar; this would account for the different value of r_{max} in Run 1.

No other data ar various pressures are available to check the constancy of r_{max} ; most investigators did not continue boiling curves down into the natural convection ragion; in the study of Farber and Scorah (109) where the entire curves are presented, the number of active sites are not reported and it is impossible to say which points on their curves correspond to the commencement (or dying away) of ebullition.

For the surface used in the present study r_{max} is taken as the mean of the values in Table 5.1, i.e. as 2.44×10^{-6} ft.

5.1 THE LOW-PRESSURE CESSATION OF NUCLEATION (ANALYSIS)

With a value of r_{max} of 2.44×10^{-6} ft. the analysis outlined in Section 3.5 is now carried out.

As indicated in Fig. 3.11, Figs. 5.1 and 5.2 give r_c vs. P_L curves at different fluxes for the boiling of ethanol and benzene. Only the stable regions of operation (Runs E.1, E.2 and B.1, and the high-flux portions of Runs E.3 and B.2) are analysed. * $r_{max} = 2.44 \times 10^{-6}$ ft. is drawn in. It is recalled that the points of intersection of the r_c curves with the r_{max} line mark the points where, according to the proposed mechanism, the size range of cavities available for nucleation becomes zero, i.e. where nucleation should theoretically cease. In Fig. 5.3 (q/A) vs. P_L is plotted for these points of intersection, i.e. Fig. 5.3 gives the theoretical cessation-of-nucleation lines for ethanol and benzene boiling on the surface employed in the present study; that is, it gives the flux at which nucleation just ceases from the largest cavity ($r_c = 2.44 \times 10^{-6}$ ft.) on the surface, as a function of system pressure.

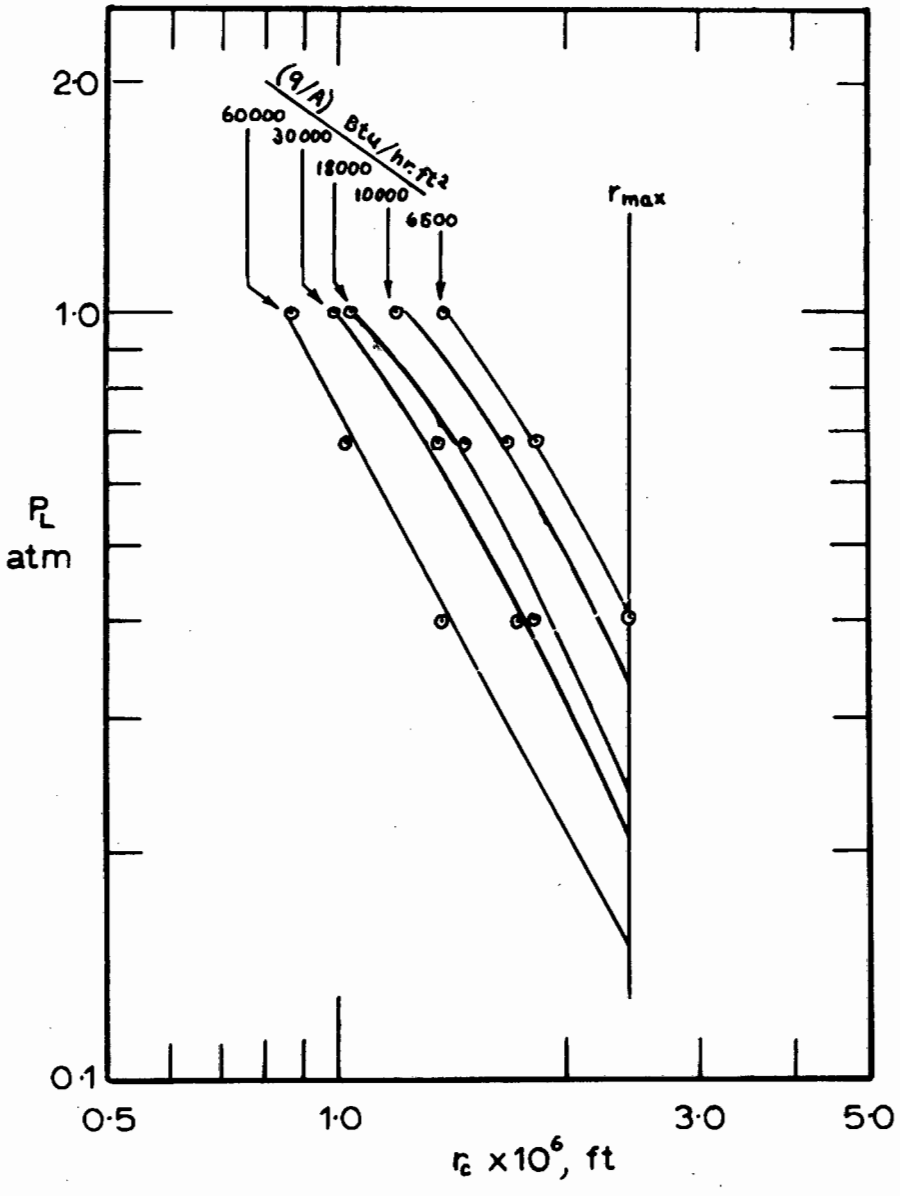

Fig. 5·1 ETHANOL : r_c vs. P_L AT VARIOUS FLUXES

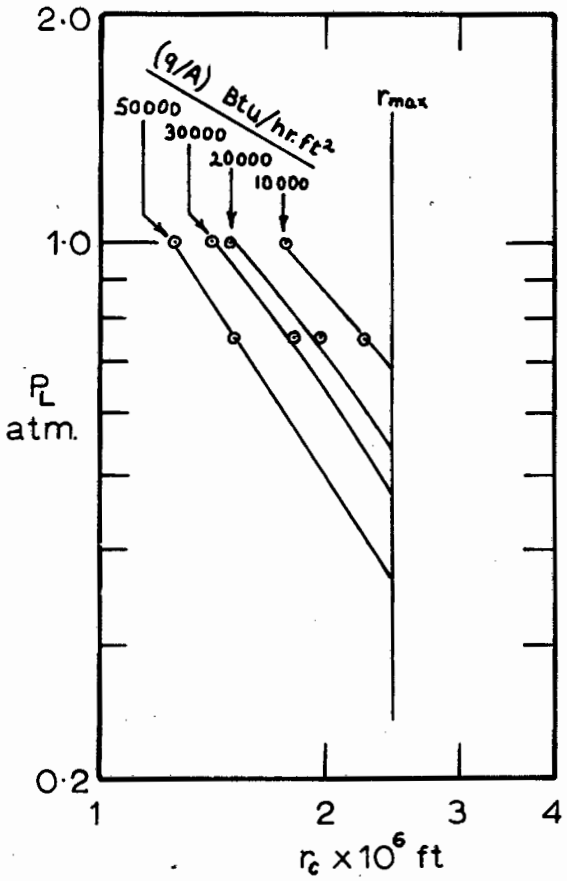

Fig. 5·2 BENZENE : r_c vs. P_L AT VARIOUS FLUXES

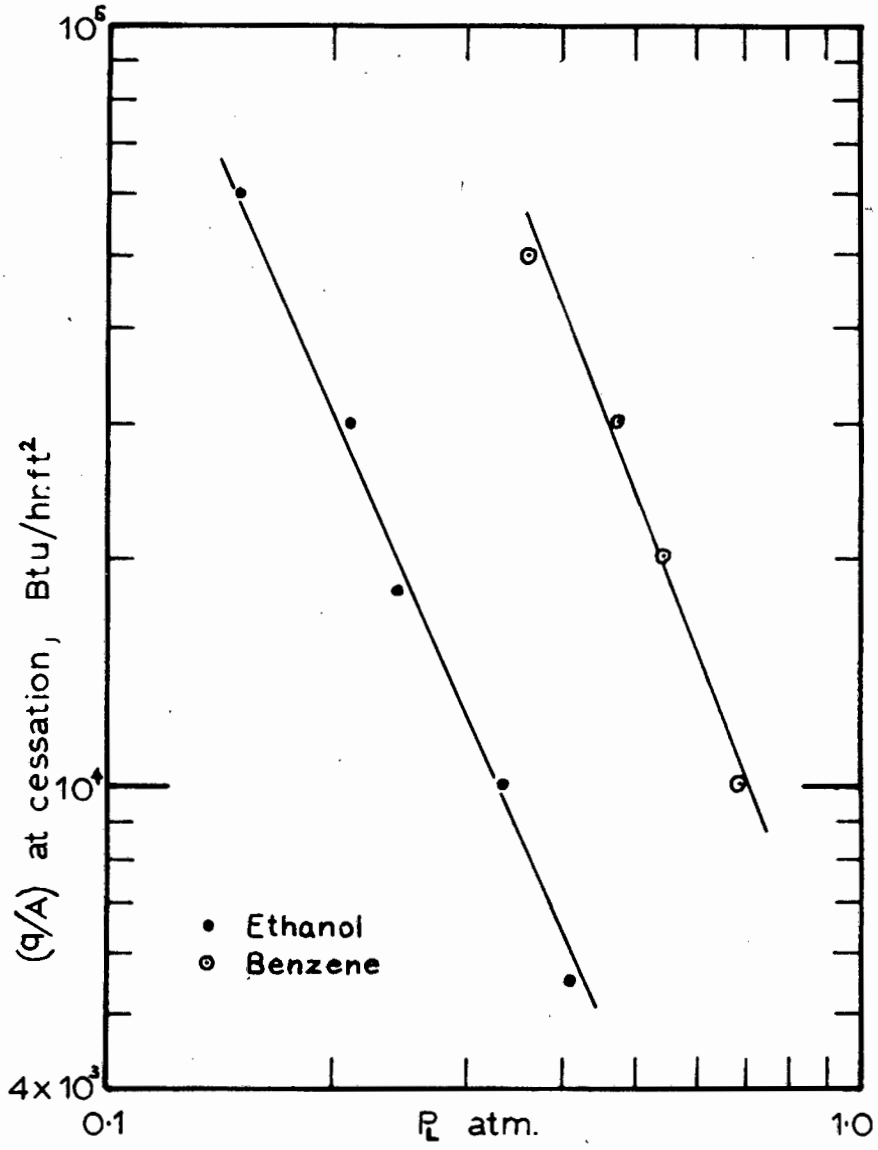

Fig. 5·3 (q/A) vs. P_L AT CESSATION OF NUCLEATION

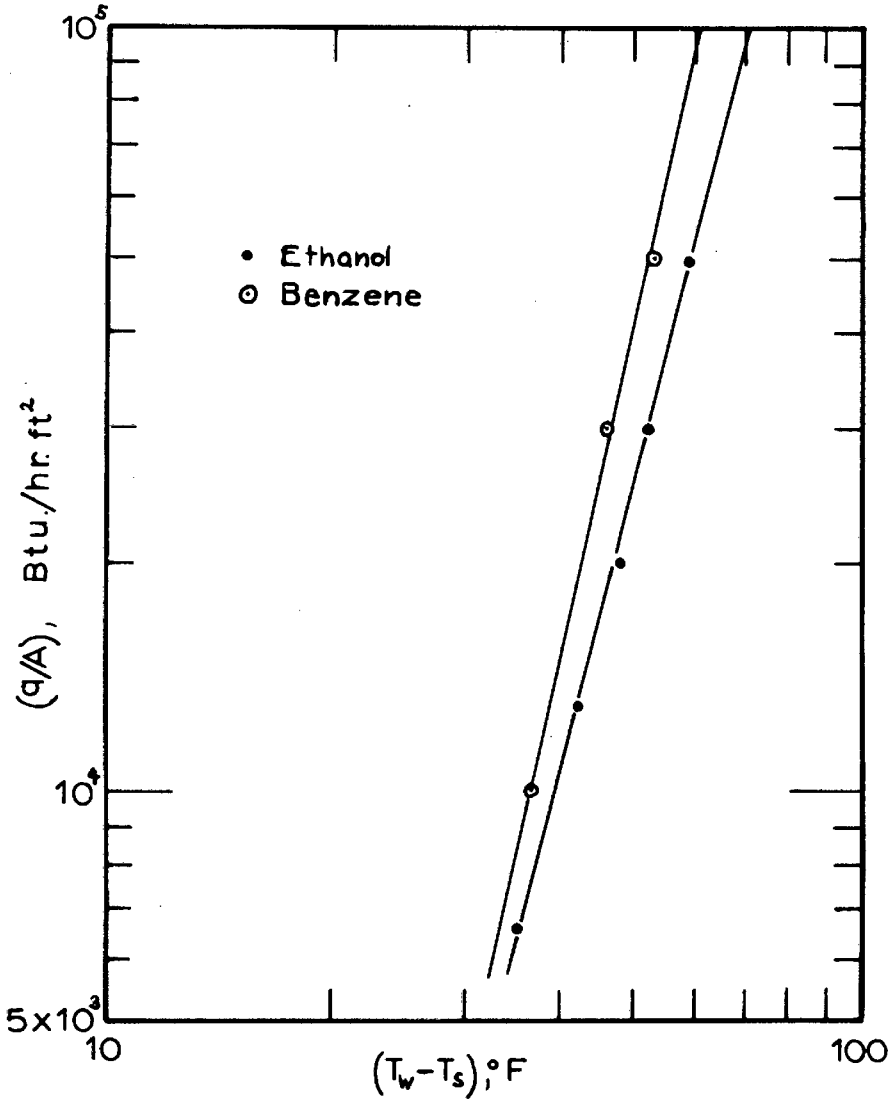

Fig. 5·4 (q/A) vs. (T_w-T_s) AT CESSATION OF NUCLEATION

During operation at a particular pressure, a flux somewhat higher than the one read from Fig. 5.3 will have a finite range of available cavity sizes associated with it, and boiling will proceed.

It is of interest to transform the information of Fig. 5.3 into a (q/A) vs. $(T_w - T_s)$ plot; the resulting curves could then be superimposed onto the figures giving the boiling runs. To this end the following procedure is adopted: For a particular (q/A) the P_L corresponding to the cessation of nucleation (from a cavity of $r_c = 2.44 \times 10^{-6}$ ft.) is read off from Fig. 5.3. The saturation temperature, T_s, corresponding to the value of P_L read off is determined from vapour-pressure data (100). By trial and error calculations a T_w is determined such that $(T_w - T_s)$, $(T_w + T_s)$ and the physical properties evaluated at $(T_w + T_s)/2$ yield, upon substitution into equation (3.19) a value of $r_c = 2.44 \times 10^{-6}$ ft. Similar calculations at different fluxes are performed for both the ethanol and the benzene data in Fig. 5.3. The resulting (q/A) vs. $(T_w - T_s)$ points are shown in Fig. 5.4. These loci of the cessation of nucleation are replotted in Figs. 4.1, 4.3 and 4.4 as dotted lines. Below these lines nucleation by the proposed mechanism cannot occur.

---

* Because of the limited pressure range in which stable operation was possible, the figures are rather approximate; this is especially the case for benzene.

5.10 DISCUSSION

From Figs 4.1, 4.3 and 4.4 it is seen that although nucleation does proceed in the region in which the present theory predicts it to be absent, it proceeds by a different mechanism. Run E.3 in Fig. 4.1 shows particularly clearly and remarkably quantitatively the change in the shape of the boiling curve when the region of theoretical absence of nucleation is entered. In all runs where the (dotted) theoretical cessation-of-nucleation curve is crossed, nucleation becomes unstable and the boiling curves assume unusual patterns. Thus the analysis presented here does not predict the complete cessation of nucelation, but the cessation of operation of the mechanism embodied in equation (5.19) i.e. the mechanism by which the wall superheat necessary for nucelation is dictated by the equilibrium (expressed by the Gibbs equation) of a vapour cap formed over a cavity mouth, with the vapour radius of curvature equal to the cavity mouth radius.

From Figs. 4.6 and 4.7 (see also section 4.1) it appears that pits and depressions of radii ranging from 10^{-5} ft. to 10^{-7} ft. are present on the heating surface. The cavity sizes predicted to be active fall within this visually observed range.

The degree to which the analysis here presented is quantitative (see Run E.3 Fig. 4.1) is surprising if one considers the experiment of Griffith and Wallis (5) (see Sections 3.1102 and 3.2) in which the boiling nucleation superheats from artificially prepared cavities differed by about an order of magnitude from those predicted by equations (3.14) and (3.19). It is possible that this discrepancy is connected with the relation between cavity radius, r_c, and the thermal boundary layer thickness, δ. Since bubble growth can only take place in a superheated liquid, another nucleation criterion for a cavity of mouth radius r_c, namely that $\delta \geq r_c$, may be advanced. δ will vary with time at a particular spot on the heating surface, being very thin just after a bubble departs and then recovering. During high-flux boiling with high active site concentrations interaction of sites must be expected. - Tien (55) has correlated the measurements of Yamagata et.al. (46), also reported (110), on the maximum δ in the region of "isolated bubbles". A correlation for δ at high fluxes does not exist, nor were Yamagata's measurements extended to the high-flux region. Hence δ in the experiment of Griffith and Wallis is unknown. However, it may be expected that δ will continue to decrease with increasing flux and consequent increase in interaction of bubble-producing sites. Thus it is possible that in Griffith and Wallis' experiment, where relatively large cavities ($r_c = 2.7 \times 10^{-3}$ in.) were punched into the surface, the situation arose where $r_c > \delta$. In that case the punched cavities were not active at all, and smaller natural cavities led to the higher superheats necessary for nucleation. Thus the analysis of the present study might be limited to "smooth surfaces" where the condition $\delta \geq r_{max}$ is satisfied.

SECTION 6 CONCLUSIONS

From the study here presented the following conclusions are drawn:-

(1) Nucleation and hence nucleate boiling cannot be made to proceed infinitely at lower and lower pressures. For a particular surface-liquid combination a particular low pressure exists below which nucleate boiling becomes unstable. At an even lower pressure the nucleate regime is altogether absent, the heat-transfer changing from natural convection straight to film boiling as the wall superheat is raised.

(2) During stable boiling nucleation proceeds from a residual vapour phase entrapped in cavities in the heating surface. The nucleation superheat for a particular cavity is determined by the equilibrium (expressed by the Gibbs equation) of a vapour cap formed over the cavity mouth, with the vapour radius of curvature equal to the cavity mouth radius.

(3) This nucleation mechanism ceases when the size range of cavities available for such nucleation becomes zero. This point marks the threshold of the unstable boiling region.

(4) This threshold may be predicted for a certain surface-liquid combination if a number of stable boiling curves determined at different pressures for the same surface-liquid combination are available, and if the points of disappearance of the last bubble (flux decreasing) are known for these curves.

APPENDIX I APPARATUS FOR BOILING TESTS

I.1 Requirements of the Apparatus

It was necessary to design an apparatus which allowed the determination of both flux and wall superheat from a metal surface to a liquid which is under essentially stagnant pool conditions and at the saturation temperature corresponding to a measured and controlled system pressure, equal to or less than atmospheric pressure.

I.2 Mechanical Details

Heat transfer took place from a thin horizontal electrically heated platinum wire immersed in the test liquid. The wire was stretched between the fastening nuts of a holder consisting of two parallel horizontal glass rods connected by copper clamping strips. Following McAdams et.al. (42) platinum potential taps of about a quarter the diameter of the heating element* were spot-welded to the wire, thereby allowing the central portion of the wire to act as test section, and eliminating end effects. The upper glass rod of the holder had two further clamps for the potential taps. Heavy current terminals and lighter potential terminals were attached to the holder. In Fig. I.1 the holder is shown attached to current and potential leads coming through the lid of the boiling vessel.

Since experiments at reduced pressure were to be carried out an air-tight boiling vessel was required. A standard hard-glass 1 litre reaction vessel (Quickfit FR1LF) with a flat ground-glass flange, see Fig. I.1, was employed. The lid (Quickfit MAF 2/2) with a similar ground flange carried five B.19 ground-glass socket joints. The holder was suspended from the current and potential leads in a hard-glass beaker fitting into the boiling vessel. Fig. I.1 shows the separate components: boiling vessel, inner vessel and lid with attached holder; Fig. I.2 illustrates the method of assembly. The boiling flask was placed in a variac-controlled heating mantle which maintained the liquid at the boiling temperature. A small hole in the inner jacket equalized the liquid levels. The inner vessel has been shown to be necessary (106) if stagnant pool conditions are to be maintained in the test liquid; if it is omitted the heat transfer from the wire varies with the power level of the external heater.

Current and potential leads were taken through the lid by braising them onto tungsten rods** fused through B.19 ground-glass stoppers which fitted into two of the sockets in the lid; details are shown in Fig. I.3.

---

* this very thin wire was obtained by picking a few strands out of a fine platinum gauze.

** obtained by breaking up an old thyratron.

Fig. I.1 COMPONENTS OF BOILING VESSEL

1. outer vessel
2. lid
3. holder with heating element
4. inner vessel

Fig. I.2 ASSEMBLY OF BOILING VESSEL

Fig. I.3 DETAILS OF LID AND ATTACHMENTS

1. stoppers with tungsten rods sealed through; thicker wires - current leads, thinner wires - potential leads.
2. insulated contacts.
3. thermometer.

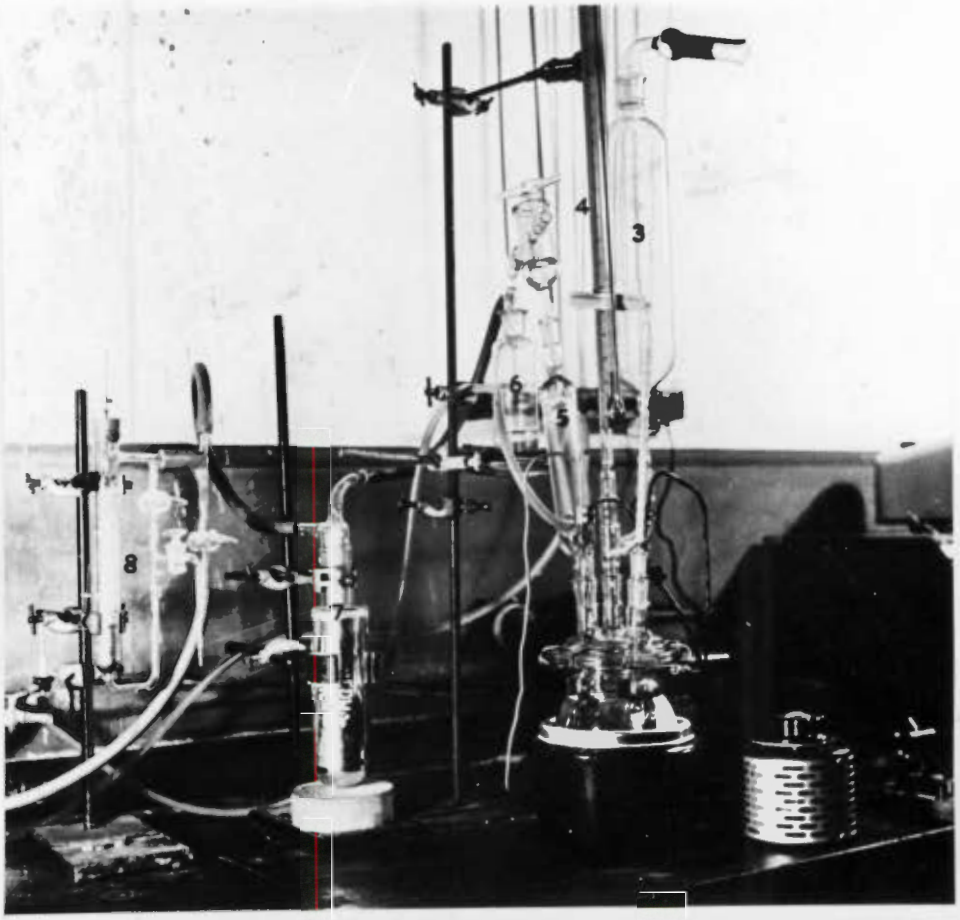

Fig. I.4 OVERALL VIEW OF APPARATUS
(Electrical Measuring Section not shown)

1. boiling vessel
2. heating mantle
3. liquid reservoir
4. manometer
5. condenser
6. liquid trap
7. vapour trap in Dewar flask
8. pressure controller

A long-stemmed Jena mercury-in-glass thermometer with a ground-glass joint and a B.19-B.14 adapter occupied a further socket in the lid and measured the liquid bulk temperature in the inner vessel; see Fig.I.3.

An adapter (Quickfit MA 1/2) with two parallel vertical necks, each carrying a socket joint, was fitted to the central socket on the lid; one neck carried a mercury manometer, the other a reservoir from which liquid could be added by opening a stopcock. The reservoir was fitted with a silica-gel drying-tube.

The last lid socket carried a double-surface reflux condenser, cooled by tap water, or, in the case of low-pressure runs, by iced water pumped through from a tank by a small centrifugal pump.

To avoid condensate splashing and consequent extraneous convection in the liquid pool, the condenser was fitted with a drip lip which directed condensate into the space between the inner and outer vessel; the bottom end of the manometer carried a wire spiral dipping into the liquid which allowed the small amounts of condensate to run into the pool without splashing.

The top of the condenser carried a vacuum and pressure release stopcock, see Fig. I.4, connected to a liquid trap by means of a drip bend with a vacuum connection (Quickfit RA 3/23).

Pressure tubing lead to a vapour trap cooled by a "dry-ice"-ethanol mixture in a Dewar flask.

A mercury-in-glass pressure controller as described by Spadaro et.al. (107) allowed any fixed subatmospheric pressure to be maintained in the system with pressure variations of about ± 0.2 mm Hg. Suction was provided by an ordinary water-jet pump.

The assembled apparatus is shown in Fig. I.4.

The vapour trap prevented the entry of uncondensed vapours into the pressure controller. The liquid trap was necessary in low-pressure runs where difficulty in nucleation often led to considerable superheating of the liquid bulk during start-up, followed by the almost explosive onset of boiling.

Only after many tests were suitable lubricants found for the ground-glass joints. Finally, Fisher "Nonaq" was employed in benzene runs and Edwards "Hard Vacuum Grease" in the ethanol tests. Both were entirely satisfactory.

I.3 Electrical System

The test wire was made to act both as a heating element and as resistance thermometer measuring T_w.

Fig I.5 depicts the electrical circuit. D.C. power was supplied from banks of 2V batteries, a total of 10V being available. The heating current was controlled by two variable resistors, and was determined by measuring the potential drop across a precision resistor in series with the heating wire. The potential drop over the test

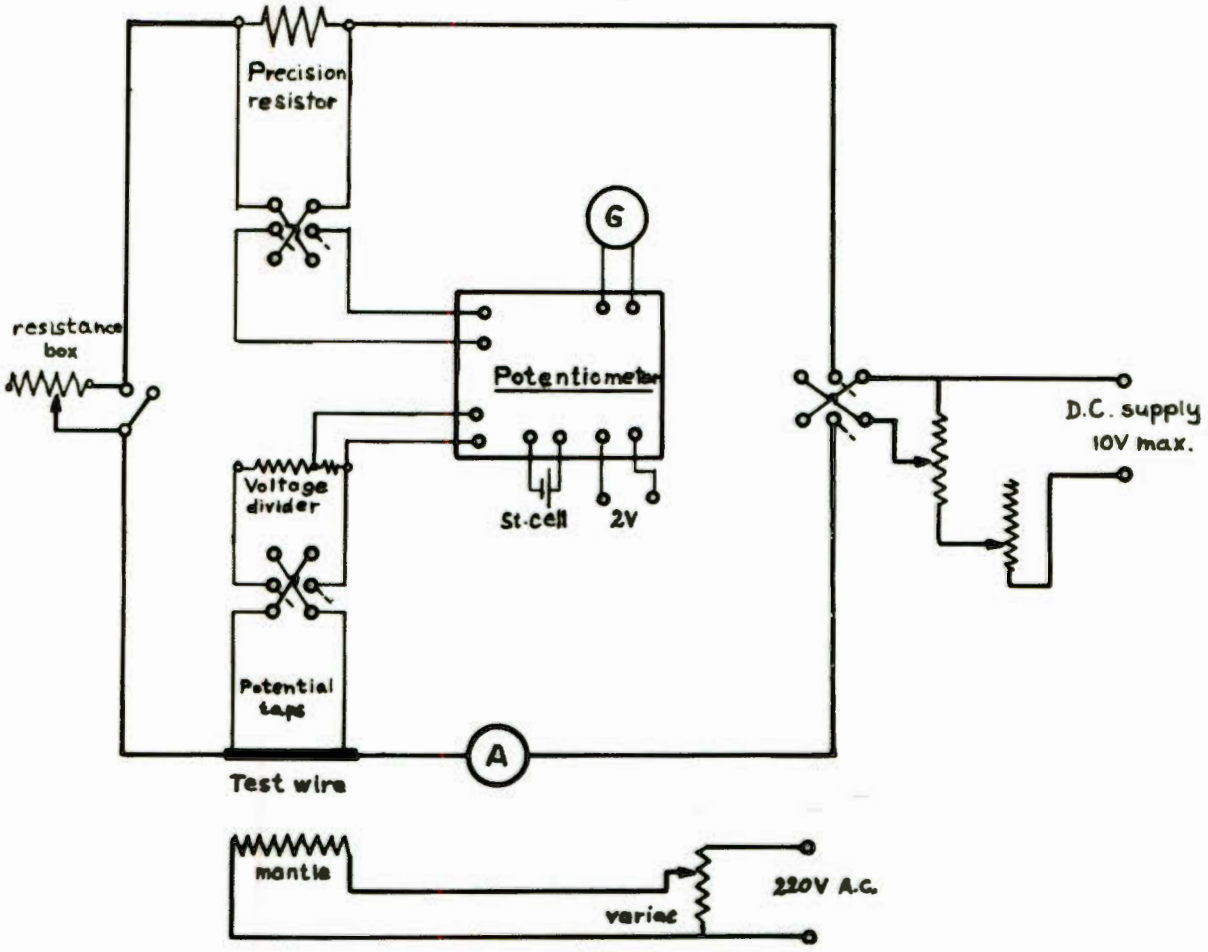

Fig. I·5 ELECTRICAL SYSTEM

section of the heating element was also measured after suitable reduction to within the range of the potentiometer by means of a voltage divider. From the values of the potential drop over the test section, and the current, the power dissipated and hence q could be calculated; the wire resistance, and hence the wire temperature could also be determined. Appendix III gives details of these calculations.

Temperature-resistance callibrations were performed by passing small currents of negligable heating effect through the wire immersed in the test liquid of known temperature, and by measuring the potential drop over the test section and over the precision resistor. Thus the wire resistance could be calculated; the wire temperature was the liquid bulk temperature. In these determinations only two volts of the supply were used; suitable resistances from a normally by-passed resistance box were switched into the circuit and the potential drop over the test section was measured directly without reduction.

Reversing keys were included in the current and potential leads; these were used to check whether thermo-electric effects were present.

Current leads and switches were of appropriate rating.

I.30 Instrument Specifications

Potentiometer - Pye, Cat.No.7565
Standard Cell - Pye, Cadmium Cell, Cat.No.35240
Galvanometer - Scalamp (multirange), Cat.No.7891/S
Precision Resistor - Robt.W.Paul, Cat.No.1022, rated at 15 amps, nominally 0.1 ohms.

APPENDIX II TEST PROCEDURE.

II.1 Calibrations and Preliminary Measurements

The precision resistor and the resistors constituting the voltage divider were calibrated against a recently certified standard Pye Four Decade Wheatstone bridge (Cat. No. 7383).

The Jena thermometer was calibrated in an oil bath against National Physical Laboratory-certified thermometers. The standard thermometers were immersed to the height of the mercury column. Test conditions were simulated for the Jena thermometer by immersing the stem up to the ground-glass joint through a hole in the lid of the the oil bath.

The test wire, stretched in the holder, was annealed in air by A.C. heating at a dull red heat for about 20 minutes. Since the platinum was of lower purity than "thermograde" it was necessary to determine the coefficient of resistance and to check the linearity of the temperature-resistance relationship. The annealed wire was immersed in a thermostatically controlled oil bath. Resistance determinations were performed by employing the calibration circuit described in Appendix I and by measuring the potential drops over the precision resistor and over the test section of the heating element when a small current of negligable heating effect was passed through the circuit. Thus the resistance could be calculated. A few determinations at different small currents were conducted at each temperature; the highest current differed from the lowest by a factor of about 20; the resistance at a particular temperature was invariant with current, thus showing that the current range was sufficiently low for heating effects to be absent. The temperature range between 20°C and 200°C was covered by 13 resistance determinations. The temperature-resistance relationship was found to be linear. The coefficient of resistance was calculated. The coefficient of two further test wires cut from different portions of the spool of wire employed was also determined, the same value as previously determined being obtained. It could thus be safely assumed that the coefficient was the same for the entire length of wire on the spool. Wires once dipped in oil were discarded.

During boiling tests proper the test wire was calibrated every now and then while immersed in the test liquid whose temperature was measured by the Jena thermometer. Procedure was as above. Calibrations during numerous preliminary tests indicated that the wire resistance did not change during tests; thus in the tests here reported (during all of which the same wire was employed) calibrations were only carried out five times and not before and after each run. This was considered sufficient. By using the previously determined coefficient the wire resistance at 0°C was calculated for ease of comparison. The calibration results are listed in Appendix V.

To allow the calculation of (q/A) the surface area of the test section had to be determined. The wire diameter was measured by a micrometer screw gauge, and the distance between the potential taps by a travelling vernier microscope.

A preliminary test to check whether thermo-electric e.m.f's were generated in the circuit was conducted. Such effects could arise from the tungsten-copper joints employed in taking the current and potential terminals through the stoppers in the lid of the boiling vessel, with one joint hot inside the vessel and the other in air. Even though pairs of such "thermocouples" generating e.m.f.'s in opposite directions were present, the possibility of a resultant e.m.f. cannot be dismissed if it is remembered that no two thermocouples, even of the same materials, act in an entirely identical manner. However, no significant difference in the potential drop over the test section and the precision resistor could be detected when measurement with the current first flowing in one direction and then with the current reversed were taken during convective heat transfer from the wire. Such small variations as were present were random. It was concluded that the circuit was essentially free from thermo-electric effects. The original intention was to take two measurements at each power setting with the current flowing in different directions as above during the actual boiling tests. This procedure was rejected as impractical when it was noticed that in the short period when no current flowed during the throwing over of the reversing key, many, and in frequent cases, all bubble-producing sites were deactivated. The latter situation, occurring invariably during low-pressure runs, could only be remedied by first raising the power input to the point of film boiling, and then lowering it again.

II.2 Procedure during tests proper.

A new test-wire complete with potential taps was fitted into the holder and annealed in air as described.

After washing with chromic acid and distilled water, thorough drying, slight greasing of all ground-glass joints and fastening of the holder to the current and potential leads, the apparatus was assembled and filled with liquid from the resevoir. The heating-mantle was switched on.

Before tests could be started the liquid and the heating element had to be thoroughly degassed. Failure to do,this yields erroneous results (7, 10,108). The liquid bulk was deaerated by prolonged boiling employing the heating-mantle. Deaeration of the heating surface was effected by prolonged high-flux boiling from the wire. The surface contamination and consequent irreproducibility reported by Rallis et.al. (10) for the boiling of water did not occur with the organic liquids here tested, probably owing to the absence of electrolytic effects.

After about six hours of boiling the first test at atmospheric pressure was started. Preliminary tests had shown that the only way in which stable reproducible boiling data could be obtained was by operating at progressively lower fluxes. This procedure was followed, about five minutes being allowed to elapse before the potential drops over the precision resistor and over the test section were measured at a particular power setting. Readings were taken from close to the peak flux, down into the natural convection region, particular attention being paid to the point of disappearance of the last bubble.

Tests on the same liquid under reduced pressures were performed without removing the test-wire. The manostat was set to the desired pressure with the suction pump operating. The Dewar flask containing the vapour trap was filled with a "dry-ice"-ethanol mixture, and the heating mantle was switched on. When boiling from the outer vessel had proceeded sufficiently long for the inner pool to be at the saturation temperature, the test-wire was raised to a high flux. In almost all cases nucleation could only be obtained by first allowing momentary film boiling to occur and then lowering the flux. Since the liquid and the test surface were already deaerated, high-flux boiling was allowed to proceed for only one hour before readings were taken. The rest of the test was conducted as above.

During operation in the unstable region (see Section 4.00) rapid fluctuations made the balancing of the potentiometer difficult. In these cases the galvanometer was operated undamped and the potentiometer setting adjusted until the galvanometer spot oscillated equally about the zero position.

Visual counting of the number of active sites on the test section, carried out when the bubble population was not too high, became extremely unreliable in the unstable region.

During runs at even lower pressure nucleation from the test wire proceeded with difficulty, if at all. Similar difficulty in nucleation occurred at the surface of the outer vessel, heated by the mantle. Often considerable superheats built up, followed by a minor explosion when boiling finally started. One or two points on the outer vessel generally remained active; if not, then the vacuum was released and a few pieces of porous porcelain (containing large cavities) were dropped into the space between the two vessels through the condenser socket, and the test recommenced. Nucleation from the procelain maintained the liquid jacket at the saturation temperature.

At the conclusion of tests with one liquid the apparatus was dismantled and cleaned. The test wire was washed and dried by A.C. heating. Assembly, start-up and test procedure were identical in both sets of tests.

In one case, run B.5, measurements were taken at progressively increasing flux.

Resistance calibrations were conducted a number of times. A test to check the reproducibility of boiling data (run E.6) was performed. Throughout the tests the heating wire remained shiny with no visible signs of fouling.

APPENDIX III COMPUTATION OF (q/A) and $(T_w - T_s)$

The power dissipated over the test section was calculated from

$$q = 3.415\ EI$$

where E = potential drop over test section, volts

I = current flowing, amps

& 3.415 = conversion factor from watts to Btu/hr.

I was determined by measuring the potential drop, V_R, over the precision resistor of 0.1023 ohms. Thus

$$I = \frac{V_R}{0.1023}$$

and

$$q = \frac{3.415\ E.V_R}{0.1023}$$

E was not measured directly but was stepped down by two resistors of 1003.6 ohms and 10,115 ohms, acting as a voltage divider. The step-down ratio was thus 11,118.6/1003.6, or

$$E = 11.079\ V$$

where V is the measured, stepped-down potential. Thus

$$q = \frac{3.415 \times 11.079\ V.V_R}{0.1023}$$

The area of the test section, A, was 4.228×10^{-4} ft^2 for the wire of 0.00760 in diameter and 5.22 cm test length employed in this study.

Thus

$$(q/A) = \frac{3.415 \times 11.079\ V.V_R}{0.1023 \times 4.228 \times 10^{-4}}$$

$$= \underline{8.747 \times 10^5\ V.V_R} \quad (\text{Btu/hr.ft}^2)$$

The resistance of the test section was calculated from

$$R = \frac{E}{I}$$

i.e.

$$R = \frac{11.079.V.\ 0.1023}{V_R}$$

$$= \underline{1.133\ \frac{V}{V_R}} \quad (\text{ohms})$$

From a calibration graph of R vs. T_w, T_w was read off. T_s was measured by the thermometer. Subtraction gave $(T_w - T_s)$.

In these calculations the radial temperature gradient in the wire has been neglected. Application of the correction given by McAdams et.al. (42) showed that an error of 0.5% at the maximum is thereby introduced into $(T_w - T_s)$.

In obtaining the calibration graph of T_w vs. R use was made of the relation

$$\frac{R^T - R^o}{TR^o} = \alpha$$

where α = coefficient of resistance
R^T = resistance at temperature T
R^o = resistance at 0^oC

The formula applies since the temperature-resistance relationship of the wire was linear.

Preliminary tests showed that $\alpha = 3.465 \times 10^{-3}$ for the impure platinum employed.

In determining R in the calibration tests E was measured directly, hence

$$R = \frac{0.1023\ E}{V_R}$$

APPENDIX IV ESTIMATE OF EXPERIMENTAL ERROR

The precision of measuring instruments was such that results were limited by fluctuations inherent in the boiling phenomenon, rather than by the accuracy of instruments.

The diameter and length of the test section were measured to within 0.2%, thus the calculated surface area should be within 0.4% .

The current-measuring resistor and the resistors constituting the voltage divider were calibrated to within 0.1% against a recently certified Wheatstone bridge. Readings on the precision potentiometer (also recently certified) were within 0.1%.

Hence it is estimated that the determination of flux is accurate to within 1%. This estimate is based on the precision of instruments and would apply if current and voltage would have been determined simultaneously. Because of fluctuations in the measured potentials, it is possible that the error in the flux may have been about 4%. Thus following McAdams et.al.(42), the small correction for change of surface area with temperature was not made.

With respect to instrument accuracy the error in R is about 0.2%. The error, taking into account potential fluctuations, is 1% at the utmost. This corresponds to a maximum possible error of about $2.5^{\circ}F$ in T_w. The mean of five temperature-resistance calibrations (see Appendix V) was used to evaluate T_w for all runs. The variation in the calibration corresponds roughly to a further $1^{\circ}F$ error, in T_w. Fluctuations in T_s were $0.5^{\circ}F$ at the utmost and occurred especially during low pressure runs. Thus the maximum possible error in $(T_w - T_s)$ is $4^{\circ}F$. The error of 0.5% in $(T_w - T_s)$ arising out of neglecting the radial temperature gradient in the wire is seen to be negligible in comparison.

These estimates refer to the determination of (q/A) and $(T_w - T_s)$ during stable runs. During low-pressure unstable boiling fluctuations were greater and the error may have been larger.

APPENDIX V RESULTS OF BOILING RUNS

V.1 Temperature-Resistance Calibrations.

V_R volts	E volts	R^T ohms	T °C	When Checked	R^o ohms
0.001535	0.003132	0.2087	17.75	After E. 1	0.1966
0.002264	0.004619	0.2087			
0.004314	0.008809	0.2089			
0.001501	0.003057	0.2083	17.2	After E.2	0.1967
0.002215	0.004512	0.2084			
0.004230	0.008618	0.2084			
0.001500	0.003055	0.2084			
0.001519	0.003090	0.2081	17.2	After B.2	0.1964
0.006383	0.01298	0.2080			
0.002328	0.004738	0.2082			
0.001569	0.003189	0.2079	17.1	After B.3	0.1965
0.002313	0.004705	0.2081			
0.004411	0.008973	0.2081			
0.001500	0.003032	0.2068	15.0	After B.5	0.1966
0.002810	0.005681	0.2068			
0.005341	0.01080	0.2069			

V.2 Results of Heat-Transfer Tests

Run: E.1 Liquid: Ethanol $T_s = 172.8^{\circ}F$

Pressure: 761 mm Hg = 1.0 atm $A = 4.228 \times 10^{-4} ft^2$

V_R volts	V volts	$(q/A) \times 10^{-3}$ Btu/hr.ft^2	R ohms	T_w °F	$(T_w - T_s)$ °F	N	Remarks
0.4806	0.1120	47.1	0.2640	211.7	38.9	-	nucleate boiling
0.4540	0.1058	42.0	0.2640	211.7	38.9	-	" "
0.4294	0.09990	37.5	0.2636	210.7	37.9	-	" "
0.4155	0.09665	35.1	0.2635	210.4	37.6	-	" "
0.3901	0.09068	30.9	0.2634	210.2	37.4	-	" "
0.3619	0.08400	26.6	0.2630	209.0	36.2	-	" "
0.3510	0.07676	22.2	0.2627	208.3	35.5	69	" "
0.3046	0.07054	18.8	0.2624	207.5	34.7	52	" "
0.2782	0.06436	15.7	0.2621	206.5	33.7	42	" "
0.2545	0.05880	13.1	0.2618	205.8	33.0	32	" "
0.2049	0.04726	8.47	0.2613	204.4	31.6	14	" "
0.1836	0.04226	6.79	0.2608	203.0	30.2	10	" "
0.1612	0.03699	5.20	0.2600	200.7	27.9	4	* " "
0.1401	0.03292	3.91	0.2581	195.4	22.6	0	* Convection
0.1246	0.02827	3.08	0.2571	192.5	19.7	0	"
0.1123	0.02540	2.49	0.2563	190.5	17.7	0	"
0.1000	0.02250	1.97	0.2549	186.4	13.6	0	"

* last bubble disappeared between these two settings.

Run: E.2 Liquid: Ethanol T_s = 155.1°F

Pressure: 514 mm Hg = 0.677 atm A = 4.228×10^{-4} ft^2

V_R volts	V volts	$(q/A) \times 10^{-3}$ Btu/hr.ft^2	R ohms	T_w °F	$(T_w - T_s)$ °F	N	Remarks
0.5505	0.1266	61.0	0.2606	202.4	47.3	-	nucleate boiling
0.5307	0.1217	56.5	0.2598	200.4	45.3	-	" "
0.5093	0.1165	51.9	0.2592	198.5	43.4	-	" "
0.4843	0.1105	46.8	0.2585	196.5	41.4	-	" "
0.4526	0.1031	40.8	0.2581	195.2	40.1	-	" "
0.4271	0.09710	36.3	0.2576	193.9	38.8	-	" "
0.4012	0.09105	31.9	0.2571	192.6	37.5	-	" "
0.3748	0.08495	27.8	0.2568	191.9	36.8	55	" "
0.3518	0.07970	24.5	0.2567	191.6	36.5	50	" "
0.2900	0.06557	16.6	0.2562	190.0	34.9	33	" "
0.2699	0.06093	14.4	0.2558	189.2	34.1	27	" "
0.2495	0.05631	12.3	0.2557	188.8	33.7	20	" "
0.2303	0.05200	10.5	0.2558	189.2	34.1	13	" "
0.2099	0.04726	8.68	0.2551	187.0	31.9	8	" "
0.1904	0.04284	7.13	0.2549	186.4	31.3	7	" "
0.1701	0.03817	5.68	0.2542	184.4	29.3	4	" "
0.1503	0.03366	4.42	0.2537	183.1	28.0	0	Last bubble disappeared

Run: E.3 Liquid: Ethanol T_s = 132.8

Pressure: 301 mm Hg = 0.396 atm A = 4.228 x 10^{-4} ft^2

V_R volts	V volts	$(q/A)x10^{-3}$ Btu/hr.ft^2	R ohms	T_w °F	$(T_w - T_s)$ °F	N	Remarks
0.5440	0.1218	58.0	0.2537	183.0	51.2	-	nucleate boiling
0.5233	0.1169	53.5	0.2531	181.3	48.5	-	" "
0.5019	0.1119	49.1	0.2526	180.1	47.3	-	" "
0.4816	0.1073	45.2	0.2524	179.7	46.9	-	" "
0.4603	0.1025	41.3	0.2523	179.4	46.6	35	" "
0.4411	0.09798	37.8	0.2517	177.5	44.7	33	" "
0.4181	0.09282	33.9	0.2515	177.0	44.2	26	" "
0.3980	0.08864	30.8	0.2515	177.0	44.2	24	" "
0.3762	0.08347	27.5	0.2514	176.7	43.9	18	" "
0.3530	0.07833	24.2	0.2514	176.7	43.9	15	" "
0.3309	0.07342	21.3	0.2514	176.7	43.9	12	" "
0.3099	0.06872	18.6	0.2512	176.1	43.3	9	" "
0.2906	0.06465	16.4	0.2521	178.7	45.9	8	" "
0.2706	0.06072	14.4	0.2542	184.4	51.6	5	" "
0.2499	0.05621	12.3	0.2548	186.2	53.4	3	" "
0.2306	0.05131	10.3	0.2521	178.7	45.9	3	" "
0.2103	0.04642	8.54	0.2501	173.2	40.4	2	" "
0.1903	0.04178	6.95	0.2487	169.5	36.7	0	last bubble disappeared
0.1701	0.03710	5.52	0.2471	164.8	32.0	0	convection

Run: E.4 Liquid: Ethanol T_s = 120.9°F

Pressure: 223 mm Hg = 0.294 atm A = 4.228×10^{-4} ft^2

V_R volts	V volts	$(q/A) \times 10^{-3}$ Btu/hr.ft^2	R ohms	T_w °F	$(T_w - T_s)$ °F	N	Remarks
0.4227	0.09468	35.0	0.2538	183.7	62.8		bubbles very unstable
0.4010	0.09025	31.6	0.2550	186.7	65.8		"
0.3788	0.08565	28.4	0.2562	190.0	69.1		"
0.3612	0.08201	25.9	0.2572	192.8	71.9	±10	"
0.3408	0.07820	23.3	0.2600	200.8	79.9	3-4	"
0.3209	0.07440	20.9	0.2627	208.3	87.4	1	"
0.3003	0.06911	18.2	0.2607	202.6	81.7	0	convection
0.2804	0.06342	15.6	0.2563	190.3	69.4	0	"

Run: E.5 Liquid: Ethanol T_s = 94.3°F

Pressure: 103 mm Hg = 0.136 atm A = 4.228×10^{-4} ft^2

0.3579	0.08212	25.7	0.2600	200.7	106.4	0	convection
0.3392	0.07705	22.9	0.2574	193.5	99.2	0	"
0.3208	0.07168	20.1	0.2532	181.8	87.5	0	"
0.3010	0.06650	17.5	0.2503	173.8	79.5	0	"
0.2802	0.06127	15.0	0.2477	166.4	72.1	0	"
0.2555	0.05464	12.2	0.2423	152.3	58.0	0	"
0.2329	0.04911	10.0	0.2389	143.3	49.0	0	"
0.2104	0.04370	8.04	0.2353	134.0	39.7	0	"

Run: E.6 Liquid: Ethanol T_s = 172.8°F

Pressure: 761 mm Hg = 1.0 atm A = 4.228×10^{-4} ft^2

0.4556	0.1060	42.2	0.2636	210.7	37.9	-	nucleate boiling
0.4040	0.09394	33.2	0.2635	210.4	37.6	-	" "
0.3613	0.08399	26.5	0.2631	209.3	36.5	-	" "
0.3019	0.07003	18.4	0.2628	208.6	35.8	48	" "
0.2305	0.05320	10.7	0.2615	204.7	31.9	23	" "

Run: B.1 Liquid: Benzene T_s = 176.5°F

Pressure: 758 mm Hg = 1.0 atm A = 4.228 x 10^{-4} ft^2

V_R volts	V volts	$(q/A)x10^{-3}$ Btu/hr.ft^2	R ohms	T_w °F	$(T_w - T_s)$ °F	N	Remarks
0.5185	0.1229	55.7	0.2686	222.9	46.4	-	nucleate boiling
0.4997	0.1183	51.7	0.2682	221.8	45.3	-	" "
0.4813	0.1136	48.0	0.2674	219.6	43.1	-	" "
0.4598	0.1084	43.6	0.2671	218.8	42.3	-	" "
0.4377	0.1032	39.5	0.2671	218.8	42.3	-	" "
0.3929	0.09259	31.8	0.2670	218.5	42.0	-	" "
0.3467	0.08162	24.8	0.2667	217.8	41.3	53	" "
0.3240	0.07621	21.6	0.2664	217.0	40.5	48	" "
0.3032	0.07110	18.9	0.2657	215.3	38.8	41	" "
0.2805	0.06530	16.2	0.2662	216.3	39.8	37	" "
0.2601	0.06093	13.9	0.2654	214.3	37.8	31	" "
0.2395	0.05594	11.7	0.2646	212.1	35.6	26	" "
0.2217	0.05182	10.0	0.2648	213.0	36.5	19	" "
0.1998	0.04654	8.13	0.2639	210.4	33.9	14	" "
0.1799	0.04180	6.58	0.2633	208.7	32.2	10	" "
0.1502	0.03473	4.56	0.2620	205.3	28.8	4	* " "
0.1302	0.02986	3.40	0.2598	199.4	22.9	0	* convection
0.1100	0.02500	2.41	0.2575	193.3	16.8	0	"
0.09002	0.02035	1.60	0.2561	189.5	13.0	0	"

* last bubble disappeared between these two settings.

Run: B.2 Liquid: Benzene T_s = 158.0°F

Pressure: 566 mm Hg = 0.745 atm A = 4.228×10^{-4} ft^2

V_R volts	V volts	$(q/A) \times 10^{-3}$ Btu/hr.ft^2	R ohms	T_w °F	$(T_w - T_s)$ °F	N	Remarks	
0.5575	0.1300	63.4	0.2642	211.0	53.0	-	nucleate boiling	
0.4869	0.1129	48.1	0.2627	207.0	49.0	-	"	"
0.4703	0.1089	44.8	0.2624	206.3	48.3	-	"	"
0.4531	0.1044	41.4	0.2611	202.7	44.7	-	"	"
0.4319	0.09953	37.6	0.2611	202.7	44.7	-	"	"
0.4111	0.09448	34.0	0.2604	201.0	43.0	-	"	"
0.3899	0.08948	30.5	0.2600	199.8	41.8	-	"	"
0.3681	0.08451	27.2	0.2601	200.2	42.2	51	"	"
0.3511	0.08052	24.7	0.2598	199.4	41.4	44	"	"
0.3319	0.07609	22.1	0.2597	199.0	41.0	42	"	"
0.2911	0.06663	17.0	0.2593	198.0	40.0	33	"	"
0.2705	0.06190	14.6	0.2593	198.0	40.0	29	"	"
0.2503	0.05716	12.5	0.2587	196.4	38.4	22	"	"
0.2304	0.05197	10.5	0.2556	188.3	30.3	19	"	"
0.2107	0.04769	8.77	0.2559	189.2	31.2	19	"	"
0.1902	0.04283	7.13	0.2551	186.7	28.7	11	"	"
0.1701	0.03820	5.68	0.2544	185.2	27.2	7	"	"
0.1502	0.03374	4.43	0.2545	185.5	27.5	3	"	"
0.1303	0.02915	3.32	0.2535	182.6	24.6	0	last bubble disappeared.	

bubbles unstable

Run: B.3 Liquid: Benzene $T_s = 134.1^{\circ}F$

Pressure: 365 mm Hg = 0.480 atm $A = 4.228 \times 10^{-4} ft^2$

V_R volts	V volts	$(q/A) \times 10^{-3}$ Btu/hr.ft^2	R ohms	T_w °F	$(T_w - T_s)$ °F	N	Remarks
0.5513	0.1245	60.0	0.2559	189.1	55.0	-	nucleate boiling,
0.5293	0.1193	55.2	0.2554	187.8	53.7	-	bubble behaviour highly irregular
0.5092	0.1147	51.1	0.2552	187.1	53.0	-	" "
0.4899	0.1101	47.2	0.2546	185.6	51.5	-	" "
0.4697	0.1054	43.3	0.2542	184.7	50.6	-	" "
0.4468	0.1002	39.2	0.2541	184.3	50.2	-	" "
0.4308	0.09610	36.2	0.2527	180.6	46.5	-	" "
0.4117	0.09086	32.7	0.2500	173.1	39.0	-	" "
0.3894	0.08586	29.2	0.2498	172.6	38.5	36	" "
0.3686	0.08203	26.4	0.2521	179.9	44.9	31	" "
0.3526	0.07795	24.0	0.2505	174.5	40.4	31	" "
0.3298	0.07341	21.2	0.2522	179.2	45.1	27	" "
0.3095	0.06923	18.7	0.2534	182.4	48.3	24	" "
0.2910	0.06426	16.4	0.2502	173.8	39.7	18	" "
0.2705	0.05968	14.1	0.2500	173.1	39.0	17	" "
0.2502	0.05513	12.1	0.2496	172.2	38.1	15	" "
0.2304	0.05076	10.2	0.2496	172.2	38.1	11	" "
0.2104	0.04618	8.50	0.2487	169.8	35.7	8	" "
0.1907	0.04167	6.95	0.2476	166.9	32.8	5	" "
0.1704	0.03699	5.51	0.2459	162.6	28.5	2	" "
0.1503	0.03262	4.29	0.2459	162.6	28.5	0	last bubble disappeared
0.1303	0.02800	3.19	0.2435	156.2	22.1	0	convection
0.1100	0.02349	2.26	0.2419	152.0	17.9	0	"

Run: B.4 Liquid: Benzene T_s = 113.7°F

Pressure: 237 mm Hg = 0.312 atm. A = 4.228×10^{-4} ft^2

V_R volts	V volts	$(q/A) \times 10^{-3}$ Btu/hr.ft^2	R ohms	T_w °F	$(T_w - T_s)$ °F	N	Remarks
0.5482	0.1202	57.6	0.2484	169.2	55.5	-	nucleate boiling, bubble behaviour highly irregular
0.5288	0.1159	53.6	0.2483	168.8	55.1	-	
0.5106	0.1113	49.7	0.2470	165.5	51.8	30	" "
0.4900	0.1068	45.8	0.2469	165.2	51.5	27	" "
0.4703	0.1022	42.0	0.2462	163.4	49.7	24	" "
0.4513	0.09780	38.6	0.2455	161.5	47.8	26	" "
0.4141	0.08977	32.5	0.2456	161.7	48.0	23	" "
0.3933	0.08508	29.3	0.2451	160.3	46.6	20	" "
0.3531	0.07626	23.6	0.2447	159.5	45.8	11	" "
0.3140	0.06796	18.7	0.2452	160.9	47.2	6	" "
0.2941	0.06358	16.4	0.2449	160.0	46.3	4	" "
0.2746	0.05944	14.3	0.2452	160.9	47.2	2	" "
0.2555	0.05494	12.3	0.2436	156.5	42.8	1	" "
0.2344	0.05012	10.3	0.2423	153.0	39.3	1	" "
0.2145	0.04504	8.45	0.2379	141.3	27.6	0	last bubble disappeared
0.1940	0.04058	6.89	0.2370	138.4	24.7	0	convection
0.1738	0.03637	5.53	0.2371	138.6	24.9	0	"

Run: B.5 Liquid: Benzene T_s = 93.2°F

Pressure: 154 mm Hg = 0.203 atm A = 4.228×10^{-4} ft^2

V_R volts	V volts	$(q/A) \times 10^{-3}$ Btu/hr.ft^2	R ohms	T_w °F	$(T_w - T_s)$ °F	N	Remarks
0.1856	0.03812	6.20	0.2327	127.6	34.4	0	convection
0.2033	0.04202	7.46	0.2342	131.4	38.2	0	"
0.2189	0.04587	8.78	0.2374	140.0	46.8	0	"
0.2343	0.04937	10.1	0.2387	143.4	50.2	0	"
0.2550	0.05444	12.1	0.2419	152.0	58.8	0	"
0.2754	0.05937	14.3	0.2442	158.0	64.8	0	"
0.3000	0.06644	17.4	0.2509	175.6	82.4	0	"
0.3201	0.07190	20.1	0.2545	185.4	93.2	0	"
0.3408	0.07786	23.2	0.2588	196.7	103.5	0	"
0.3559	0.08192	25.5	0.2608	202.1	108.9	1	bubbles irregular
0.3764	0.08356	27.6	0.2515	177.3	84.1	3	" "
0.3926	0.08610	29.6	0.2485	169.3	76.1	4	went over to film boiling

APPENDIX VI PHOTOMICROGRAPHS: APPARATUS & TECHNIQUE

Apparatus:

Microscope	-	Zeiss "Standard Research"
Objective	-	Neofluar 40X
Eyepiece	-	Komplan 8X
Condenser	-	achromatic, aplanatic (N.A. 1.4)
Camera	-	Alpa - Reflex
Film	-	Kodak PLUS X

Technique:

Illumination	-	oblique, monochromatic green, phase contrast.
Exposure	-	10 seconds.

NOMENCLATURE

a	acceleration of bubble
A	heat transfer area
c_L	specific heat of liquid
C_1, C_2 etc.	constants
C_D	drag coefficient
C_{sf}	constant defined by equation (2.8)
D	tube or wire diameter
D_d	bubble diameter at departure
E	potential drop over test section
f	bubble frequency
Δf_o^*	activation energy
ΔF	change in Gibbs free energy
ΔF_{max}	change in Gibbs free energy to form bubble of critical size
g	gravitation acceleration
g_c	conversion factor from mass to force units
G_b	bubble mass flow rate
h	heat transfer coefficient; Planck's constant in Section 3.
I	heating current
J	mechanical equivalent of heat
k	Boltzmann's constant
k_L	thermal conductivity of liquid
K	constant
Ku	Kutateladze's number defined in equation (2.29)
ℓ^*	characteristic length, see equation (2.19)
L	length of test section
m	constant
n	constant
N/A	number of active sites per unit area
N	Avogadro's number
$P = P_L$	absolute pressure in system (liquid)
P_B	absolute pressure inside bubble
ΔP	superheat-vapour-pressure difference
q	heat per unit time
(q/A)	heat flux
$(q/A)_b$	flux due to latent heat transport by departing bubbles
$(q/A)_c$	critical (peak) flux
R	bubble radius of curvature, bubble radius
$\dot{R}$	radial bubble growth rate
R_o	critical radius of bubble (homogeneous nucleation)

R^{o}	resistance of heating element at $0^{o}C$
R^{T}	resistance of heating element at temperature T
R'_{o}	radius of curvature of bubble, see Figs. 3.3, 3.4 and 3.5
R_{c}	radius of curvature of bubble over cavity mouth
Re	Reynolds number
r_{c}	mouth radius of smallest cavity capable of nucleation, or cavity mouth radius in general
r_{max}	cavity mouth radius of largest cavity on surface
r_{s}	radius of curvature of surface projection
T	temperature (usually absolute)
T_{w}	wall temperature
T_{s}	liquid saturation temperature
$(T_{w} - T_{s})$	wall superheat
t	time
U_{L}	superficial liquid velocity
U_{c}	critical superficial vapour velocity (at flooding)
u_{b}	linear bubble velocity
V	volume of bubble
V	measured, stepped-down voltage drop over test section
V_{R}	voltage drop over precision resistor
v_{L}	specific volume of liquid
v_{V}	specific volume of vapour
W	reversible work to form a bubble
W_{max}	reversible work to form a bubble of critical size
$\alpha = \alpha_{L}$	thermal diffusibity of liquid
β	contact angle measured through liquid
δ	superheat-layer thickness
λ_{V}	latent heat of vaporization
μ_{L}	viscosity of liquid
ρ_{L}	liquid density
ρ_{V}	vapour density
σ	surface tension

LITERATURE CITED

(1) "Nuclear Engineering", ed. C.F.Bonilla, McGraw Hill (1957) p.400

(2) Bankoff, S.C: Trans.A.S.M.E. 79, 735 (1957)

(3) Courty, C. and A.Fousy: Chem.Eng.Prog.Symposium, Series 51,No.17,1(1955)

(4) Westwater, J.W., H.B.Clark and P.S.Strenge: Chem.Eng.Prog.Symposium Series 55, No.29, 103 (1959)

(5) Griffith, P. and J.D.Wallis: Chem.Eng.Prog.Symposium Series 56, No.30, 49 (1960)

(6) Bankoff, S.G., A.J.Hajjar and B.B.McClothin: J.Appl.Phys.29, 1759 (1958)

(7) Dutkiewicz, R.K.: S.African Mech.Eng. 7, 231 (1958)

(8) Vos, A.S. and S.J.D.van Stralen: Chem.Eng.Sci. 5, 50 (1956)

(9) Dean, R.B.: J.Appl.Phys. 15, 446 (1944)

(10) Rallis, C.J., R.V.Greenland and A.Kok: S.African Mech.Eng. 10, 171 (1961)

(11) Westwater, J.W.: Advances in Chemical Engineering, 1, 22; Ed.T.B.Drew and J.W.Hoopes, Academic Press Inc., New York (1956)

(12) Forster, H.K.: J.Appl.Phys. 25, 1067 (1954)

(13) Forster, H.K. and N.Zuber: J.Appl.Phys. 25, 474 (1954)

(14) Plesset, M.S. and S.A.Zwick: J.Appl.Phys. 23, 95 (1952)

(15) Plesset, M.S. and S.A.Zwick: J.Appl.Phys. 25, 493 (1954)

(16) Griffith, P: Trans.A.S.M.E. 80, 721 (1958)

(17) Dergarabedian, P.: J.Appl.Mech. 20, 537 (1953)

(18) Forster, H.K. and N.Zuber: A.I.Ch.E. Journal 1, 531 (1955)

(19) Levy, S: Trans.A.S.M.E., Journal of Heat Trans.81, 37 (1959)

(20) Labountzov, D.A.: Teploenergetika 7, 76 (1960) *

(21) Van Stralen, S.J.D.: Chem.Eng.Sci. 5, 290 (1956)

(22) Cryder, D.S. and E.R.Gilliland: Ind.Eng.Chem. 24, 1382 (1932)

(23) Cryder, D.S. and A.C.Finalborgo: Trans.Am.Inst.Chem.Eng. 33, 346 (1937)

(24) Jakob, M. and W.Linke: Physik.Z. 36, 267 (1935)

(25) Insinger, T.H. and H.Bliss: Trans.Am.Inst.Chem.Eng. 36, 491 (1940)

(26) Bonilla, C.F. and C.W.Perry: Trans.Am.Inst.Chem.Eng. 37, 685 (1941)

(27) Hughmark, G.A.: Int.Journal Heat & Mass Trans. 5, 667 (1962)

(28) Jakob, M.: "Heat Transfer" 1, 627, John Wiley & Sons, Inc. New York (1949)

(29) Gunther, F.C. and F.Kreith: "Head Transfer and Fluid Mechanics Institute", 113, A.S.M.E. Publication, New York (1949)

(30) Rohsenow, W.M. and J.A.Clark: Trans. A.S.M.E. 73, 609 (1951)

(31) Hyman, S. and D.J.Carliell: B.Sc. Thesis in Mech.Eng. (C.J.Rallis supervisor) Witwatersrand University, S.Africa (1961)

(32) Rohsenow, W.M.: Trans. A.S.M.E. 74, 969 (1952)

(33) Rohsenow, W.M.: Univ.Michigan Heat Trans. Symposium, 101 (1952)

(34) Fritz, W.: Physik Z. 36, 379 (1935)

(35) McAdams, W.H.: "Heat Transmission", 3rd ed., 382, McGraw Hill Book Co., Inc., New York (1954)

(36) Cichelli, M.T. and C.F. Bonilla: Trans.Am.Inst.Chem.Eng. 41, 755 (1945)

(37) Kurihara, H.M. and J.E.Myers: A.I.Ch.E. Journal 6, 83 (1960)

(38) Westwater, J.W.: "Advances in Chemical Engineering" 1, 13, Ed. T.B.Drew and J.W.Hoopes, Academic Press, Inc., New York (1956)

(39) Kazakova, E.A.: Eng.Digest 12, 81 (1951)

(40) Zuber, N.: A.I.Ch.E. Journal 3, No.3, 9S (1957)

(41) Zuber, N. and E.Fried: Am.Rocket Soc., Propellants, Cumbustion and Liquid Rockets Conference, Palm Beach, Florida (1961), Paper No. 1709-61

(42) Engelberg-Forster, K. and R.Greif: Tran. A.S.M.E., Jour.of Heat Trans. 81, 43 (1959)

(43) Jakob, M.: Mech. Eng. 58, 643 and 729 (1936)

(44) Gilmour, C.H.: A.S.M.E.-A.I.Ch.E. 2nd Nat.Heat Trans.Conference, Chicago (1958) A.I.Ch.E. Paper No.27 *

(45) Gaertner, R.F. and J.W.Westwater: Chem.Eng.Prog.Symposium Ser. 56, No.30, 39 (1960)

(46) Yamagata, K., F.Kirano, K.Nishikawa and H.Matsuoka: Mem.Fac.Eng. Kyushu University, 15, No.1, 97 (1955)*

(47) Jakob, M.: "Temperature, Its Measurements and Control in Science and Industry", 834, Reinhold Pub.Co., New York (1941)

(48) Mixon, F.D., W.Y.Chon and K.O.Beatty: Chem.Eng.Prog.Symposium Ser., 56, No.30, 75 (1960)

(49) Bankoff, S.G. and J.P.Mason: A.I.Ch.E. Journal 8, 30 (1962)

(50) Bankoff, S.G.: A.I.Ch.E. Journal 8, 63 (1962)

(51) Moore, F.D. and R.B.Mesler: A.I.Ch.E. Journal 7, 620 (1961)

(52) Hsu, S.T. and F.W.Schmidt: Trans.A.S.M.E., Jour.of Heat Trans. 83, 254 (1961)

(53) Chang, Y.P.: Trans. A.S.M.E. 79, 1501 (1951)

(54) Chang, Y.P. and N.W.Snyder: Chem.Eng.Prog.Symposium Ser. 56, No.30, 25 (1960)

(55) Tien, C.L.: Int.Jour.Head & Mass Trans. 5, 533 (1962)

(56) Westwater, J.W. and J.G.Santangelo: Ind.Eng.Chem. 47, 1605 (1955)

(57) Rohsenow, W.M. and P.Griffith: Chem.Eng.Prog.Symposium Ser. 52, No.18, 47 (1956)

(58) Jakob, M.: "Heat Transfer", p.633, John Wiley & Sons Inc., New York, (1949)

(59) McAdams, W.H.: "Heat Transmission", 3rd ed., p.380, McGraw-Hill Book Co. Inc., New York (1954)

(60) Perkins, A.S. and J.W.Westwater: A.I.Ch.E.Jour. 2, 471 (1956)

(61) Cole, R.: A.I.Ch.E. Journal 6, 533 (1960)

(62) McFadden, P.W. and P.Grassmann: Int.Journal Ht.& Mass Trans. 5, 169 (1962)

(63) Zuber, N.: Trans. A.S.M.E. 80, 711 (1958)

(64) Kutateladze, S.S.: Izv.Akad.Nauk.USSR, Otd.Tekh.Nauk, No.4, 524 (1951) See (63) *

(65) Sterman, L.S.: Zhur.Tekh.Fiz. 23, 341 (1953) See (61) *

(66) Borishanskii, V.M.: Zhur.Tekh.Fiz. 26, 452 (1956) *

(67) Zuber, N., M.Tribus and J.W.Westwater: Int.Ht.Trans.Conference, Boulder, Colorado (1961) Paper No.27

(68) Bragg, S.L. and I.E.Smith: Int. Jour.Heat & Mass Trans. 3, 252 (1961)

(69) Bromley, L.A.: Chem.Eng.Prog. 46, 221 (1950)

(70) Lamb, H.: "Hydrodynamics", 6th ed., Dover Publications, New York (1955)

(71) McAdams, W.H., J.N.Addoms, P.R.M.Rinaldo and R.S.Day: Chem.Eng. Prog. 44, 639 (1948)

(72) Zuber, N. and M.Tribus: U.S.Atomic Energy Report AECU-3631 (1958) A.E.C.Technical Information Service, Oak Ridge, Tenn. *

(73) Bradfield, W.S., R.O.Bankdoll and J.J.Byrne: Convair Scientific Research Laboratory, San Diego, Cal., Research Note 35 (1960)*

(74) Berenson, P.: M.I.T., Cambridge, Mass.; D.I.C.Tech.Rpt. 17, (1960)*

(75) Bankoff, S.G. and V.S.Mehra: Ind.Eng.Chem.Fundamentals 1, 38 (1962)

(76) Siemes, W. and M.Borchers: Chemie Inginiear Tech. 28, 787 (1956)

(77) Elgin, J.G. and F.B.Weiss: Ind.Eng.Chem. 31, 435 (1939)

(78) Souders, M. and G.G.Brown: Ind.Eng,Chem. 26, 98 (1934)

(79) Birkhoff, G. and E.H.Zarantonello: "Jets, Waves and Cavities", Academic Press, New York (1958)

(80) Mulford, R.N., J.Nigan, J.Dash and W.Keller: A.E.C.Report LA-1416, A.E.C. Tech.Inf.Ser. (1952)*

(81) Class, C.R., J.R.DeHaan, M.Piccone and R.B.Cast: "Advances in Cryogenic Engineering" 5, 254 (K.D.Timmerhaus, ed.) Plenum Press, New York (1960) *

(82) Westwater, J.W.: "Advances in Chemical Engineering" 1, 25-27, Ed. T.B.Drew and J.W.Hoopes, Academic Press, Inc. New York, 1956)

(83) Volmer, M.: Z.Elektrochemie 35, 555 (1929)

(84) Fisher, J.C.: J.Appl.Physics, 19, 1062 (1948)

(85) Kutateladze, S.S.: Int.Journal Heat & Mass Tran. 4, 31 (1961)

(86) Bankoff, S.G.: Jour.Phys.Chem. 60, 952, (1956)

(87) Bankoff, S.G.: A.I.Ch.E. 4, 24 (1958)

(88) Kermeen, R.W., J.T.McGraw and B.R.Parkin: Trans.A.S.M.E. 77, 533 (1955)

(89) Jakob, M. and W.Fritz: Forsch. Gebiete Ingenieurw. 2, 435 (1931)

(90) Griffith, P.: Reply to Discussion of (5)

(91) Bankoff, S.G.: Chem.Eng.Prog.Symposium Ser. 55, No.29, 87 (1959)

(92) Bankoff, S.G.: Discussion of (5)

(93) Trefethen, L.: J.Appl.Phys. 28, 923 (1957)

(94) Gordon, K.F. T.Singh and E.Y.Weissmann: Int.Jour.Heat & Mass Trans. 3, 90 (1961)

(95) Gibbs, J.W.: "The Scientific Papers of J.Willard Gibbs" 1, 366, Longmans, Greene and Co., New York (1906)

(96) Thomson, Sir W. (Lord Kelvin): Phil.Mag. 42, Ser.4, 448 (1871)

(97) Rohsenow, W.M.: University of Michigan Heat Trans.Symposium, 108 (1952)

(98) "International Critical Tables", ed. E.W.Washburn, McGraw-Hill Book Co. Inc., New York (1926)

(99) "Landolt-Börnstein, Zahlenwerte und Funktionen", ed. A.Eucken, Springer Verlag, Berlin (1951)

(100) "Chemical Engineers' Handbook" 3rd ed., ed J.H.Perry, McGraw-Hill Book Co. Inc., New York (1950)

(101) Gröber-Erk-Grigull, "Die Grundgesetze der Wärmeübertragung", Springer Verlag, Berlin (1961)

(102) Mesler, R.B. and J.T.Banchero: A.I.Ch.E. Jour. 4, 102 (1958)

(103) Akin, G.A. and W.H.McAdams: Trans. Am.Inst.Chem.Eng. 35, 137 (1939)

(104) Sarukhanian, G.: Chemie-Ingenieur-Tech. 25, 477 (1953)

(105) Van Stralen, S.J.D.: British Chem.Eng. 6, 834 (1961)

(106) Kok, A.: M.Sc. Thesis in Mech.Eng. (C.J.Rallis supervisor), Witwatersrand University, S.Africa (1960)

(107) Spadaro, J.J., H.L.I.Vix and E.A.Gastrock: Ind.Eng.Chem. (Anal.Secn.) 18, 214 (1946)

(108) Pike, F.P., P.D.Miller and K.O.Beatty: Chen.Eng.Prog. Symposium Ser. 51, No.17, 13 (1955)

(109) Farber, E.A. and R.L.Scorah: Trans.A.S.M.E. 70, 369 (1948)

(110) Nishikawa,K. and K.Yamagata: Int.Jour.Heat & Mass Trans. 1 219 (1960)

* Literature not studied in original form.

ACKNOWLEDGEMENTS

To Dr. A.D.Carr of this Department and to Mr. C.J.Rallis of the Department of Mechanical Engineering, Witwatersrand University, I offer my sincerest thanks for their guidance and encouragement throughout this study. I would also thank Mr. D.Williams of the Department of Botany for the careful preparation of the photomicrographs.